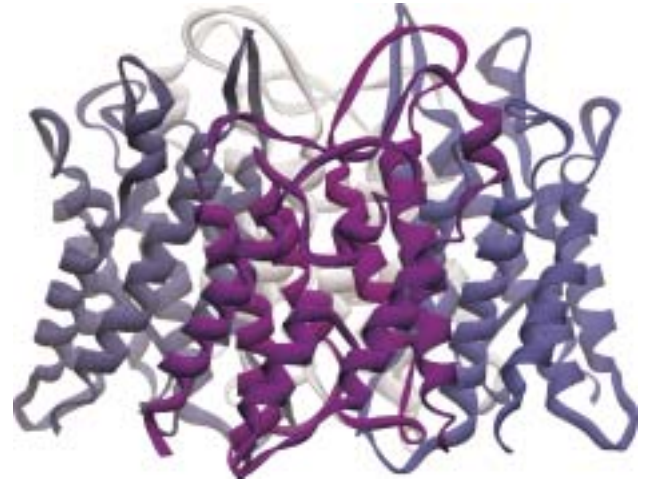


# 7

## TRANSPORT OF IONS AND SMALL MOLECULES ACROSS CELL MEMBRANES



Aquaporin, the water channel, consists of four identical transmembrane polypeptides.

The plasma membrane is a selectively permeable barrier between the cell and the extracellular environment. Its permeability properties ensure that essential molecules such as ions, glucose, amino acids, and lipids readily enter the cell, metabolic intermediates remain in the cell, and waste compounds leave the cell. In short, the selective permeability of the plasma membrane allows the cell to maintain a constant internal environment. In Chapter 5, we learned about the components and structural organization of cell membranes. Movement of virtually all molecules and ions across cellular membranes is mediated by selective **membrane transport proteins** embedded in the phospholipid bilayer. Because different cell types require different mixtures of low-molecular-weight compounds, the plasma membrane of each cell type contains a specific set of transport proteins that allow only certain ions and molecules to cross. Similarly, organelles within the cell often have a different internal environment from that of the surrounding cytosol, and organelle membranes contain specific transport proteins that maintain this difference.

We begin our discussion by reviewing some general principles of transport across membranes and distinguishing three major classes of transport proteins. In subsequent sections, we describe the structure and operation of specific examples of each class and show how members of families of homologous transport proteins have different properties that enable different cell types to function appropriately. We also explain how specific combinations of transport proteins in different subcellular membranes enable cells to carry out essential physiological processes, including the maintenance of cytosolic pH, the accumulation of sucrose and salts in

plant cell vacuoles, and the directed flow of water in both plants and animals. Epithelial cells, such as those lining the small intestine, transport ions, sugars and other small molecules, and water from one side to the other. We shall see how, in order to do this, their plasma membranes are organized into at least two discrete regions, each with its own set of transport proteins. The last two sections of the chapter focus on the panoply of transport proteins that allow nerve cells to generate and conduct the type of electric signal called an **action potential** along their entire length and to transmit these signals to other cells, inducing a change in the electrical properties of the receiving cells.

### OUTLINE

- 7.1 Overview of Membrane Transport
- 7.2 ATP-Powered Pumps and the Intracellular Ionic Environment
- 7.3 Nongated Ion Channels and the Resting Membrane Potential
- 7.4 Cotransport by Symporters and Antiporters
- 7.5 Movement of Water
- 7.6 Transepithelial Transport
- 7.7 Voltage-Gated Ion Channels and the Propagation of Action Potentials in Nerve Cells
- 7.8 Neurotransmitters and Receptor and Transport Proteins in Signal Transmission at Synapses

## 7.1 Overview of Membrane Transport

The phospholipid bilayer, the basic structural unit of biomembranes, is essentially impermeable to most water-soluble molecules, ions, and water itself. After describing the factors that influence the permeability of lipid membranes, we briefly compare the three major classes of membrane proteins that increase the permeability of biomembranes. We then examine operation of the simplest type of transport protein to illustrate basic features of protein-mediated transport. Finally, two common experimental systems used in studying the functional properties of transport proteins are described.

### Few Molecules Cross Membranes by Passive Diffusion

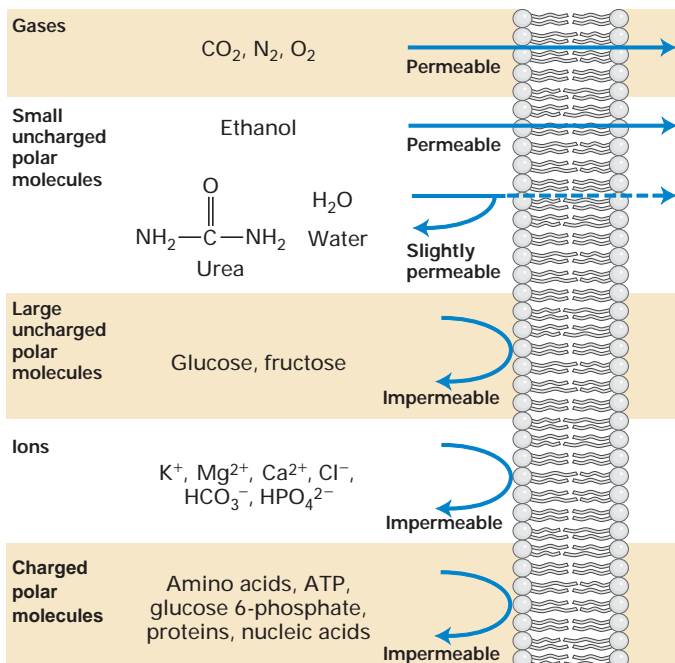
Gases, such as  $O_2$  and  $CO_2$ , and small, uncharged polar molecules, such as urea and ethanol, can readily move by **passive (simple) diffusion** across an artificial membrane composed of pure phospholipid or of phospholipid and cholesterol (Figure 7-1). Such molecules also can diffuse across cellular membranes without the aid of transport proteins. No metabolic energy is expended because movement is from a high to a low concentration of the molecule, down its chemical con-

centration gradient. As noted in Chapter 2, such transport reactions are spontaneous because they have a positive  $\Delta S$  value (increase in entropy) and thus a negative  $\Delta G$  (decrease in free energy).

The relative diffusion rate of any substance across a pure phospholipid bilayer is proportional to its concentration gradient across the layer and to its hydrophobicity and size; charged molecules are also affected by any electric potential across the membrane (see below). When a phospholipid bilayer separates two aqueous compartments, membrane permeability can be easily determined by adding a small amount of radioactive material to one compartment and measuring its rate of appearance in the other compartment. The greater the concentration gradient of the substance, the faster its rate of diffusion across a bilayer.

The hydrophobicity of a substance is measured by its partition coefficient  $K$ , the equilibrium constant for its partition between oil and water. The higher a substance's partition coefficient, the more lipid-soluble it is. The first and rate-limiting step in transport by passive diffusion is movement of a molecule from the aqueous solution into the hydrophobic interior of the phospholipid bilayer, which resembles oil in its chemical properties. This is the reason that the more hydrophobic a molecule is, the faster it diffuses across a pure phospholipid bilayer. For example, diethylurea, with an ethyl group ( $CH_3CH_2-$ ) attached to each nitrogen atom of urea, has a  $K$  of 0.01, whereas urea has a  $K$  of 0.0002 (see Figure 7-1). Diethylurea, which is 50 times ( $0.01/0.0002$ ) more hydrophobic than urea, will diffuse through phospholipid bilayer membranes about 50 times faster than urea. Diethylurea also enters cells about 50 times faster than urea. Similarly, fatty acids with longer hydrocarbon chains are more hydrophobic than those with shorter chains and will diffuse more rapidly across a pure phospholipid bilayer at all concentrations.

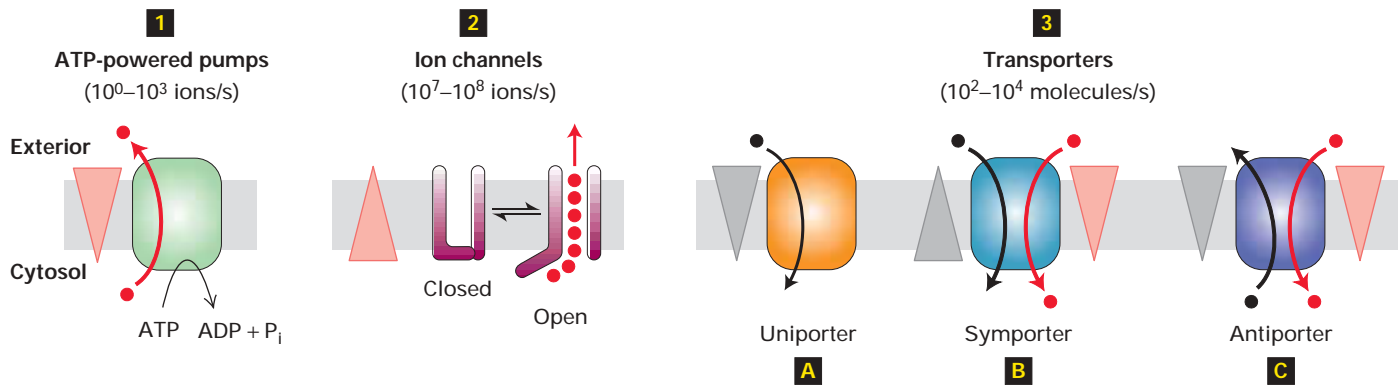
If a transported substance carries a net charge, its movement is influenced by both its concentration gradient and the **membrane potential**, the electric potential (voltage) across the membrane. The combination of these two forces, called the **electrochemical gradient**, determines the energetically favorable direction of transport of a charged molecule across a membrane. The electric potential that exists across most cellular membranes results from a small imbalance in the concentration of positively and negatively charged ions on the two sides of the membrane. We discuss how this ionic imbalance, and resulting potential, arise and are maintained in Sections 7.2 and 7.3.



▲ FIGURE 7-1 Relative permeability of a pure phospholipid bilayer to various molecules. A bilayer is permeable to small hydrophobic molecules and small uncharged polar molecules, slightly permeable to water and urea, and essentially impermeable to ions and to large polar molecules.

### Membrane Proteins Mediate Transport of Most Molecules and All Ions Across Biomembranes

As is evident from Figure 7-1, very few molecules and no ions can cross a pure phospholipid bilayer at appreciable rates by passive diffusion. Thus transport of most molecules



▲ FIGURE 7-2 Overview of membrane transport proteins.

Gradients are indicated by triangles with the tip pointing toward lower concentration, electrical potential, or both. **1** Pumps utilize the energy released by ATP hydrolysis to power movement of specific ions (red circles) or small molecules against their electrochemical gradient. **2** Channels permit movement of specific ions (or water) down their electrochemical gradient. Transporters, which fall into three groups, facilitate movement

of specific small molecules or ions. Uniporters transport a single type of molecule down its concentration gradient **3A**. Cotransport proteins (symporters, **3B**, and antiporters, **3C**) catalyze the movement of one molecule *against* its concentration gradient (black circles), driven by movement of one or more ions down an electrochemical gradient (red circles). Differences in the mechanisms of transport by these three major classes of proteins account for their varying rates of solute movement.

into and out of cells requires the assistance of specialized membrane proteins. Even transport of molecules with a relatively large partition coefficient (e.g., water and urea) is frequently accelerated by specific proteins because their transport by passive diffusion usually is not sufficiently rapid to meet cellular needs.

All transport proteins are transmembrane proteins containing multiple membrane-spanning segments that generally are  $\alpha$  helices. By forming a protein-lined pathway across the membrane, transport proteins are thought to allow movement of hydrophilic substances without their coming into contact with the hydrophobic interior of the membrane. Here we introduce the various types of transport proteins covered in this chapter (Figure 7-2).

**ATP-powered pumps** (or simply **pumps**) are **ATPases** that use the energy of ATP hydrolysis to move ions or small molecules across a membrane *against* a chemical concentration gradient or electric potential or both. This process, referred to as **active transport**, is an example of a coupled chemical reaction (Chapter 2). In this case, transport of ions or small molecules “uphill” against an electrochemical gradient, which requires energy, is coupled to the hydrolysis of ATP, which releases energy. The overall reaction—ATP hydrolysis and the “uphill” movement of ions or small molecules—is energetically favorable.

**Channel proteins** transport water or specific types of ions and hydrophilic small molecules *down* their concentration or electric potential gradients. Such protein-assisted transport sometimes is referred to as **facilitated diffusion**. Channel proteins form a hydrophilic passageway across the membrane through which multiple water molecules or ions move simultaneously, single file at a very rapid rate. Some ion chan-

nels are open much of the time; these are referred to as *non-gated* channels. Most ion channels, however, open only in response to specific chemical or electrical signals; these are referred to as *gated* channels.

**Transporters** (also called *carriers*) move a wide variety of ions and molecules across cell membranes. Three types of transporters have been identified. **Uniporters** transport a single type of molecule *down* its concentration gradient via facilitated diffusion. Glucose and amino acids cross the plasma membrane into most mammalian cells with the aid of uniporters. In contrast, **antiporters** and **symporters** couple the movement of one type of ion or molecule *against* its concentration gradient with the movement of one or more different ions *down* its concentration gradient. These proteins often are called *cotransporters*, referring to their ability to transport two different solutes simultaneously.

Like ATP pumps, cotransporters mediate coupled reactions in which an energetically unfavorable reaction (i.e., uphill movement of molecules) is coupled to an energetically favorable reaction. Note, however, that the nature of the energy-supplying reaction driving active transport by these two classes of proteins differs. ATP pumps use energy from hydrolysis of ATP, whereas cotransporters use the energy stored in an electrochemical gradient. This latter process sometimes is referred to as *secondary active transport*.

Table 7-1 summarizes the four mechanisms by which small molecules and ions are transported across cellular membranes. In this chapter, we focus on the properties and operation of the membrane proteins that mediate the three protein-dependent transport mechanisms. Conformational changes are essential to the function of all transport proteins.

TABLE 7-1 Mechanisms for Transporting Ions and Small Molecules Across Cell Membranes

Property	Transport Mechanism			
	Passive Diffusion	Facilitated Diffusion	Active Transport	Cotransport*
Requires specific protein	–	+	+	+
Solute transported against its gradient	–	–	+	+
Coupled to ATP hydrolysis	–	–	+	–
Driven by movement of a cotransported ion down its gradient	–	–	–	+
Examples of molecules transported	O <sub>2</sub> , CO <sub>2</sub> , steroid hormones, many drugs	Glucose and amino acids (uniporters); ions and water (channels)	Ions, small hydrophilic molecules, lipids (ATP-powered pumps)	Glucose and amino acids (symporters); various ions and sucrose (antiporters)

\*Also called *secondary active transport*.

ATP-powered pumps and transporters undergo a cycle of conformational change exposing a binding site (or sites) to one side of the membrane in one conformation and to the other side in a second conformation. Because each such cycle results in movement of only one (or a few) substrate molecules, these proteins are characterized by relatively slow rates of transport ranging from  $10^0$  to  $10^4$  ions or molecules per second (see Figure 7-2). Ion channels shuttle between a closed state and an open state, but many ions can pass through an open channel without any further conformational change. For this reason, channels are characterized by very fast rates of transport, up to  $10^8$  ions per second.

### Several Features Distinguish Uniport Transport from Passive Diffusion

The protein-mediated movement of glucose and other small hydrophilic molecules across a membrane, known as **uniport** transport, exhibits the following distinguishing properties:

1. The rate of facilitated diffusion by uniporters is far higher than passive diffusion through a pure phospholipid bilayer.
2. Because the transported molecules never enter the hydrophobic core of the phospholipid bilayer, the partition coefficient  $K$  is irrelevant.
3. Transport occurs via a limited number of uniporter molecules, *rather than throughout the phospholipid bilayer*. Consequently, there is a maximum transport rate  $V_{\max}$  that is achieved when the concentration gradient across the

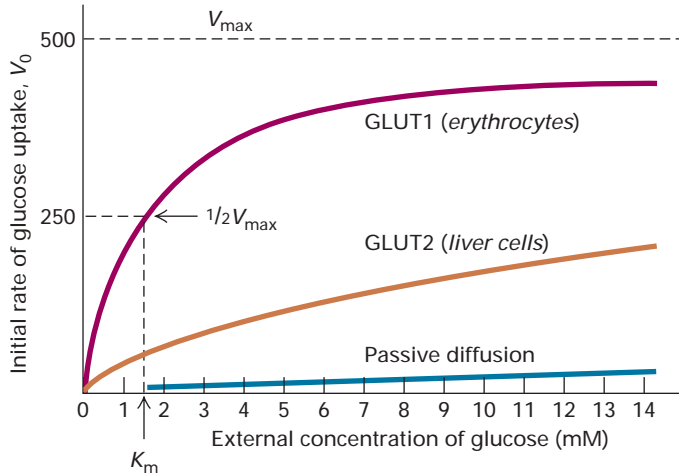
membrane is very large and each uniporter is working at its maximal rate.

4. Transport is specific. Each uniporter transports only a single species of molecule or a single group of closely related molecules. A measure of the affinity of a transporter for its substrate is  $K_m$ , which is the concentration of substrate at which transport is half-maximal.

These properties also apply to transport mediated by the other classes of proteins depicted in Figure 7-2.

One of the best-understood uniporters is the glucose transporter *GLUT1* found in the plasma membrane of erythrocytes. The properties of GLUT1 and many other transport proteins from mature erythrocytes have been extensively studied. These cells, which have no nucleus or other internal organelles, are essentially “bags” of hemoglobin containing relatively few other intracellular proteins and a single membrane, the plasma membrane (see Figure 5-3a). Because the erythrocyte plasma membrane can be isolated in high purity, isolating and purifying a transport protein from mature erythrocytes is a straightforward procedure.

Figure 7-3 shows that glucose uptake by erythrocytes and liver cells exhibits kinetics characteristic of a simple enzyme-catalyzed reaction involving a single substrate. The kinetics of transport reactions mediated by other types of proteins are more complicated than for uniporters. Nonetheless, all protein-assisted transport reactions occur faster than allowed by passive diffusion, are substrate-specific as reflected in lower  $K_m$  values for some substrates than others, and exhibit a maximal rate ( $V_{\max}$ ).



### GLUT1 Uniporter Transports Glucose into Most Mammalian Cells

Most mammalian cells use blood glucose as the major source of cellular energy and express GLUT1. Since the glucose concentration usually is higher in the extracellular medium (blood in the case of erythrocytes) than in the cell, GLUT1 generally catalyzes the net import of glucose from the extracellular medium into the cell. Under this condition,  $V_{\max}$  is achieved at high external glucose concentrations.

Like other uniporters, GLUT1 alternates between two conformational states: in one, a glucose-binding site faces the outside of the membrane; in the other, a glucose-binding site faces the inside. Figure 7-4 depicts the sequence of events occurring during the unidirectional transport of glucose from the cell exterior inward to the cytosol. GLUT1 also can catalyze the net export of glucose from the cytosol to the extra-

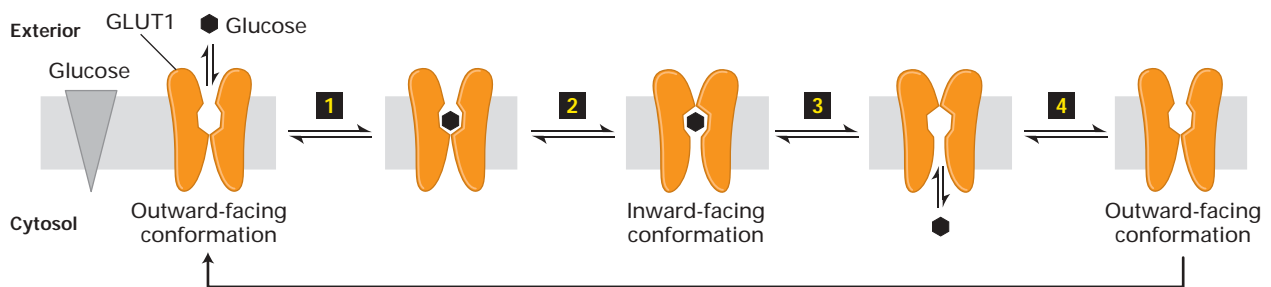
◀ **EXPERIMENTAL FIGURE 7-3 Cellular uptake of glucose mediated by GLUT proteins exhibits simple enzyme kinetics and greatly exceeds the calculated rate of glucose entry solely by passive diffusion.** The initial rate of glucose uptake (measured as micromoles per milliliter of cells per hour) in the first few seconds is plotted against increasing glucose concentration in the extracellular medium. In this experiment, the initial concentration of glucose in the cells is always zero. Both GLUT1, expressed by erythrocytes, and GLUT2, expressed by liver cells, greatly increase the rate of glucose uptake (red and orange curves) compared with that associated with passive diffusion (blue curve) at all external concentrations. Like enzyme-catalyzed reactions, GLUT-facilitated uptake of glucose exhibits a maximum rate ( $V_{\max}$ ). The  $K_m$  is the concentration at which the rate of glucose uptake is half maximal. GLUT2, with a  $K_m$  of about 20 mM, has a much lower affinity for glucose than GLUT1, with a  $K_m$  of about 1.5 mM.

cellular medium exterior when the glucose concentration is higher inside the cell than outside.

The kinetics of the unidirectional transport of glucose from the outside of a cell inward via GLUT1 can be described by the same type of equation used to describe a simple enzyme-catalyzed chemical reaction. For simplicity, let's assume that the substrate glucose,  $S$ , is present initially only on the outside of the membrane. In this case, we can write:



where  $S_{\text{out}} - \text{GLUT1}$  represents GLUT1 in the outward-facing conformation with a bound glucose. By a similar derivation used to arrive at the Michaelis-Menten equation



▲ **FIGURE 7-4 Model of uniport transport by GLUT1.** In one conformation, the glucose-binding site faces outward; in the other, the binding site faces inward. Binding of glucose to the outward-facing site (step **1**) triggers a conformational change in the transporter that results in the binding site's facing inward toward the cytosol (step **2**). Glucose then is released to the inside of the cell (step **3**). Finally, the transporter undergoes the

reverse conformational change, regenerating the outward-facing binding site (step **4**). If the concentration of glucose is higher inside the cell than outside, the cycle will work in reverse (step **4** → step **1**), resulting in net movement of glucose from inside to out. The actual conformational changes are probably smaller than those depicted here.

in Chapter 3, we can derive the following expression for  $v$ , the initial transport rate for S into the cell catalyzed by GLUT1:

$$v = \frac{V_{\max}}{1 + \frac{K_m}{C}} \quad (7-1)$$

where  $C$  is the concentration of  $S_{\text{out}}$  (initially, the concentration of  $S_{\text{in}} = 0$ ).  $V_{\max}$ , the rate of transport when all molecules of GLUT1 contain a bound S, occurs at an infinitely high  $S_{\text{out}}$  concentration. The lower the value of  $K_m$ , the more tightly the substrate binds to the transporter, and the greater the transport rate at a fixed concentration of substrate. Equation 7-1 describes the curve for glucose uptake by erythrocytes shown in Figure 7-3 as well as similar curves for other uniporters.

For GLUT1 in the erythrocyte membrane, the  $K_m$  for glucose transport is 1.5 millimolar (mM); at this concentration roughly half the transporters with outward-facing binding sites would have a bound glucose and transport would occur at 50 percent of the maximal rate. Since blood glucose is normally 5 mM, the erythrocyte glucose transporter usually is functioning at 77 percent of the maximal rate, as can be seen from Figure 7-3. GLUT1 and the very similar GLUT3 are expressed by erythrocytes and other cells that need to take up glucose from the blood continuously at high rates; the rate of glucose uptake by such cells will remain high regardless of small changes in the concentration of blood glucose.

In addition to glucose, the isomeric sugars D-mannose and D-galactose, which differ from D-glucose in the configuration at only one carbon atom, are transported by GLUT1 at measurable rates. However, the  $K_m$  for glucose (1.5 mM) is much lower than the  $K_m$  for D-mannose (20 mM) or D-galactose (30 mM). Thus GLUT1 is quite specific, having a much higher affinity (indicated by a lower  $K_m$ ) for the normal substrate D-glucose than for other substrates.

GLUT1 accounts for 2 percent of the protein in the plasma membrane of erythrocytes. After glucose is transported into the erythrocyte, it is rapidly phosphorylated, forming glucose 6-phosphate, which cannot leave the cell. Because this reaction, the first step in the metabolism of glucose (see Figure 8-4), is rapid, the intracellular concentration of glucose does not increase as glucose is taken up by the cell. Consequently, the glucose concentration gradient across the membrane is maintained, as is the rate of glucose entry into the cell.

### The Human Genome Encodes a Family of Sugar-Transporting GLUT Proteins

The human genome encodes 12 proteins, GLUT1–GLUT12, that are highly homologous in sequence, and all are thought to contain 12 membrane-spanning  $\alpha$  helices. Detailed studies

on GLUT1 have shown that the amino acid residues in the transmembrane  $\alpha$  helices are predominantly hydrophobic; several helices, however, bear amino acid residues (e.g., serine, threonine, asparagine, and glutamine) whose side chains can form hydrogen bonds with the hydroxyl groups on glucose. These residues are thought to form the inward-facing and outward-facing glucose-binding sites in the interior of the protein (see Figure 7-4).

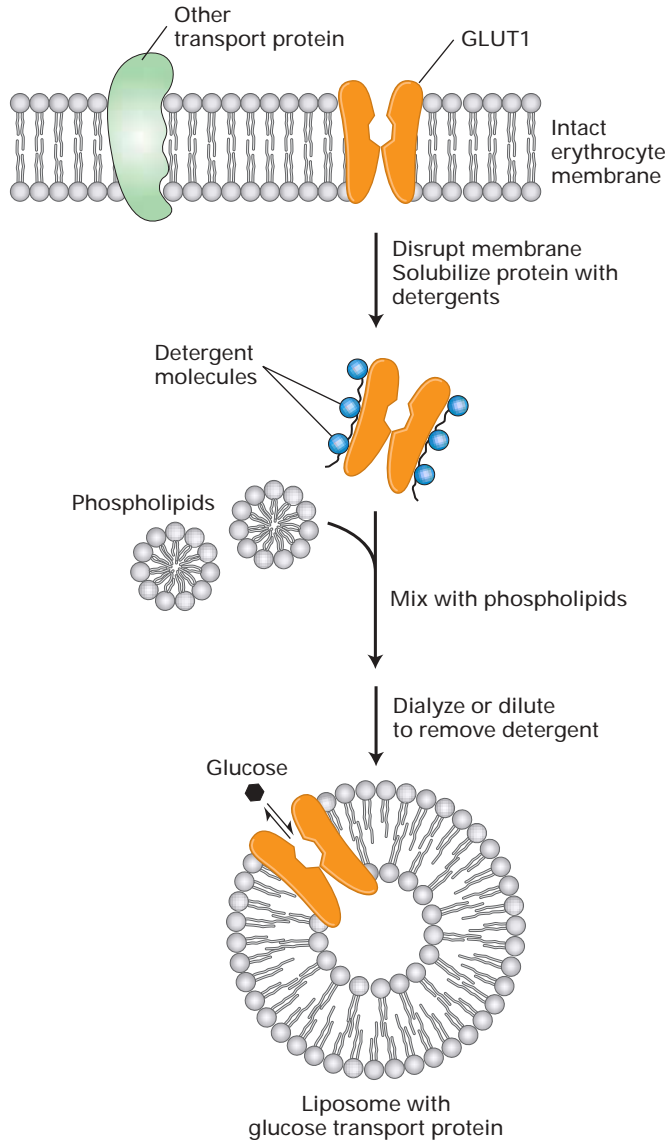
The structures of all GLUT isoforms are quite similar, and all transport sugars. Nonetheless, their differential expression in various cell types and isoform-specific functional properties enable different body cells to regulate glucose metabolism independently and at the same time maintain a constant concentration of glucose in the blood. For instance, GLUT2, expressed in liver and the insulin-secreting  $\beta$  cells of the pancreas, has a  $K_m$  of  $\approx 20$  mM, about 13 times higher than the  $K_m$  of GLUT1. As a result, when blood glucose rises from its basal level of 5 mM to 10 mM or so after a meal, the rate of glucose influx will almost double in GLUT2-expressing cells, whereas it will increase only slightly in GLUT1-expressing cells (see Figure 7-3). In liver, the “excess” glucose brought into the cell is stored as the polymer **glycogen**. In islet  $\beta$  cells, the rise in glucose triggers secretion of the hormone **insulin**, which in turn lowers blood glucose by increasing glucose uptake and metabolism in muscle and by inhibiting glucose production in liver.

Another GLUT isoform, GLUT4, is expressed only in fat and muscle cells, the cells that respond to insulin by increasing their uptake of glucose, thereby removing glucose from the blood. In the absence of insulin, GLUT4 is found in intracellular membranes, not on the plasma membrane, and obviously is unable to facilitate glucose uptake. By a process detailed in Chapter 15, insulin causes these GLUT4-rich internal membranes to fuse with the plasma membrane, increasing the number of GLUT4 molecules on the cell surface and thus the rate of glucose uptake. Defects in this process, one principal mechanism by which insulin lowers blood glucose, lead to diabetes, a disease marked by continuously high blood glucose.

In contrast to GLUT1–GLUT4, which all transport glucose at physiological concentrations, GLUT5 transports fructose. The properties of other members of the GLUT family have not yet been studied in detail.

### Transport Proteins Can Be Enriched Within Artificial Membranes and Cells

Although transport proteins can be isolated from membranes and purified, the functional properties of these proteins can be studied only when they are associated with a membrane. Most cellular membranes contain many different types of transport proteins but a relatively low concentration of any particular one, making functional studies of a single protein difficult. To facilitate such studies, researchers use two ap-



▲ **EXPERIMENTAL FIGURE 7-5** Liposomes containing a single type of transport protein are very useful in studying functional properties of transport proteins.

Here, all the integral proteins of the erythrocyte membrane are solubilized by a nonionic detergent, such as octylglucoside. The glucose uniporter GLUT1 can be purified by chromatography on a column containing a specific monoclonal antibody and then incorporated into liposomes made of pure phospholipids.

proaches for enriching a transport protein of interest so that it predominates in the membrane.

In one common approach, a specific transport protein is extracted and purified; the purified protein then is reincorporated into pure phospholipid bilayer membranes, such as **liposomes** (Figure 7-5). Alternatively, the gene encoding a specific transport protein can be expressed at high levels in

a cell type that normally does not express it. The difference in transport of a substance by the transfected and by control nontransfected cells will be due to the expressed transport protein. In these systems, the functional properties of the various membrane proteins can be examined without ambiguity.

## KEY CONCEPTS OF SECTION 7.1

### Overview of Membrane Transport

- The plasma membrane regulates the traffic of molecules into and out of the cell.
- With the exception of gases (e.g., O<sub>2</sub> and CO<sub>2</sub>) and small hydrophobic molecules, most molecules cannot diffuse across the phospholipid bilayer at rates sufficient to meet cellular needs.
- Three classes of transmembrane proteins mediate transport of ions, sugars, amino acids, and other metabolites across cell membranes: ATP-powered pumps, channels, and transporters (see Figure 7-2).
- In active transport, a transport protein couples movement of a substrate against its concentration gradient to ATP hydrolysis.
- In facilitated diffusion, a transport protein assists in the movement of a specific substrate (molecule or ion) down its concentration gradient.
- In secondary active transport, or cotransport, a transport protein couples movement of a substrate against its concentration gradient to the movement of a second substrate down its concentration gradient (see Table 7-1).
- Protein-catalyzed transport of a solute across a membrane occurs much faster than passive diffusion, exhibits a  $V_{\max}$  when the limited number of transporter molecules are saturated with substrate, and is highly specific for substrate (see Figure 7-3).
- Uniport proteins, such as the glucose transporters (GLUTs), are thought to shuttle between two conformational states, one in which the substrate-binding site faces outward and one in which the binding site faces inward (see Figure 7-4).
- All members of the GLUT protein family transport sugars and have similar structures. Differences in their  $K_m$  values, expression in different cell types, and substrate specificities are important for proper sugar metabolism in the body.
- Two common experimental systems for studying the functions of transport proteins are liposomes containing a purified transport protein (see Figure 7-5) and cells transfected with the gene encoding a particular transport protein.

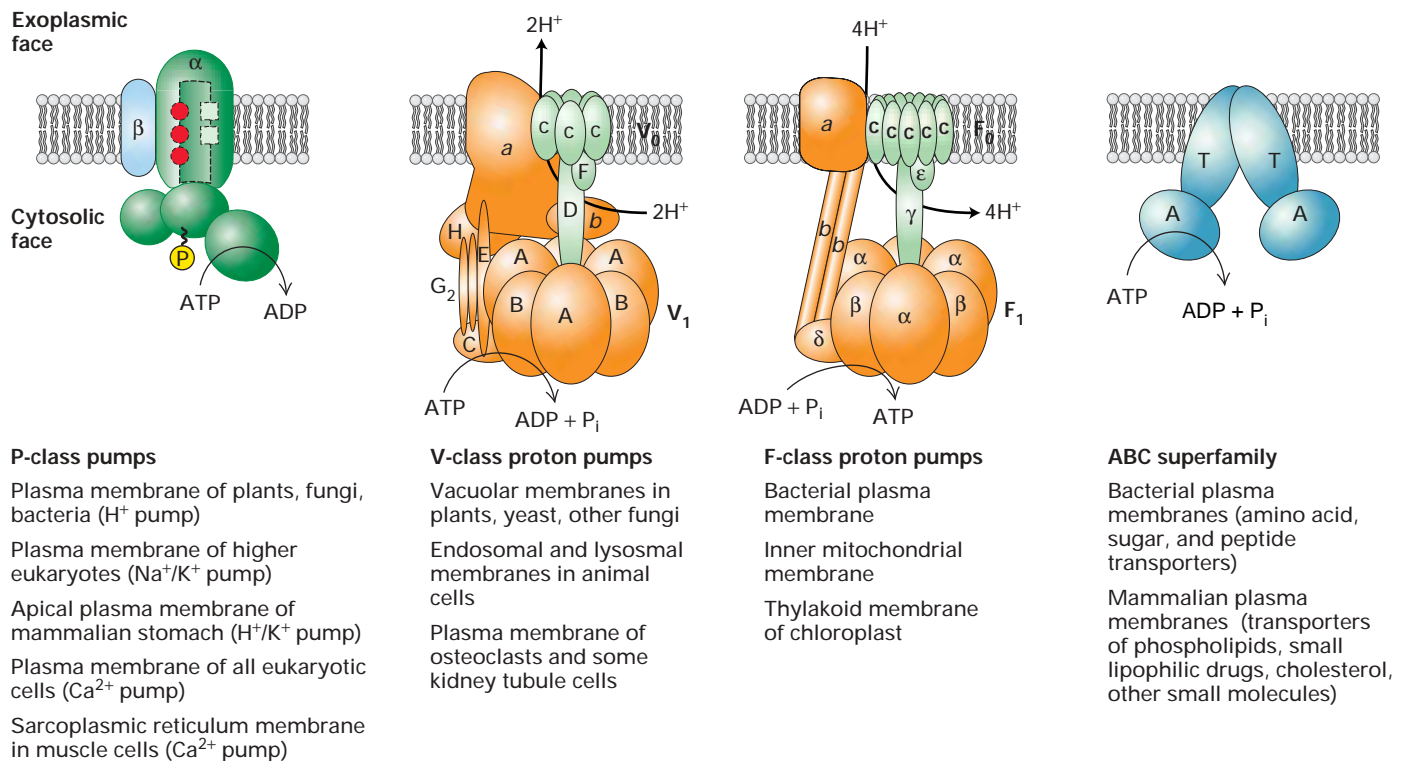
## 7.2 ATP-Powered Pumps and the Intracellular Ionic Environment

We turn now to the ATP-powered pumps, which transport ions and various small molecules against their concentration gradients. All ATP-powered pumps are transmembrane proteins with one or more binding sites for ATP located on the cytosolic face of the membrane. Although these proteins commonly are called *ATPases*, they normally do not hydrolyze ATP into ADP and  $P_i$  unless ions or other molecules are simultaneously transported. Because of this tight coupling between ATP hydrolysis and transport, the energy stored in the phosphoanhydride bond is not dissipated but rather used to move ions or other molecules uphill against an electrochemical gradient.

### Different Classes of Pumps Exhibit Characteristic Structural and Functional Properties

The general structures of the four classes of ATP-powered pumps are depicted in Figure 7-6, with specific examples in each class listed below. Note that the members of three classes (P, F, and V) transport ions only, whereas members of the ABC superfamily primarily transport small molecules.

All *P-class ion pumps* possess two identical catalytic  $\alpha$  subunits that contain an ATP-binding site. Most also have two smaller  $\beta$  subunits that usually have regulatory functions. During the transport process, at least one of the  $\alpha$  subunits is phosphorylated (hence the name “P” class), and the transported ions are thought to move through the phosphorylated subunit. The sequence around the phosphorylated residue is homologous in different pumps. This class includes the  $Na^+/K^+$  ATPase in the plasma membrane, which main-



▲ **FIGURE 7-6 The four classes of ATP-powered transport proteins.** The location of specific pumps are indicated below each class. P-class pumps are composed of a catalytic  $\alpha$  subunit, which becomes phosphorylated as part of the transport cycle. A  $\beta$  subunit, present in some of these pumps, may regulate transport. F-class and V-class pumps do not form phosphoprotein intermediates and transport only protons. Their structures are similar and contain similar proteins, but none of their subunits are related to those of P-class pumps. V-class pumps couple ATP hydrolysis to transport of protons against a concentration gradient, whereas F-class pumps normally operate in the

direction to utilize energy in a proton concentration or electrochemical gradient to synthesize ATP. All members of the large ABC superfamily of proteins contain two transmembrane (T) domains and two cytosolic ATP-binding (A) domains, which couple ATP hydrolysis to solute movement. These core domains are present as separate subunits in some ABC proteins (depicted here), but are fused into a single polypeptide in other ABC proteins. [See T. Nishi and M. Forgac, 2002, *Nature Rev. Mol. Cell Biol.* **3**:94; G. Chang and C. Roth, 2001, *Science* **293**:1793; C. Toyoshima et al., 2000, *Nature* **405**:647; D. McIntosh, 2000, *Nature Struct. Biol.* **7**:532; and T. Elston, H. Wang, and G. Oster, 1998, *Nature* **391**:510.]



tains the low cytosolic  $\text{Na}^+$  and high cytosolic  $\text{K}^+$  concentrations typical of animal cells. Certain  $\text{Ca}^{2+}$  ATPases pump  $\text{Ca}^{2+}$  ions out of the cytosol into the external medium; others pump  $\text{Ca}^{2+}$  from the cytosol into the endoplasmic reticulum or into the specialized ER called the *sarcoplasmic reticulum*, which is found in muscle cells. Another member of the P class, found in acid-secreting cells of the mammalian stomach, transports protons ( $\text{H}^+$  ions) out of and  $\text{K}^+$  ions into the cell. The  $\text{H}^+$  pump that generates and maintains the membrane electric potential in plant, fungal, and bacterial cells also belongs to this class.

The structures of *F-class* and *V-class ion pumps* are similar to one another but unrelated to and more complicated than P-class pumps. F- and V-class pumps contain several different transmembrane and cytosolic subunits. All known V and F pumps transport only protons, in a process that does not involve a phosphoprotein intermediate. V-class pumps generally function to maintain the low pH of plant vacuoles and of lysosomes and other acidic vesicles in animal cells by pumping protons from the cytosolic to the exoplasmic face of the membrane against a proton electrochemical gradient. F-class pumps are found in bacterial plasma membranes and in mitochondria and chloroplasts. In contrast to V pumps, they generally function to power the synthesis of ATP from ADP and  $\text{P}_i$  by movement of protons from the exoplasmic to the cytosolic face of the membrane down the proton electrochemical gradient. Because of their importance in ATP synthesis in chloroplasts and mitochondria, F-class proton pumps, commonly called ATP synthases, are treated separately in Chapter 8.

The final class of ATP-powered pumps contains more members and is more diverse than the other classes. Referred to as the **ABC (ATP-binding cassette) superfamily**, this class includes several hundred different transport proteins found in organisms ranging from bacteria to humans. Each ABC protein is specific for a single substrate or group of related substrates, which may be ions, sugars, amino acids, phospholipids, peptides, polysaccharides, or even proteins. All ABC transport proteins share a structural organization consisting of four “core” domains: two transmembrane (T) domains, forming the passageway through which transported molecules cross the membrane, and two cytosolic ATP-binding (A) domains. In some ABC proteins, mostly in bacteria, the core domains are present in four separate polypeptides; in others, the core domains are fused into one or two multidomain polypeptides.

### ATP-Powered Ion Pumps Generate and Maintain Ionic Gradients Across Cellular Membranes

The specific ionic composition of the cytosol usually differs greatly from that of the surrounding extracellular fluid. In virtually all cells—including microbial, plant, and animal cells—the cytosolic pH is kept near 7.2 regardless of the extracellular pH. Also, the cytosolic concentration of  $\text{K}^+$  is

much higher than that of  $\text{Na}^+$ . In addition, in both invertebrates and vertebrates, the concentration of  $\text{K}^+$  is 20–40 times higher in cells than in the blood, while the concentration of  $\text{Na}^+$  is 8–12 times lower in cells than in the blood (Table 7-2). Some  $\text{Ca}^{2+}$  in the cytosol is bound to the negatively charged groups in ATP and other molecules, but it is the concentration of free, unbound  $\text{Ca}^{2+}$  that is critical to its functions in signaling pathways and muscle contraction. The concentration of free  $\text{Ca}^{2+}$  in the cytosol is generally less than 0.2 micromolar ( $2 \times 10^{-7}$  M), a thousand or more times lower than that in the blood. Plant cells and many microorganisms maintain similarly high cytosolic concentrations of  $\text{K}^+$  and low concentrations of  $\text{Ca}^{2+}$  and  $\text{Na}^+$  even if the cells are cultured in very dilute salt solutions.

The ion pumps discussed in this section are largely responsible for establishing and maintaining the usual ionic gradients across the plasma and intracellular membranes. In carrying out this task, cells expend considerable energy. For

**TABLE 7-2** Typical Intracellular and Extracellular Ion Concentrations

Ion	Cell (mM)	Blood (mM)
SQUID AXON (INVERTEBRATE)*		
$\text{K}^+$	400	20
$\text{Na}^+$	50	440
$\text{Cl}^-$	40–150	560
$\text{Ca}^{2+}$	0.0003	10
$\text{X}^\dagger$	300–400	5–10
MAMMALIAN CELL (VERTEBRATE)		
$\text{K}^+$	139	4
$\text{Na}^+$	12	145
$\text{Cl}^-$	4	116
$\text{HCO}_3^-$	12	29
$\text{X}^-$	138	9
$\text{Mg}^{2+}$	0.8	1.5
$\text{Ca}^{2+}$	<0.0002	1.8

\*The large nerve axon of the squid has been widely used in studies of the mechanism of conduction of electric impulses.

† $\text{X}^-$  represents proteins, which have a net negative charge at the neutral pH of blood and cells.

example, up to 25 percent of the ATP produced by nerve and kidney cells is used for ion transport, and human erythrocytes consume up to 50 percent of their available ATP for this purpose; in both cases, most of this ATP is used to power the  $\text{Na}^+/\text{K}^+$  pump.

In cells treated with poisons that inhibit the aerobic production of ATP (e.g., 2,4-dinitrophenol in aerobic cells), the ion concentrations inside the cell gradually approach those of the exterior environment as ions move through channels in the plasma membrane down their electrochemical gradients. Eventually treated cells die: partly because protein synthesis requires a high concentration of  $\text{K}^+$  ions and partly because in the absence of a  $\text{Na}^+$  gradient across the cell membrane, a cell cannot import certain nutrients such as amino acids. Studies on the effects of such poisons provided early evidence for the existence of ion pumps.

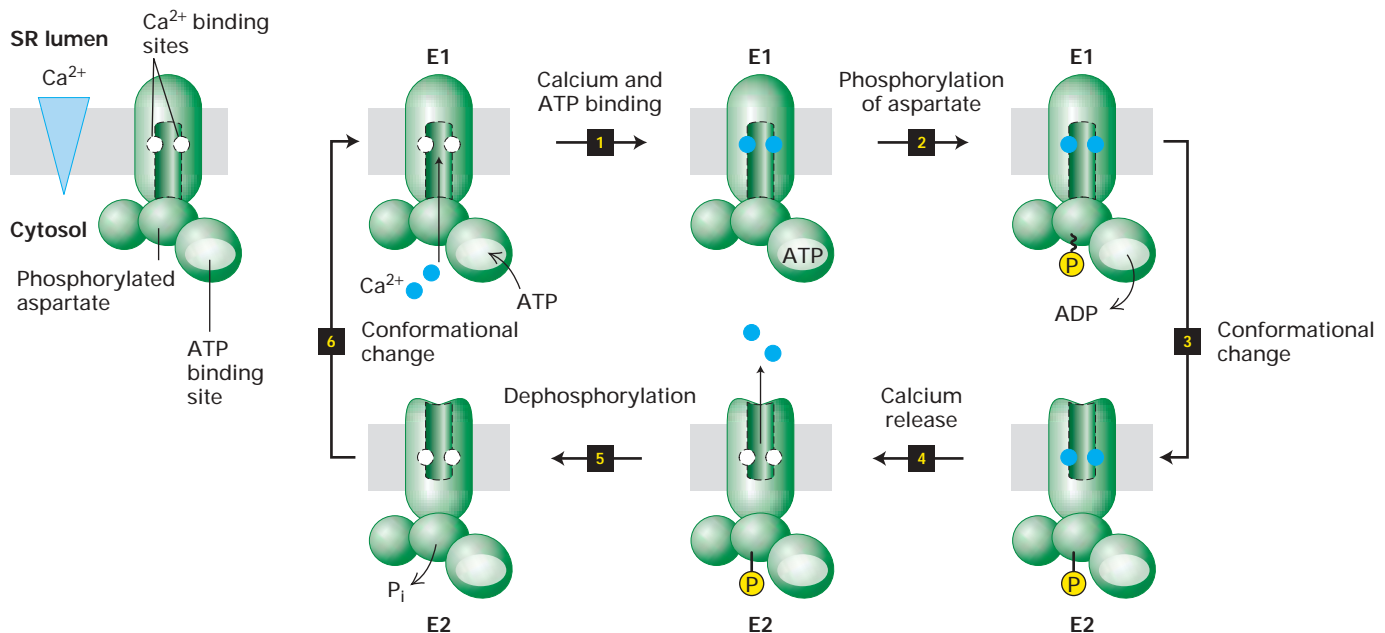
### Muscle $\text{Ca}^{2+}$ ATPase Pumps $\text{Ca}^{2+}$ Ions from the Cytosol into the Sarcoplasmic Reticulum

In skeletal muscle cells,  $\text{Ca}^{2+}$  ions are concentrated and stored in the sarcoplasmic reticulum (SR); release of stored  $\text{Ca}^{2+}$  ions from the SR lumen into the cytosol causes con-

traction, as discussed in Chapter 19. A P-class  $\text{Ca}^{2+}$  ATPase located in the SR membrane of skeletal muscle pumps  $\text{Ca}^{2+}$  from the cytosol into the lumen of the SR, thereby inducing muscle relaxation. Because this *muscle calcium pump* constitutes more than 80 percent of the integral protein in SR membranes, it is easily purified and has been studied extensively.

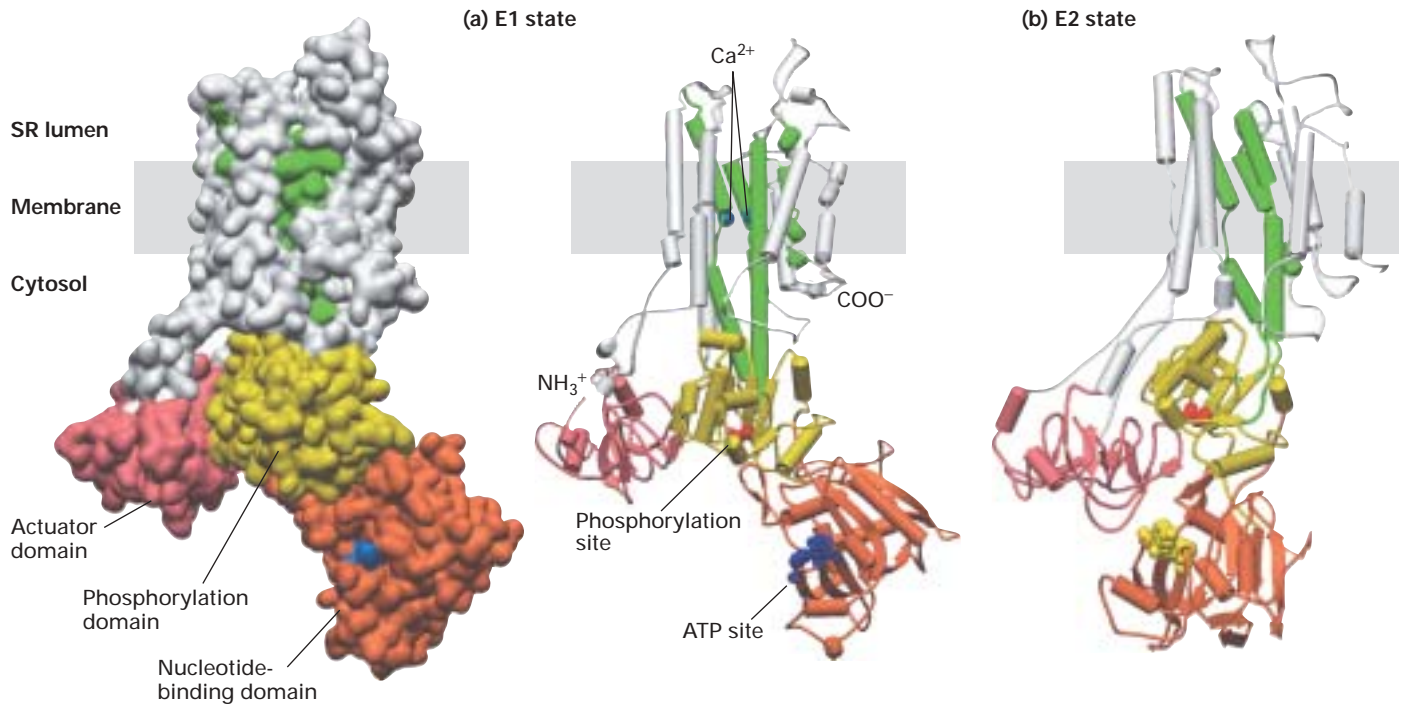
In the cytosol of muscle cells, the free  $\text{Ca}^{2+}$  concentration ranges from  $10^{-7}$  M (resting cells) to more than  $10^{-6}$  M (contracting cells), whereas the *total*  $\text{Ca}^{2+}$  concentration in the SR lumen can be as high as  $10^{-2}$  M. However, two soluble proteins in the lumen of SR vesicles bind  $\text{Ca}^{2+}$  and serve as a reservoir for intracellular  $\text{Ca}^{2+}$ , thereby reducing the concentration of free  $\text{Ca}^{2+}$  ions in the SR vesicles and consequently the energy needed to pump  $\text{Ca}^{2+}$  ions into them from the cytosol. The activity of the muscle  $\text{Ca}^{2+}$  ATPase increases as the free  $\text{Ca}^{2+}$  concentration in the cytosol rises. Thus in skeletal muscle cells, the calcium pump in the SR membrane can supplement the activity of a similar  $\text{Ca}^{2+}$  pump located in the plasma membrane to assure that the cytosolic concentration of free  $\text{Ca}^{2+}$  in resting muscle remains below  $1 \mu\text{M}$ .

The current model for the mechanism of action of the  $\text{Ca}^{2+}$  ATPase in the SR membrane involves two conformational states of the protein termed E1 and E2. Coupling of



▲ **FIGURE 7-7 Operational model of the  $\text{Ca}^{2+}$  ATPase in the SR membrane of skeletal muscle cells.** Only one of the two catalytic  $\alpha$  subunits of this P-class pump is depicted. E1 and E2 are alternative conformations of the protein in which the  $\text{Ca}^{2+}$ -binding sites are accessible to the cytosolic and exoplasmic faces, respectively. An ordered sequence of steps (**1–6**), as diagrammed here, is essential for coupling ATP hydrolysis and the transport of  $\text{Ca}^{2+}$  ions across the membrane. In the figure,

~P indicates a high-energy acyl phosphate bond; -P indicates a low-energy phosphoester bond. Because the affinity of  $\text{Ca}^{2+}$  for the cytosolic-facing binding sites in E1 is a thousandfold greater than the affinity of  $\text{Ca}^{2+}$  for the exoplasmic-facing sites in E2, this pump transports  $\text{Ca}^{2+}$  unidirectionally from the cytosol to the SR lumen. See the text and Figure 7-8 for more details. [See C. Toyoshima et al., 2000, *Nature* **405**:647; P. Zhang et al., 1998, *Nature* **392**:835; and W. P. Jencks, 1989, *J. Biol. Chem.* **264**:18855.]



▲ **FIGURE 7-8 Structure of the catalytic  $\alpha$  subunit of the muscle  $\text{Ca}^{2+}$  ATPase.** (a) Three-dimensional models of the protein in the E1 state based on the structure determined by x-ray crystallography. There are 10 transmembrane  $\alpha$  helices, four of which (green) contain residues that site-specific mutagenesis studies have identified as participating in  $\text{Ca}^{2+}$  binding. The cytosolic segment forms three domains: the nucleotide-binding domain (orange), the phosphorylation domain (yellow), and the actuator domain (pink) that connects two of the membrane-spanning helices. (b) Hypothetical model of the pump in the E2 state, based on a

lower-resolution structure determined by electron microscopy of frozen crystals of the pure protein. Note the differences between the E1 and E2 states in the conformations of the nucleotide-binding and actuator domains; these changes probably power the conformational changes of the membrane-spanning  $\alpha$  helices (green) that constitute the  $\text{Ca}^{2+}$ -binding sites, converting them from one in which the  $\text{Ca}^{2+}$ -binding sites are accessible to the cytosolic face (E1 state) to one in which they are accessible to the exoplasmic face (E2 state). [Adapted from C. Xu, 2002, *J. Mol. Biol.* **316**:201, and D. McIntosh, 2000, *Nature Struct. Biol.* **7**:532.]

ATP hydrolysis with ion pumping involves several steps that must occur in a defined order, as shown in Figure 7-7. When the protein is in the E1 conformation, two  $\text{Ca}^{2+}$  ions bind to two high-affinity binding sites accessible from the cytosolic side and an ATP binds to a site on the cytosolic surface (step 1). The bound ATP is hydrolyzed to ADP in a reaction that requires  $\text{Mg}^{2+}$ , and the liberated phosphate is transferred to a specific aspartate residue in the protein, forming the high-energy acyl phosphate bond denoted by  $\text{E1} \sim \text{P}$  (step 2). The protein then undergoes a conformational change that generates E2, which has two low-affinity  $\text{Ca}^{2+}$ -binding sites accessible to the SR lumen (step 3). The free energy of hydrolysis of the aspartyl-phosphate bond in  $\text{E1} \sim \text{P}$  is greater than that in  $\text{E2} - \text{P}$ , and this reduction in free energy of the aspartyl-phosphate bond can be said to power the  $\text{E1} \rightarrow \text{E2}$  conformational change. The  $\text{Ca}^{2+}$  ions spontaneously dissociate from the low-affinity sites to enter the SR lumen (step 4), following which the aspartyl-phosphate bond is hydrolyzed (step 5). Dephosphorylation powers the  $\text{E2} \rightarrow \text{E1}$  conformational change (step 6), and E1 is ready to transport two more  $\text{Ca}^{2+}$  ions.

Much evidence supports the model depicted in Figure 7-7. For instance, the muscle calcium pump has been isolated with phosphate linked to an aspartate residue, and spectroscopic studies have detected slight alterations in protein conformation during the  $\text{E1} \rightarrow \text{E2}$  conversion. The 10 membrane-spanning  $\alpha$  helices in the catalytic subunit are thought to form the passageway through which  $\text{Ca}^{2+}$  ions move, and mutagenesis studies have identified amino acids in four of these helices that are thought to form the two  $\text{Ca}^{2+}$ -binding sites (Figure 7-8). Cryoelectron microscopy and x-ray crystallography of the protein in different conformational states also revealed that the bulk of the catalytic subunit consists of cytosolic globular domains that are involved in ATP binding, phosphorylation of aspartate, and transduction of the energy released by hydrolysis of the aspartyl phosphate into conformational changes in the protein. These domains are connected by a “stalk” to the membrane-embedded domain.

All P-class ion pumps, regardless of which ion they transport, are phosphorylated on a highly conserved aspartate residue during the transport process. Thus the operational

model in Figure 7-7 is generally applicable to all these ATP-powered ion pumps. In addition, the catalytic  $\alpha$  subunits of all the P pumps examined to date have a similar molecular weight and, as deduced from their amino acid sequences derived from cDNA clones, have a similar arrangement of transmembrane  $\alpha$  helices (see Figure 7-8). These findings strongly suggest that all these proteins evolved from a common precursor, although they now transport different ions.

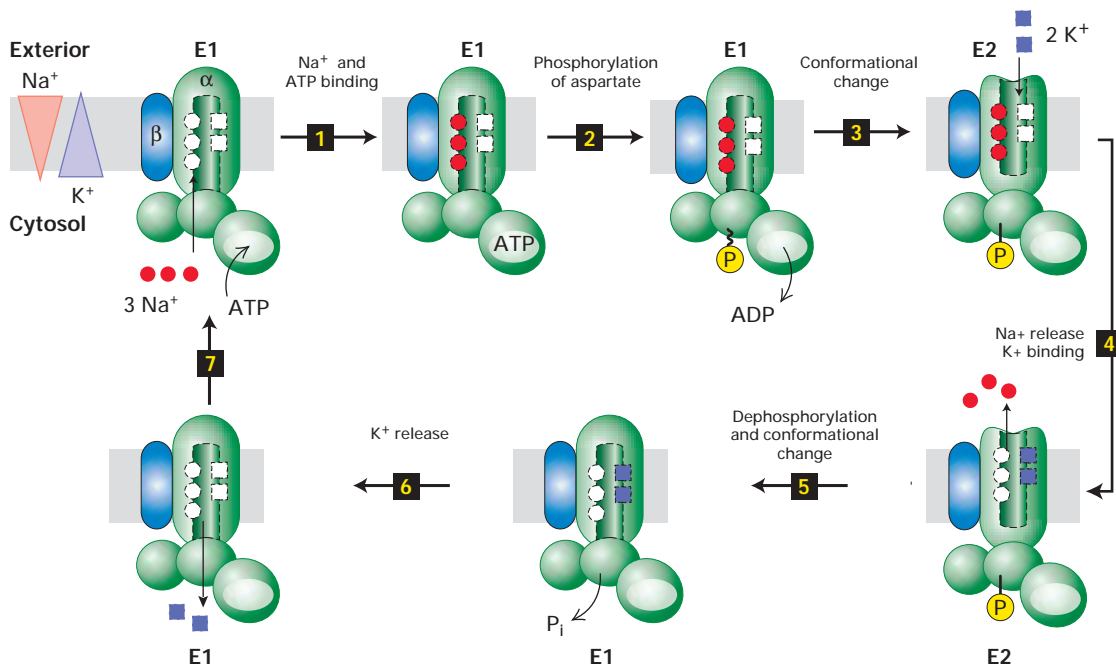
### Calmodulin-Mediated Activation of Plasma-Membrane $\text{Ca}^{2+}$ ATPase Leads to Rapid $\text{Ca}^{2+}$ Export

As we explain in Chapter 13, small increases in the concentration of free  $\text{Ca}^{2+}$  ions in the cytosol trigger a variety of cellular responses. In order for  $\text{Ca}^{2+}$  to function in intracellular signaling, the concentration of  $\text{Ca}^{2+}$  ions free in the cytosol usually must be kept below 0.1 – 0.2  $\mu\text{M}$ . Animal, yeast, and probably plant cells express plasma-membrane  $\text{Ca}^{2+}$  ATPases that transport  $\text{Ca}^{2+}$  out of the cell against its electrochemical gradient. The catalytic  $\alpha$  subunit of these P-class pumps is similar in structure and sequence to the  $\alpha$  subunit of the muscle SR  $\text{Ca}^{2+}$  pump.

The activity of plasma-membrane  $\text{Ca}^{2+}$  ATPases is regulated by **calmodulin**, a cytosolic  $\text{Ca}^{2+}$ -binding protein (see Figure 3-28). A rise in cytosolic  $\text{Ca}^{2+}$  induces the binding of  $\text{Ca}^{2+}$  ions to calmodulin, which triggers allosteric activation of the  $\text{Ca}^{2+}$  ATPase. As a result, the export of  $\text{Ca}^{2+}$  ions from the cell accelerates, quickly restoring the low concentration of free cytosolic  $\text{Ca}^{2+}$  characteristic of the resting cell.

### $\text{Na}^+/\text{K}^+$ ATPase Maintains the Intracellular $\text{Na}^+$ and $\text{K}^+$ Concentrations in Animal Cells

A second important P-class ion pump present in the plasma membrane of all animal cells is the  **$\text{Na}^+/\text{K}^+$  ATPase**. This ion pump is a tetramer of subunit composition  $\alpha_2\beta_2$ . (Classic Experiment 7.1 describes the discovery of this enzyme.) The small, glycosylated  $\beta$  polypeptide helps newly synthesized  $\alpha$  subunits to fold properly in the endoplasmic reticulum but apparently is not involved directly in ion pumping. The amino acid sequence and predicted secondary structure of the catalytic  $\alpha$  subunit are very similar to those of the muscle SR  $\text{Ca}^{2+}$  ATPase (see Figure 7-8). In particular, the  $\text{Na}^+/\text{K}^+$  ATPase has a stalk on the cytosolic face that links



▲ FIGURE 7-9 Operational model of the  $\text{Na}^+/\text{K}^+$  ATPase in the plasma membrane. Only one of the two catalytic  $\alpha$  subunits of this P-class pump is depicted. It is not known whether just one or both subunits in a single ATPase molecule transport ions. Ion pumping by the  $\text{Na}^+/\text{K}^+$  ATPase involves phosphorylation, dephosphorylation, and conformational changes similar to those in the muscle

$\text{Ca}^{2+}$  ATPase (see Figure 7-7). In this case, hydrolysis of the E2-P intermediate powers the E2  $\rightarrow$  E1 conformational change and concomitant transport of two ions ( $\text{K}^+$ ) inward.  $\text{Na}^+$  ions are indicated by red circles;  $\text{K}^+$  ions, by purple squares; high-energy acyl phosphate bond, by  $\sim\text{P}$ ; low-energy phosphoester bond, by  $-\text{P}$ . [See K. Sweadner and C. Donnet, 2001, *Biochem. J.* 356:6875, for details of the structure of the  $\alpha$  subunit.]



domains containing the ATP-binding site and the phosphorylated aspartate to the membrane-embedded domain. The overall transport process moves three  $\text{Na}^+$  ions out of and two  $\text{K}^+$  ions into the cell per ATP molecule hydrolyzed.

The mechanism of action of the  $\text{Na}^+/\text{K}^+$  ATPase, outlined in Figure 7-9, is similar to that of the muscle calcium pump, except that ions are pumped in both directions across the membrane. In its E1 conformation, the  $\text{Na}^+/\text{K}^+$  ATPase has three high-affinity  $\text{Na}^+$ -binding sites and two low-affinity  $\text{K}^+$ -binding sites accessible to the cytosolic surface of the protein. The  $K_m$  for binding of  $\text{Na}^+$  to these cytosolic sites is 0.6 mM, a value considerably lower than the intracellular  $\text{Na}^+$  concentration of  $\approx 12$  mM; as a result,  $\text{Na}^+$  ions normally will fully occupy these sites. Conversely, the affinity of the cytosolic  $\text{K}^+$ -binding sites is low enough that  $\text{K}^+$  ions, transported inward through the protein, dissociate from E1 into the cytosol despite the high intracellular  $\text{K}^+$  concentration. During the E1  $\rightarrow$  E2 transition, the three bound  $\text{Na}^+$  ions become accessible to the exoplasmic face, and simultaneously the affinity of the three  $\text{Na}^+$ -binding sites becomes reduced. The three  $\text{Na}^+$  ions, transported outward through the protein and now bound to the low-affinity  $\text{Na}^+$  sites exposed to the exoplasmic face, dissociate one at a time into the extracellular medium despite the high extracellular  $\text{Na}^+$  concentration. Transition to the E2 conformation also generates two high-affinity  $\text{K}^+$  sites accessible to the exoplasmic face. Because the  $K_m$  for  $\text{K}^+$  binding to these sites (0.2 mM) is lower than the extracellular  $\text{K}^+$  concentration (4 mM), these sites will fill with  $\text{K}^+$  ions. Similarly, during the E2  $\rightarrow$  E1 transition, the two bound  $\text{K}^+$  ions are transported inward and then released into the cytosol.

Certain drugs (e.g., ouabain and digoxin) bind to the exoplasmic domain of the plasma-membrane  $\text{Na}^+/\text{K}^+$  ATPase and specifically inhibit its ATPase activity. The resulting disruption in the  $\text{Na}^+/\text{K}^+$  balance of cells is strong evidence for the critical role of this ion pump in maintaining the normal  $\text{K}^+$  and  $\text{Na}^+$  ion concentration gradients.

### V-Class $\text{H}^+$ ATPases Pump Protons Across Lysosomal and Vacuolar Membranes

All V-class ATPases transport only  $\text{H}^+$  ions. These proton pumps, present in the membranes of lysosomes, endosomes, and plant vacuoles, function to acidify the lumen of these organelles. The pH of the lysosomal lumen can be measured precisely in living cells by use of particles labeled with a pH-sensitive fluorescent dye. After these particles are phagocytosed by cells and transferred to lysosomes, the lysosomal pH can be calculated from the spectrum of the fluorescence emitted. Maintenance of the 100-fold or more proton gradient between the lysosomal lumen (pH  $\approx 4.5$ – $5.0$ ) and the cytosol (pH  $\approx 7.0$ ) depends on ATP production by the cell.

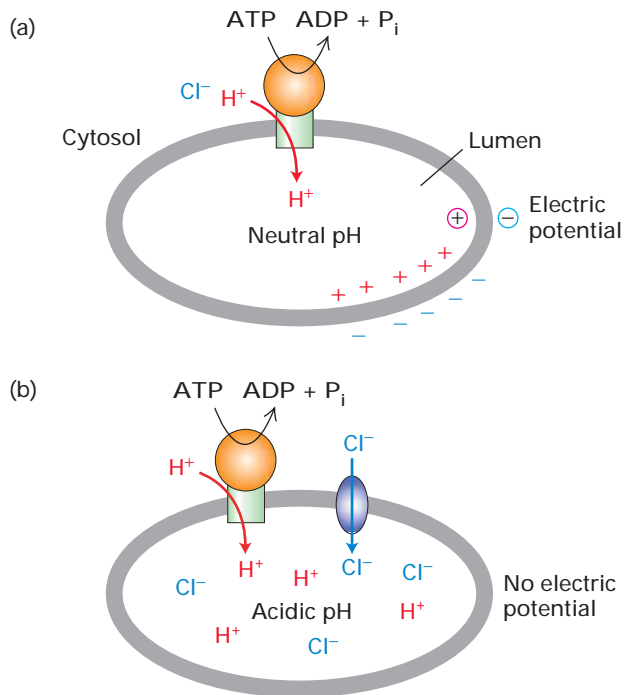
The ATP-powered proton pumps in lysosomal and vacuolar membranes have been isolated, purified, and incor-

porated into liposomes. As illustrated in Figure 7-6 (center), these V-class proton pumps contain two discrete domains: a cytosolic hydrophilic domain ( $V_1$ ) and a transmembrane domain ( $V_0$ ) with multiple subunits in each domain. Binding and hydrolysis of ATP by the B subunits in  $V_1$  provide the energy for pumping of  $\text{H}^+$  ions through the proton-conducting channel formed by the c and a subunits in  $V_0$ . Unlike P-class ion pumps, V-class proton pumps are not phosphorylated and dephosphorylated during proton transport. The structurally similar F-class proton pumps, which we describe in the next chapter, normally operate in the “reverse” direction to generate ATP rather than pump protons and their mechanism of action is understood in great detail.

Pumping of relatively few protons is required to acidify an intracellular vesicle. To understand why, recall that a solution of pH 4 has a  $\text{H}^+$  ion concentration of  $10^{-4}$  moles per liter, or  $10^{-7}$  moles of  $\text{H}^+$  ions per milliliter. Since there are  $6.02 \times 10^{23}$  molecules per mole (Avogadro’s number), then a milliliter of a pH 4 solution contains  $6.02 \times 10^{16}$   $\text{H}^+$  ions. Thus at pH 4, a primary spherical lysosome with a volume of  $4.18 \times 10^{-15}$  ml (diameter of 0.2  $\mu\text{m}$ ) will contain just 252 protons.

By themselves ATP-powered proton pumps cannot acidify the lumen of an organelle (or the extracellular space) because these pumps are *electrogenic*; that is, a net movement of electric charge occurs during transport. Pumping of just a few protons causes a buildup of positively charged  $\text{H}^+$  ions on the exoplasmic (inside) face of the organelle membrane. For each  $\text{H}^+$  pumped across, a negative ion (e.g.,  $\text{OH}^-$  or  $\text{Cl}^-$ ) will be “left behind” on the cytosolic face, causing a buildup of negatively charged ions there. These oppositely charged ions attract each other on opposite faces of the membrane, generating a charge separation, or electric potential, across the membrane. As more and more protons are pumped, the excess of positive charges on the exoplasmic face repels other  $\text{H}^+$  ions, soon preventing pumping of additional protons long before a significant transmembrane  $\text{H}^+$  concentration gradient had been established (Figure 7-10a). In fact, this is the way that P-class  $\text{H}^+$  pumps generate a cytosol-negative potential across plant and yeast plasma membranes.

In order for an organelle lumen or an extracellular space (e.g., the lumen of the stomach) to become acidic, movement of protons must be accompanied either by (1) movement of an equal number of anions (e.g.,  $\text{Cl}^-$ ) in the same direction or by (2) movement of equal numbers of a different cation in the opposite direction. The first process occurs in lysosomes and plant vacuoles whose membranes contain V-class  $\text{H}^+$  ATPases and anion channels through which accompanying  $\text{Cl}^-$  ions move (Figure 7-10b). The second process occurs in the lining of the stomach, which contains a P-class  $\text{H}^+/\text{K}^+$  ATPase that is not electrogenic and pumps one  $\text{H}^+$  outward and one  $\text{K}^+$  inward. Operation of this pump is discussed later in the chapter.



▲ FIGURE 7-10 Effect of proton pumping by V-class ion pumps on H<sup>+</sup> concentration gradients and electric potential gradients across cellular membranes. (a) If an intracellular organelle contains only V-class pumps, proton pumping generates an electric potential across the membrane, luminal-side positive, but no significant change in the intraluminal pH. (b) If the organelle membrane also contains Cl<sup>-</sup> channels, anions passively follow the pumped protons, resulting in an accumulation of H<sup>+</sup> ions (low luminal pH) but no electric potential across the membrane.

### Bacterial Permeases Are ABC Proteins That Import a Variety of Nutrients from the Environment

As noted earlier, all members of the very large and diverse ABC superfamily of transport proteins contain two transmembrane (T) domains and two cytosolic ATP-binding (A) domains (see Figure 7-6). The T domains, each built of six membrane-spanning  $\alpha$  helices, form the pathway through which the transported substance (substrate) crosses the membrane and determine the substrate specificity of each ABC protein. The sequences of the A domains are  $\approx 30$ –40 percent homologous in all members of this superfamily, indicating a common evolutionary origin. Some ABC proteins also contain an additional exoplasmic substrate-binding subunit or regulatory subunit.

The plasma membrane of many bacteria contains numerous *permeases* that belong to the ABC superfamily. These proteins use the energy released by hydrolysis of ATP to transport specific amino acids, sugars, vitamins, or even peptides into the cell. Since bacteria frequently grow in soil or pond water where the concentration of nutrients is low, these

ABC transport proteins enable the cells to import nutrients against substantial concentration gradients. Bacterial permeases generally are inducible; that is, the quantity of a transport protein in the cell membrane is regulated by both the concentration of the nutrient in the medium and the metabolic needs of the cell.

In *E. coli* histidine permease, a typical bacterial ABC protein, the two transmembrane domains and two cytosolic ATP-binding domains are formed by four separate subunits. In gram-negative bacteria such as *E. coli*, the outer membrane contains **porins** that render them highly permeable to most small molecules (see Figure 5-14). A soluble histidine-binding protein is located in the periplasmic space between the outer membrane and plasma membrane. This soluble protein binds histidine tightly and directs it to the T subunits of the permease, through which histidine crosses the plasma membrane powered by ATP hydrolysis. Mutant *E. coli* cells that are defective in any of the histidine permease subunits or the soluble binding protein are unable to transport histidine into the cell, but are able to transport other amino acids whose uptake is facilitated by other transport proteins. Such genetic analyses provide strong evidence that histidine permease and similar ABC proteins function to transport various solutes into bacterial cells.

### About 50 ABC Small-Molecule Pumps Are Known in Mammals

Discovery of the first eukaryotic ABC protein to be recognized came from studies on tumor cells and cultured cells that exhibited resistance to several drugs with unrelated chemical structures. Such cells eventually were shown to express elevated levels of a *multidrug-resistance (MDR) transport protein* known as *MDR1*. This protein uses the energy derived from ATP hydrolysis to *export* a large variety of drugs from the cytosol to the extracellular medium. The *Mdr1* gene is frequently amplified in multidrug-resistant cells, resulting in a large overproduction of the MDR1 protein.

Most drugs transported by MDR1 are small hydrophobic molecules that diffuse from the medium across the plasma membrane, unaided by transport proteins, into the cell cytosol, where they block various cellular functions. Two such drugs are colchicine and vinblastine, which block assembly of microtubules. ATP-powered export of such drugs by MDR1 reduces their concentration in the cytosol. As a result, a much higher extracellular drug concentration is required to kill cells that express MDR1 than those that do not. That MDR1 is an ATP-powered small-molecule pump has been demonstrated with liposomes containing the purified protein (see Figure 7-5). The ATPase activity of these liposomes is enhanced by different drugs in a dose-dependent manner corresponding to their ability to be transported by MDR1.

About 50 different mammalian ABC transport proteins are now recognized (see Table 18-2). These are expressed in

abundance in the liver, intestines, and kidney—sites where natural toxic and waste products are removed from the body. Substrates for these ABC proteins include sugars, amino acids, cholesterol, peptides, proteins, toxins, and xenobiotics. Thus the normal function of MDR1 most likely is to transport various natural and metabolic toxins into the bile, intestinal lumen, or forming urine. During the course of its evolution, MDR1 appears to have acquired the ability to transport drugs whose structures are similar to those of these endogenous toxins. Tumors derived from MDR-expressing cell types, such as hepatomas (liver cancers), frequently are resistant to virtually all chemotherapeutic agents and thus difficult to treat, presumably because the tumors exhibit increased expression of the MDR1 or the related MDR2.

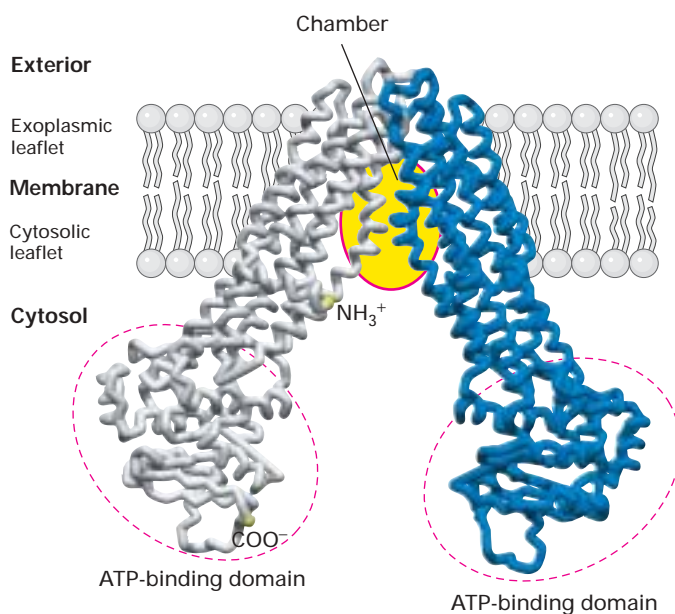


Several human genetic diseases are associated with defective ABC proteins. X-linked adrenoleukodystrophy (ALD), for instance, is characterized by a defective ABC transport protein (ABCD1) that is localized to peroxisomal membranes. This protein normally regulates import of very long chain fatty acids into peroxisomes, where they undergo oxidation; in its absence these fatty acids accumulate in the cytosol and cause cellular damage. Tangiers disease is marked by a deficiency of the plasma-membrane ABC protein (ABCA1) that transports phospholipids and possibly cholesterol (Chapter 18).

A final example is cystic fibrosis (CF), which is caused by a mutation in the gene encoding the *cystic fibrosis transmembrane regulator* (*CFTR*). This  $\text{Cl}^-$  transport protein is expressed in the apical plasma membranes of epithelial cells in the lung, sweat glands, pancreas, and other tissues. For instance, *CFTR* protein is important for reabsorption of  $\text{Cl}^-$  into cells of sweat glands, and babies with cystic fibrosis, if licked, often taste “salty.” An increase in cyclic AMP (cAMP), a small intracellular signaling molecule, causes phosphorylation of *CFTR* and stimulates  $\text{Cl}^-$  transport by such cells from normal individuals, but not from CF individuals who have a defective *CFTR* protein. (The role of cAMP in numerous signaling pathways is covered in Chapter 13.) The sequence and predicted structure of the *CFTR* protein, based on analysis of the cloned gene, are very similar to those of MDR1 protein except for the presence of an additional domain, the regulatory (R) domain, on the cytosolic face. Moreover, the  $\text{Cl}^-$ -transport activity of *CFTR* protein is enhanced by the binding of ATP. Given its similarity to other ABC proteins, *CFTR* may also function as an ATP-powered pump of some still unidentified molecule. ■

### ABC Proteins That Transport Lipid-Soluble Substrates May Operate by a Flippase Mechanism

The substrates of mammalian MDR1 are primarily planar, lipid-soluble molecules with one or more positive charges;

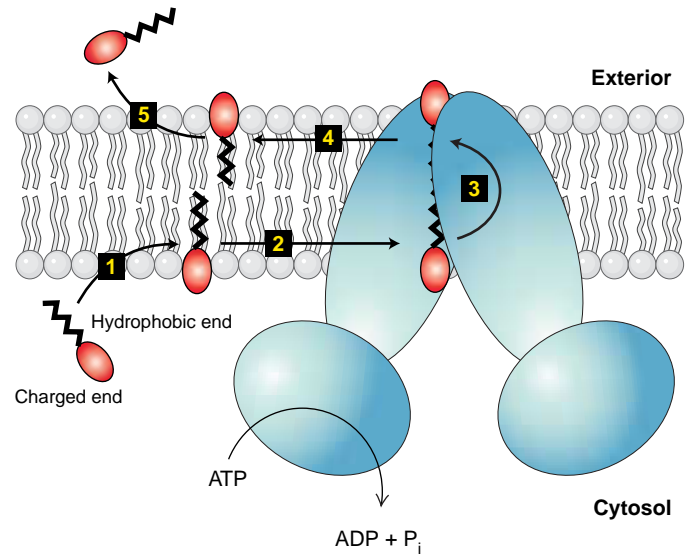


▲ **FIGURE 7-11 Structural model of *E. coli* lipid flippase, an ABC protein homologous to mammalian MDR1.** The V-shaped protein encloses a “chamber” within the bilayer where it is hypothesized that bound substrates are flipped across the membrane, as depicted in Figure 7-12. Each identical subunit in this homodimeric protein has one transmembrane domain, comprising six  $\alpha$  helices, and one cytosolic domain where ATP binding occurs. [Adapted from G. Chang and C. Roth, 2001, *Science* 293:1793.]

they all compete with one another for transport by MDR1, suggesting that they bind to the same site or sites on the protein. In contrast to bacterial ABC proteins, all four domains of MDR1 are fused into a single 170,000-MW protein. The recently determined three-dimensional structure of a homologous *E. coli* lipid-transport protein reveals that the molecule is V shaped, with the apex in the membrane and the arms containing the ATP-binding sites protruding into the cytosol (Figure 7-11).

Although the mechanism of transport by MDR1 and similar ABC proteins has not been definitively demonstrated, a likely candidate is the *flippase model* depicted in Figure 7-12. According to this model, MDR1 “flips” a charged substrate molecule from the cytosolic to the exoplasmic leaflet, an energetically unfavorable reaction powered by the coupled ATPase activity of the protein. Support for the flippase model of transport by MDR1 comes from MDR2, a homologous protein present in the region of the liver cell plasma membrane that faces the bile duct. As detailed in Chapter 18, MDR2 has been shown to flip phospholipids from the cytosolic-facing leaflet of the plasma membrane to the exoplasmic leaflet, thereby generating an excess of phospholipids in the exoplasmic leaflet; these phospholipids then peel off into the bile duct and form an essential part of the bile.

► **FIGURE 7-12 Flippase model of transport by MDR1 and similar ABC proteins.** Step **1**: The hydrophobic portion (black) of a substrate molecule moves spontaneously from the cytosol into the cytosolic-facing leaflet of the lipid bilayer, while the charged end (red) remains in the cytosol. Step **2**: The substrate diffuses laterally until encountering and binding to a site on the MDR1 protein within the bilayer. Step **3**: The protein then “flips” the charged substrate molecule into the exoplasmic leaflet, an energetically unfavorable reaction powered by the coupled hydrolysis of ATP by the cytosolic domain. Steps **4** and **5**: Once in the exoplasmic face, the substrate again can diffuse laterally in the membrane and ultimately moves into the aqueous phase on the outside of the cell. [Adapted from P. Borst, N. Zelcer, and A. van Helvoort, 2000, *Biochim. Biophys. Acta* **1486**:128.]



## KEY CONCEPTS OF SECTION 7.2

### ATP-Powered Pumps and the Intracellular Ionic Environment

- Four classes of transmembrane proteins couple the energy-releasing hydrolysis of ATP with the energy-requiring transport of substances against their concentration gradient: P-, V-, and F-class pumps and ABC proteins (see Figure 7-6).
- The combined action of P-class  $\text{Na}^+/\text{K}^+$  ATPases in the plasma membrane and homologous  $\text{Ca}^{2+}$  ATPases in the plasma membrane or sarcoplasmic reticulum creates the usual ion milieu of animal cells: high  $\text{K}^+$ , low  $\text{Ca}^{2+}$ , and low  $\text{Na}^+$  in the cytosol; low  $\text{K}^+$ , high  $\text{Ca}^{2+}$ , and high  $\text{Na}^+$  in the extracellular fluid.
- In P-class pumps, phosphorylation of the  $\alpha$  (catalytic) subunit and a change in conformational states are essential for coupling ATP hydrolysis to transport of  $\text{H}^+$ ,  $\text{Na}^+$ ,  $\text{K}^+$ , or  $\text{Ca}^{2+}$  ions (see Figures 7-7 and 7-9).
- V- and F-class ATPases, which transport protons exclusively, are large, multisubunit complexes with a proton-conducting channel in the transmembrane domain and ATP-binding sites in the cytosolic domain.
- V-class  $\text{H}^+$  pumps in animal lysosomal and endosomal membranes and plant vacuole membranes are responsible for maintaining a lower pH inside the organelles than in the surrounding cytosol (see Figure 7-10b).
- All members of the large and diverse ABC superfamily of transport proteins contain four core domains: two transmembrane domains, which form a pathway for solute movement and determine substrate specificity, and two cytosolic ATP-binding domains (see Figure 7-11).
- The ABC superfamily includes bacterial amino acid and sugar permeases and about 50 mammalian proteins (e.g.,

MDR1, ABCA1) that transport a wide array of substrates including toxins, drugs, phospholipids, peptides, and proteins.

- According to the flippase model of MDR activity, a substrate molecule diffuses into the cytosolic leaflet of the plasma membrane, then is flipped to the exoplasmic leaflet in an ATP-powered process, and finally diffuses from the membrane into the extracellular space (see Figure 7-12).

## 7.3 Nongated Ion Channels and the Resting Membrane Potential

In addition to ATP-powered ion pumps, which transport ions against their concentration gradients, the plasma membrane contains channel proteins that allow the principal cellular ions ( $\text{Na}^+$ ,  $\text{K}^+$ ,  $\text{Ca}^{2+}$ , and  $\text{Cl}^-$ ) to move through them at different rates down their concentration gradients. Ion concentration gradients generated by pumps and selective movements of ions through channels constitute the principal mechanism by which a difference in voltage, or electric potential, is generated across the plasma membrane. The magnitude of this electric potential generally is  $\approx 70$  millivolts (mV) with the inside of the cell always negative with respect to the outside. This value does not seem like much until we consider the thickness of the plasma membrane (3.5 nm). Thus the voltage gradient across the plasma membrane is 0.07 V per  $3.5 \times 10^{-7}$  cm, or 200,000 volts per centimeter! (To appreciate what this means, consider that high-voltage transmission lines for electricity utilize gradients of about 200,000 volts per kilometer.)

The ionic gradients and electric potential across the plasma membrane play a role in many biological processes. As noted previously, a rise in the cytosolic  $\text{Ca}^{2+}$  concentration is an important regulatory signal, initiating contraction in muscle cells and triggering secretion of digestive enzymes



in the exocrine pancreatic cells. In many animal cells, the combined force of the  $\text{Na}^+$  concentration gradient and membrane electric potential drives the uptake of amino acids and other molecules against their concentration gradient by ion-linked symport and antiport proteins (see Section 7.4). And the conduction of action potentials by nerve cells depends on the opening and closing of ion channels in response to changes in the membrane potential (see Section 7.7).

Here we discuss the origin of the membrane electric potential in resting cells, how ion channels mediate the selective movement of ions across a membrane, and useful experimental techniques for characterizing the functional properties of channel proteins.

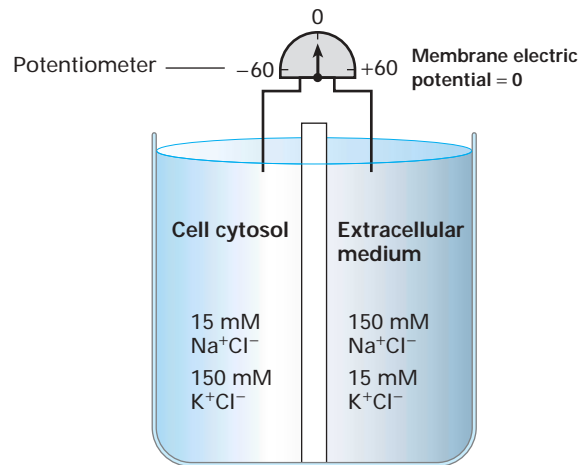
### Selective Movement of Ions Creates a Transmembrane Electric Potential Difference

To help explain how an electric potential across the plasma membrane can arise, we first consider a set of simplified experimental systems in which a membrane separates a 150 mM NaCl/15 mM KCl solution on the right from a 15 mM NaCl/150 mM KCl solution on the left. A potentiometer (voltmeter) is connected to both solutions to measure any difference in electric potential across the membrane. If the membrane is impermeable to all ions, no ions will flow across it and no electric potential will be generated, as shown in Figure 7-13a.

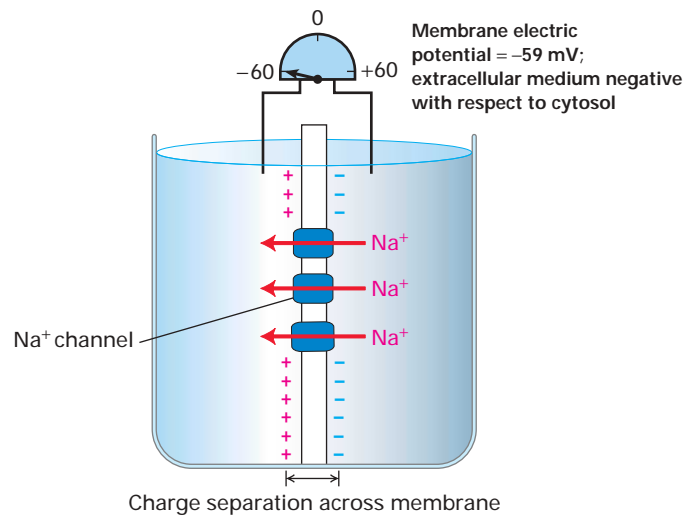
Now suppose that the membrane contains  $\text{Na}^+$ -channel proteins that accommodate  $\text{Na}^+$  ions but exclude  $\text{K}^+$  and  $\text{Cl}^-$  ions (Figure 7-13b).  $\text{Na}^+$  ions then tend to move down their concentration gradient from the right side to the left, leaving an excess of negative  $\text{Cl}^-$  ions compared with  $\text{Na}^+$  ions on the right side and generating an excess of positive  $\text{Na}^+$  ions compared with  $\text{Cl}^-$  ions on the left side. The excess  $\text{Na}^+$  on the left and  $\text{Cl}^-$  on the right remain near the respective surfaces of the membrane because the excess positive charges on one side of the membrane are attracted to the excess negative charges on the other side. The resulting separation of charge across the membrane constitutes an electric

► **EXPERIMENTAL FIGURE 7-13** Generation of a transmembrane electric potential (voltage) depends on the selective movement of ions across a semipermeable membrane. In this experimental system, a membrane separates a 15 mM NaCl/150 mM KCl solution (*left*) from a 150 mM NaCl/15 mM KCl solution (*right*): these ion concentrations are similar to those in cytosol and blood, respectively. If the membrane separating the two solutions is impermeable to all ions (a), no ions can move across the membrane and no difference in electric potential is registered on the potentiometer connecting the two solutions. If the membrane is selectively permeable only to  $\text{Na}^+$  (b) or to  $\text{K}^+$  (c), then diffusion of ions through their respective channels leads to a separation of charge across the membrane. At equilibrium, the membrane potential caused by the charge separation becomes equal to the Nernst potential  $E_{\text{Na}}$  or  $E_{\text{K}}$  registered on the potentiometer. See the text for further explanation.

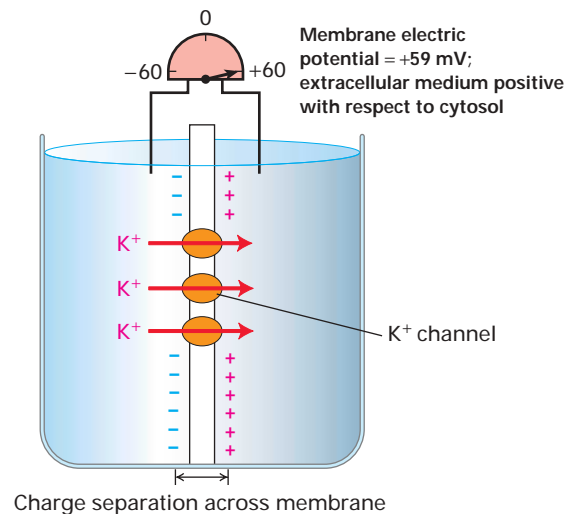
(a) Membrane impermeable to  $\text{Na}^+$ ,  $\text{K}^+$ , and  $\text{Cl}^-$



(b) Membrane permeable only to  $\text{Na}^+$



(c) Membrane permeable only to  $\text{K}^+$



potential, or voltage, with the right side of the membrane having excess negative charge with respect to the left.

As more and more  $\text{Na}^+$  ions move through channels across the membrane, the magnitude of this charge difference (i.e., voltage) increases. However, continued right-to-left movement of the  $\text{Na}^+$  ions eventually is inhibited by the mutual repulsion between the excess positive ( $\text{Na}^+$ ) charges accumulated on the left side of the membrane and by the attraction of  $\text{Na}^+$  ions to the excess negative charges built up on the right side. The system soon reaches an equilibrium point at which the two opposing factors that determine the movement of  $\text{Na}^+$  ions—the membrane electric potential and the ion concentration gradient—balance each other out. At equilibrium, no net movement of  $\text{Na}^+$  ions occurs across the membrane. Thus this *semipermeable* membrane, like all biological membranes, acts like a *capacitor*—a device consisting of a thin sheet of nonconducting material (the hydrophobic interior) surrounded on both sides by electrically conducting material (the polar phospholipid head groups and the ions in the surrounding aqueous solution)—that can store positive charges on one side and negative charges on the other.

If a membrane is permeable only to  $\text{Na}^+$  ions, then at equilibrium the measured electric potential across the membrane equals the sodium equilibrium potential in volts,  $E_{\text{Na}}$ . The magnitude of  $E_{\text{Na}}$  is given by the *Nernst equation*, which is derived from basic principles of physical chemistry:

$$E_{\text{Na}} = \frac{RT}{ZF} \ln \frac{[\text{Na}_i]}{[\text{Na}_o]} \quad (7-2)$$

where  $R$  (the gas constant) = 1.987 cal/(degree · mol), or 8.28 joules/(degree · mol);  $T$  (the absolute temperature in degrees Kelvin) = 293 K at 20 °C;  $Z$  (the charge, also called the valency) here equal to +1;  $F$  (the Faraday constant) 23,062 cal/(mol · V), or 96,000 coulombs/(mol · V); and  $[\text{Na}_i]$  and  $[\text{Na}_o]$  are the  $\text{Na}^+$  concentrations on the left and right sides, respectively, at equilibrium. At 20 °C, Equation 7-2 reduces to

$$E_{\text{Na}} = 0.059 \log_{10} \frac{[\text{Na}_i]}{[\text{Na}_o]} \quad (7-3)$$

If  $[\text{Na}_i]/[\text{Na}_o] = 0.1$ , a tenfold ratio of concentrations as in Figure 7-13b, then  $E_{\text{Na}} = -0.059$  V (or  $-59$  mV), with the right side negative with respect to the left.

If the membrane is permeable only to  $\text{K}^+$  ions and not to  $\text{Na}^+$  or  $\text{Cl}^-$  ions, then a similar equation describes the potassium equilibrium potential  $E_{\text{K}}$ :

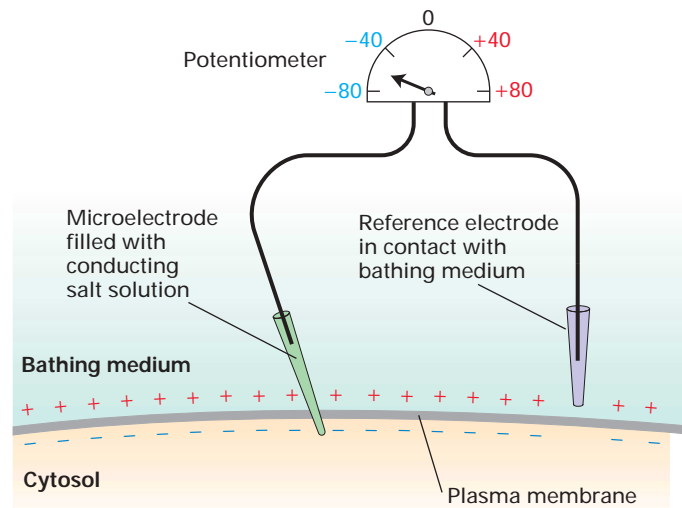
$$E_{\text{K}} = \frac{RT}{ZF} \ln \frac{[\text{K}_i]}{[\text{K}_o]} \quad (7-4)$$

The *magnitude* of the membrane electric potential is the same (59 mV for a tenfold difference in ion concentrations), except that the right side is now *positive* with respect to the left (Figure 7-13c), opposite to the polarity obtained across a membrane selectively permeable to  $\text{Na}^+$  ions.

## The Membrane Potential in Animal Cells Depends Largely on Resting $\text{K}^+$ Channels

The plasma membranes of animal cells contain many open  $\text{K}^+$  channels but few open  $\text{Na}^+$ ,  $\text{Cl}^-$ , or  $\text{Ca}^{2+}$  channels. As a result, the major ionic movement across the plasma membrane is that of  $\text{K}^+$  from the inside outward, powered by the  $\text{K}^+$  concentration gradient, leaving an excess of negative charge on the inside and creating an excess of positive charge on the outside, similar to the experimental system shown in Figure 7-13c. Thus the outward flow of  $\text{K}^+$  ions through these channels, called **resting  $\text{K}^+$  channels**, is the major determinant of the inside-negative membrane potential. Like all channels, these alternate between an open and a closed state, but since their opening and closing are not affected by the membrane potential or by small signaling molecules, these channels are called *nongated*. The various gated channels discussed in later sections open only in response to specific ligands or to changes in membrane potential.

Quantitatively, the usual resting membrane potential of  $-70$  mV is close to but lower in magnitude than that of the potassium equilibrium potential calculated from the Nernst equation because of the presence of a few open  $\text{Na}^+$  channels. These open  $\text{Na}^+$  channels allow the net inward flow of  $\text{Na}^+$  ions, making the cytosolic face of the plasma membrane more positive, that is, less negative, than predicted by the



### ▲ EXPERIMENTAL FIGURE 7-14 The electric potential across the plasma membrane of living cells can be measured.

A microelectrode, constructed by filling a glass tube of extremely small diameter with a conducting fluid such as a KCl solution, is inserted into a cell in such a way that the surface membrane seals itself around the tip of the electrode. A reference electrode is placed in the bathing medium. A potentiometer connecting the two electrodes registers the potential, in this case  $-60$  mV. A potential difference is registered only when the microelectrode is inserted into the cell; no potential is registered if the microelectrode is in the bathing fluid.

Nernst equation for  $K^+$ . The  $K^+$  concentration gradient that drives the flow of ions through resting  $K^+$  channels is generated by the  $Na^+/K^+$  ATPase described previously (see Figure 7-9). In the absence of this pump, or when it is inhibited, the  $K^+$  concentration gradient cannot be maintained and eventually the magnitude of the membrane potential falls to zero.

Although resting  $K^+$  channels play the dominant role in generating the electric potential across the plasma membrane of animal cells, this is not the case in plant and fungal cells. The inside-negative membrane potential in these cells is generated by transport of  $H^+$  ions out of the cell by P-class proton pumps (see Figure 7-10a).

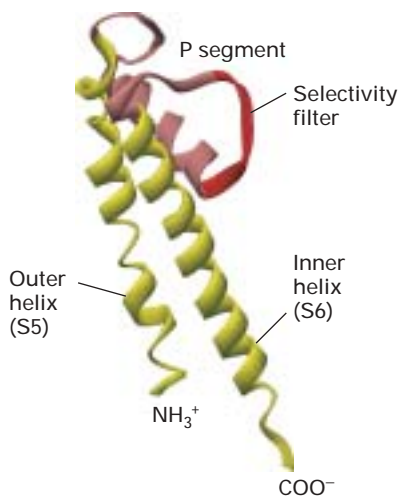
The potential across the plasma membrane of large cells can be measured with a microelectrode inserted inside the cell and a reference electrode placed in the extracellular fluid. The two are connected to a potentiometer capable of measuring small potential differences (Figure 7-14). In virtually all cells the inside (cytosolic face) of the cell membrane is negative relative to the outside; typical membrane potentials range between  $-30$  and  $-70$  mV. The potential across the surface membrane of most animal cells generally does not vary with time. In contrast, neurons and muscle cells—the principal types of electrically active cells—undergo controlled changes in their membrane potential that we discuss later.

### Ion Channels Contain a Selectivity Filter Formed from Conserved Transmembrane $\alpha$ Helices and P Segments

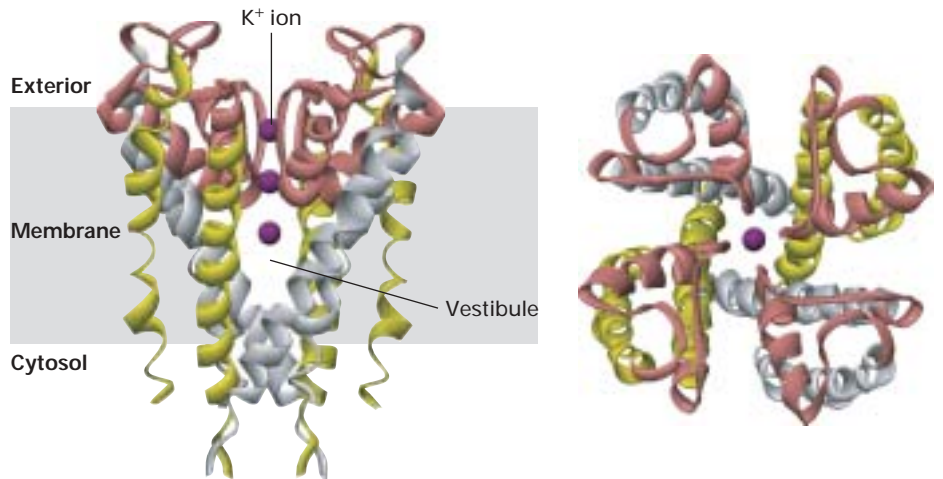
All ion channels exhibit specificity for particular ions:  $K^+$  channels allow  $K^+$  but not closely related  $Na^+$  ions to enter, whereas  $Na^+$  channels admit  $Na^+$  but not  $K^+$ . Determination of the three-dimensional structure of a bacterial  $K^+$  channel first revealed how this exquisite ion selectivity is achieved. As the sequences of other  $K^+$ ,  $Na^+$ , and  $Ca^{2+}$  channels subsequently were determined, it became apparent that all such proteins share a common structure and probably evolved from a single type of channel protein.

Like all other  $K^+$  channels, bacterial  $K^+$  channels are built of four identical subunits symmetrically arranged around a central pore (Figure 7-15). Each subunit contains two membrane-spanning  $\alpha$  helices (S5 and S6) and a short P (pore domain) segment that partly penetrates the membrane bilayer. In the tetrameric  $K^+$  channel, the eight transmembrane  $\alpha$  helices (two from each subunit) form an “inverted teepee,” generating a water-filled cavity called the vestibule in the central portion of the channel. Four extended loops that are part of the P segments form the actual *ion-selectivity filter* in the narrow part of the pore near the exoplasmic surface above the vestibule.

(a) Single subunit



(b) Tetrameric channel



▲ **Figure 7-15 Structure of resting  $K^+$  channel from the bacterium *Streptomyces lividans*.** All  $K^+$  channel proteins are tetramers comprising four identical subunits each containing two conserved membrane-spanning  $\alpha$  helices, called by convention S5 and S6 (yellow), and a shorter P, or pore segment (pink). (a) One of the subunits, viewed from the side, with key structural features indicated. (b) The complete tetrameric channel viewed from the side (*left*) and the top, or extracellular, end (*right*). The P segments are located near the exoplasmic surface and connect the S5 and

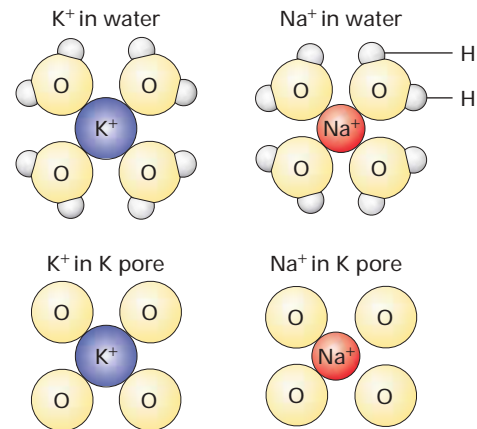
S6  $\alpha$  helices; they consist of a nonhelical “turret,” which lines the upper part of the pore; a short  $\alpha$  helix; and an extended loop that protrudes into the narrowest part of the pore and forms the ion-selectivity filter. This filter allows  $K^+$  (purple spheres) but not other ions to pass. Below the filter is the central cavity or vestibule lined by the inner, or S6  $\alpha$ , helices. The subunits in gated  $K^+$  channels, which open and close in response to specific stimuli, contain additional transmembrane helices not shown here. [See Y. Zhou et al., 2001, *Nature* 414:43.]

Several types of evidence support the role of P segments in ion selection. First, the amino acid sequence of the P segment is highly homologous in all known  $K^+$  channels and different from that in other ion channels. Second, mutation of amino acids in this segment alters the ability of a  $K^+$  channel to distinguish  $Na^+$  from  $K^+$ . Finally, replacing the P segment of a bacterial  $K^+$  channel with the homologous segment from a mammalian  $K^+$  channel yields a chimeric protein that exhibits normal selectivity for  $K^+$  over other ions. Thus all  $K^+$  channels are thought to use the same mechanism to distinguish  $K^+$  over other ions.

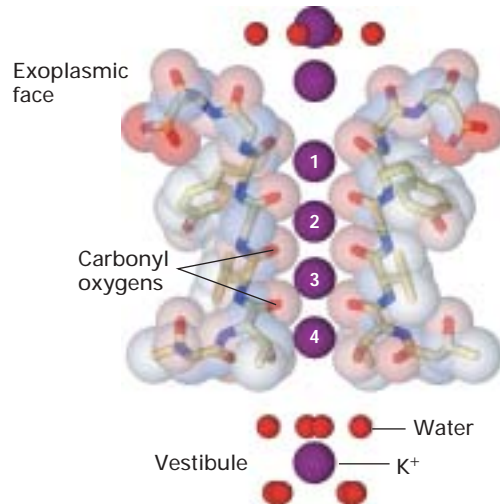
The ability of the ion-selectivity filter in  $K^+$  channels to select  $K^+$  over  $Na^+$  is due mainly to backbone carbonyl oxygens on glycine residues located in a Gly-Tyr-Gly sequence that is found in an analogous position in the P segment in every known  $K^+$  channel. As a  $K^+$  ion enters the narrow selectivity filter, it loses its water of hydration but becomes bound to eight backbone carbonyl oxygens, two from the extended loop in each P segment lining the channel (Figure 7-16a, *left*). As a result, a relatively low activation energy is required for passage of  $K^+$  ions through the channel. Because a dehydrated  $Na^+$  ion is too small to bind to all eight carbonyl oxygens that line the selectivity filter, the activation energy for passage of  $Na^+$  ions is relatively high (Figure 7-16a, *right*). This difference in activation energies favors

► **Figure 7-16 Mechanism of ion selectivity and transport in resting  $K^+$  channels.** (a) Schematic diagrams of  $K^+$  and  $Na^+$  ions hydrated in solution and in the pore of a  $K^+$  channel. As  $K^+$  ions pass through the selectivity filter, they lose their bound water molecules and become coordinated instead to eight backbone carbonyl oxygens, four of which are shown, that are part of the conserved amino acids in the channel-lining loop of each P segment. The smaller  $Na^+$  ions cannot perfectly coordinate with these oxygens and therefore pass through the channel only rarely. (b) High-resolution electron-density map obtained from x-ray crystallography showing  $K^+$  ions (purple spheres) passing through the selectivity filter. Only two of the diagonally opposed channel subunits are shown. Within the selectivity filter each unhydrated  $K^+$  ion interacts with eight carbonyl oxygen atoms (red sticks) lining the channel, two from each of the four subunits, as if to mimic the eight waters of hydration. (c) Interpretation of the electron-density map showing the two alternating states by which  $K^+$  ions move through the channel. In State 1, moving from the exoplasmic side of the channel inward one sees a hydrated  $K^+$  ion with its eight bound water molecules,  $K^+$  ions at positions 1 and 3 within the selectivity filter, and a fully hydrated  $K^+$  ion within the vestibule. During  $K^+$  movement each ion in State 1 moves one step inward, forming State 2. Thus in State 2 the  $K^+$  ion on the exoplasmic side of the channel has lost four of its eight waters, the ion at position 1 in State 1 has moved to position 2, and the ion at position 3 in State 1 has moved to position 4. In going from State 2 to State 1 the  $K^+$  at position 4 moves into the vestibule and picks up eight water molecules, while another hydrated  $K^+$  ion moves into the channel opening and the other  $K^+$  ions move down one step. [Part (a) adapted from C. Armstrong, 1998, *Science* **280**:56. Parts (b) and (c) adapted from Y. Zhou et al., 2001, *Nature* **414**:43.]

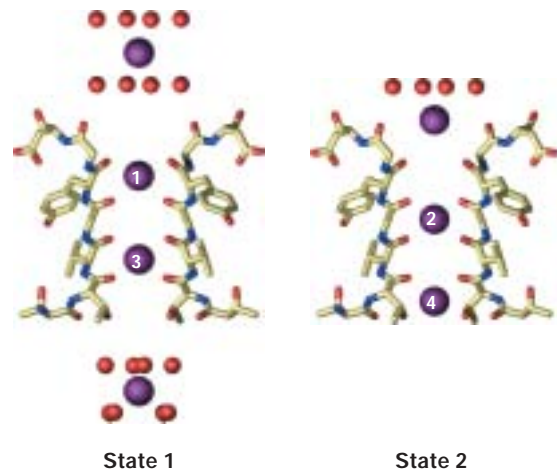
(a)  $K^+$  and  $Na^+$  ions in the pore of a  $K^+$  channel (top view)



(b)  $K^+$  ions in the pore of a  $K^+$  channel (side view)



(c) Ion movement through selectivity filter



passage of  $K^+$  ions over  $Na^+$  by a factor of thousand. Calcium ions are too large to pass through a  $K^+$  channel with or without their bound water.

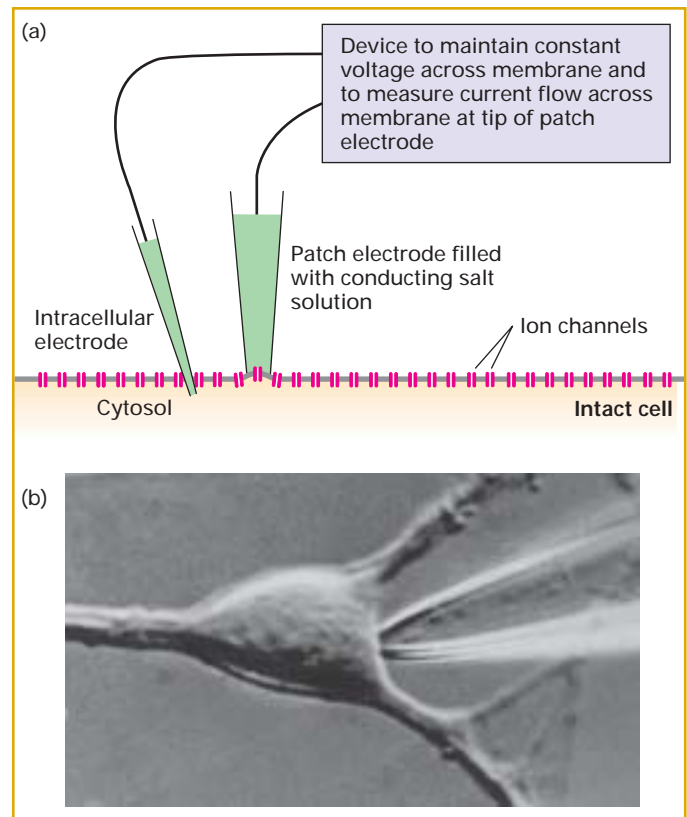
Recent x-ray crystallographic studies reveal that the channel contains  $K^+$  ions within the selectivity filter even when it is closed; without these ions the channel probably would collapse. These ions are thought to be present either at positions 1 and 3 or at 2 and 4, each boxed by eight carbonyl oxygen atoms (Figure 7-16b and c).  $K^+$  ions move simultaneously through the channel such that when the ion on the exoplasmic face that has been partially stripped of its water of hydration moves into position 1, the ion at position 2 jumps to position 3 and the one at position 4 exits the channel (Figure 7-16c).

Although the amino acid sequences of the P segment in  $Na^+$  and  $K^+$  channels differ somewhat, they are similar enough to suggest that the general structure of the ion-selectivity filters are comparable in both types of channels. Presumably the diameter of the filter in  $Na^+$  channels is small enough that it permits dehydrated  $Na^+$  ions to bind to the backbone carbonyl oxygens but excludes the larger  $K^+$  ions from entering.

### Patch Clamps Permit Measurement of Ion Movements Through Single Channels

The technique of **patch clamping** enables workers to investigate the opening, closing, regulation, and ion conductance of a *single* ion channel. In this technique, the inward or outward movement of ions across a patch of membrane is quantified from the amount of electric current needed to maintain the membrane potential at a particular “clamped” value (Figure 7-17a, b). To preserve electroneutrality and to keep the membrane potential constant, the entry of each positive ion (e.g., a  $Na^+$  ion) into the cell through a channel in the patch of membrane is balanced by the addition of an electron

into the cytosol through a microelectrode inserted into the cytosol; an electronic device measures the numbers of electrons (current) required to counterbalance the inflow of ions through the membrane channels. Conversely, the exit of each positive ion from the cell (e.g., a  $K^+$  ion) is balanced by the withdrawal of an electron from the cytosol. The patch-clamping technique can be employed on whole cells or isolated membrane patches to measure the effects of different substances and ion concentrations on ion flow (Figure 7-17c).



► **EXPERIMENTAL FIGURE 7-17** Current flow through individual ion channels can be measured by patch-clamping technique. (a) Basic experimental arrangement for measuring current flow through individual ion channels in the plasma membrane of a living cell. The patch electrode, filled with a current-conducting saline solution, is applied, with a slight suction, to the plasma membrane. The 0.5- $\mu\text{m}$ -diameter tip covers a region that contains only one or a few ion channels. The second electrode is inserted through the membrane into the cytosol. A recording device measures current flow only through the channels in the patch of plasma membrane. (b) Photomicrograph of the cell body of a cultured neuron and the tip of a patch pipette touching the cell membrane. (c) Different patch-clamping configurations. Isolated, detached patches are the best configurations for studying the effects on channels of different ion concentrations and solutes such as extracellular hormones and intracellular second messengers (e.g., cAMP). [Part (b) from B. Sakmann, 1992, *Neuron* 8:613 (Nobel lecture); also published in E. Neher and B. Sakmann, 1992, *Sci. Am.* 266(3):44. Part (c) adapted from B. Hille, 1992, *Ion Channels of Excitable Membranes*, 2d ed., Sinauer Associates, p. 89.]

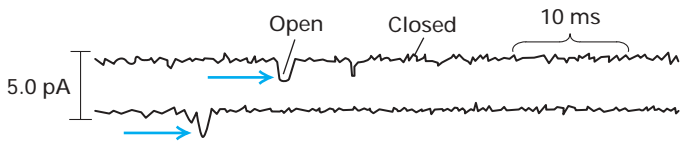
(c) Tip of micropipette  
Ion channel

**On-cell patch** measures indirect effect of extracellular solutes on channels within membrane patch on intact cell

Cytosolic face  
Exoplasmic face

**Inside-out patch** measures effects of intracellular solutes on channels within isolated patch

**Outside-out patch** measures effects of extracellular solutes on channels within isolated patch



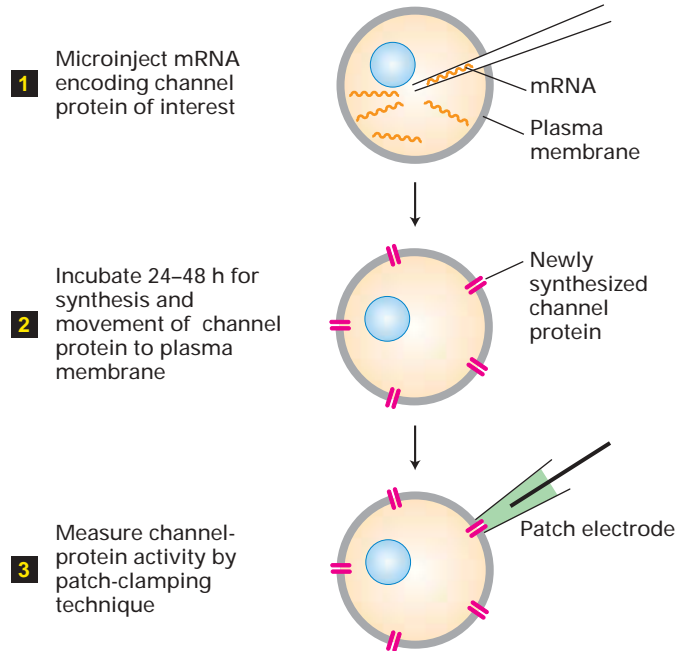
**▲ EXPERIMENTAL FIGURE 7-18 Ion flux through individual Na<sup>+</sup> channels can be calculated from patch-clamp tracings.**

Two inside-out patches of muscle plasma membrane were clamped at a potential of slightly less than that of the resting membrane potential. The patch electrode contained NaCl. The transient pulses of electric current in picoamperes (pA), recorded as large downward deviations (blue arrows), indicate the opening of a Na<sup>+</sup> channel and movement of Na<sup>+</sup> ions inward across the membrane. The smaller deviations in current represent background noise. The average current through an open channel is 1.6 pA, or  $1.6 \times 10^{-12}$  amperes. Since 1 ampere = 1 coulomb (C) of charge per second, this current is equivalent to the movement of about 9900 Na<sup>+</sup> ions per channel per millisecond:  $(1.6 \times 10^{-12} \text{ C/s})(10^{-3} \text{ s/ms})(6 \times 10^{23} \text{ molecules/mol}) \div 96,500 \text{ C/mol}$ . [See F. J. Sigworth and E. Neher, 1980, *Nature* **287**:447.]

The patch-clamp tracings in Figure 7-18 illustrate the use of this technique to study the properties of voltage-gated Na<sup>+</sup> channels in the plasma membrane of muscle cells. As we discuss later, these channels normally are closed in resting muscle cells and open following nervous stimulation. Patches of muscle membrane, each containing one Na<sup>+</sup> channel, were clamped at a voltage slightly less than the resting membrane potential. Under these circumstances, transient pulses of current cross the membrane as individual Na<sup>+</sup> channels open and then close. Each channel is either fully open or completely closed. From such tracings, it is possible to determine the time that a channel is open and the ion flux through it. For the channels measured in Figure 7-18, the flux is about 10 million Na<sup>+</sup> ions per channel per second, a typical value for ion channels. Replacement of the NaCl within the patch pipette (corresponding to the outside of the cell) with KCl or choline chloride abolishes current through the channels, confirming that they conduct only Na<sup>+</sup> ions.

**Novel Ion Channels Can Be Characterized by a Combination of Oocyte Expression and Patch Clamping**

Cloning of human disease-causing genes and sequencing of the human genome have identified many genes encoding putative channel proteins, including 67 putative K<sup>+</sup> channel proteins. One way of characterizing the function of these proteins is to transcribe a cloned cDNA in a cell-free system to produce the corresponding mRNA. Injection of this mRNA into frog oocytes and patch-clamp measurements on the newly synthesized channel protein can often reveal its function (Figure 7-19). This experimental approach is especially useful because frog oocytes normally do not express any channel proteins, so only the channel under study is



**▲ EXPERIMENTAL FIGURE 7-19 Oocyte expression assay is useful in comparing the function of normal and mutant forms of a channel protein.**

A follicular frog oocyte is first treated with collagenase to remove the surrounding follicle cells, leaving a denuded oocyte, which is microinjected with mRNA encoding the channel protein under study. [Adapted from T. P. Smith, 1988, *Trends Neurosci.* **11**:250.]

present in the membrane. In addition, because of the large size of frog oocytes, patch-clamping studies are technically easier to perform on them than on smaller cells.



This approach has provided insight into the underlying defect in polycystic kidney disease, the most common single-gene disorder leading to kidney failure. Mutations in either of two proteins, PKD1 or PKD2, produce the clinical symptoms of polycystic kidney disease in which fluid-filled cysts accumulate throughout the organ. The amino acid sequence of PDK2 is consistent with its being an ion-channel protein, and it contains a conserved P segment. When expressed in oocytes, PDK2 mediates transport of Na<sup>+</sup>, K<sup>+</sup>, and Ca<sup>2+</sup> ions. In contrast, the sequence of PKD1 differs substantially from that of channel proteins, and it has a long extracellular domain that probably binds to a component of the extracellular matrix. Coexpression of PKD1 with PKD2 in frog oocyte eggs modifies the cation-transporting activity of PDK2. These findings provided the first, albeit partial, molecular understanding of cyst formation characteristic of polycystic kidney disease and also suggest that some channel proteins may be regulated in complex ways. Indeed, most Na<sup>+</sup> and K<sup>+</sup> channel proteins are associated with other transmembrane or cytosolic proteins that are thought to regulate their opening, closing, or ion conductivity. ■

## Na<sup>+</sup> Entry into Mammalian Cells Has a Negative Change in Free Energy ( $\Delta G$ )

As mentioned earlier, two forces govern the movement of ions across selectively permeable membranes: the voltage and the ion concentration gradient across the membrane. The sum of these forces, which may act in the same direction or in opposite directions, constitutes the electrochemical gradient. To calculate the **free-energy change**  $\Delta G$  corresponding to the transport of any ion across a membrane, we need to consider the independent contributions from each of the forces to the electrochemical gradient.

For example, when Na<sup>+</sup> moves from outside to inside the cell, the free-energy change generated from the Na<sup>+</sup> concentration gradient is given by

$$\Delta G_c = RT \ln \frac{[\text{Na}_{\text{in}}]}{[\text{Na}_{\text{out}}]} \quad (7-5)$$

At the concentrations of Na<sub>in</sub> and Na<sub>out</sub> shown in Figure 7-20, which are typical for many mammalian cells,  $\Delta G_c$ , the change in free energy due to the concentration gradient, is  $-1.45$  kcal for transport of 1 mol of Na<sup>+</sup> ions from outside to inside the cell, assuming there is no membrane electric potential. The free-energy change generated from the membrane electric potential is given by

$$\Delta G_m = FE \quad (7-6)$$

where  $F$  is the Faraday constant and  $E$  is the membrane electric potential. If  $E = -70$  mV, then  $\Delta G_m$ , the free-energy change due to the membrane potential, is  $-1.61$  kcal for transport of 1 mol of Na<sup>+</sup> ions from outside to inside the cell, assuming there is no Na<sup>+</sup> concentration gradient. Since both forces do in fact act on Na<sup>+</sup> ions, the total  $\Delta G$  is the sum of the two partial values:

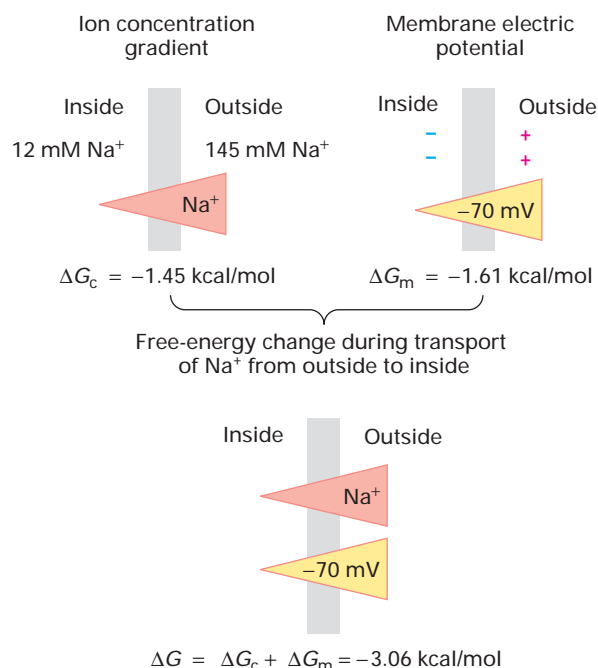
$$\Delta G = \Delta G_c + \Delta G_m = (-1.45) + (-1.61) = -3.06 \text{ kcal/mol}$$

In this example, the Na<sup>+</sup> concentration gradient and the membrane electric potential contribute almost equally to the total  $\Delta G$  for transport of Na<sup>+</sup> ions. Since  $\Delta G$  is  $<0$ , the inward movement of Na<sup>+</sup> ions is thermodynamically favored. As discussed in the next section, certain cotransport proteins use the inward movement of Na<sup>+</sup> to power the uphill movement of other ions and several types of small molecules into or out of animal cells. The rapid, energetically favorable movement of Na<sup>+</sup> ions through gated Na<sup>+</sup> channels also is critical in generating action potentials in nerve and muscle cells.

### KEY CONCEPTS OF SECTION 7.3

#### Nongated Ion Channels and the Resting Membrane Potential

- An inside-negative electric potential (voltage) of 50–70 mV exists across the plasma membrane of all cells.
- In animal cells, the membrane potential is generated primarily by movement of cytosolic K<sup>+</sup> ions through resting



▲ **FIGURE 7-20** Transmembrane forces acting on Na<sup>+</sup> ions. As with all ions, the movement of Na<sup>+</sup> ions across the plasma membrane is governed by the sum of two separate forces—the ion concentration gradient and the membrane electric potential. At the internal and external Na<sup>+</sup> concentrations typical of mammalian cells, these forces usually act in the same direction, making the inward movement of Na<sup>+</sup> ions energetically favorable.

K<sup>+</sup> channels to the external medium. Unlike the more common gated ion channels, which open only in response to various signals, these nongated K<sup>+</sup> channels are usually open.

- In plants and fungi, the membrane potential is maintained by the ATP-driven pumping of protons from the cytosol to the exterior of the cell.
- K<sup>+</sup> channels are assembled from four identical subunits, each of which has at least two conserved membrane-spanning  $\alpha$  helices and a nonhelical P segment that lines the ion pore (see Figure 7-15).
- The ion specificity of K<sup>+</sup> channel proteins is due mainly to coordination of the selected ion with the carbonyl oxygen atoms of specific amino acids in the P segments, thus lowering the activation energy for passage of the selected K<sup>+</sup> compared with other ions (see Figure 7-16).
- Patch-clamping techniques, which permit measurement of ion movements through single channels, are used to determine the ion conductivity of a channel and the effect of various signals on its activity (see Figure 7-17).
- Recombinant DNA techniques and patch clamping allow the expression and functional characterization of channel proteins in frog oocytes (see Figure 7-19).

■ The electrochemical gradient across a semipermeable membrane determines the direction of ion movement through channel proteins. The two forces constituting the electrochemical gradient, the membrane electric potential and the ion concentration gradient, may act in the same or opposite directions (see Figure 7-20).

## 7.4 Cotransport by Symporters and Antiporters

Besides ATP-powered pumps, cells have a second, discrete class of proteins that transport ions and small molecules, such as glucose and amino acids, against a concentration gradient. As noted previously, cotransporters use the energy stored in the electrochemical gradient of  $\text{Na}^+$  or  $\text{H}^+$  ions to power the uphill movement of another substance, which may be a small organic molecule or a different ion. For instance, the energetically favored movement of a  $\text{Na}^+$  ion (the cotransported ion) into a cell across the plasma membrane, driven both by its concentration gradient and by the transmembrane voltage gradient, can be coupled to movement of the transported molecule (e.g., glucose) against its concentration gradient. An important feature of such **cotransport** is that neither molecule can move alone; movement of both molecules together is obligatory, or *coupled*.

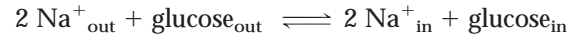
Cotransporters share some features with uniporters such as the GLUT proteins. The two types of transporters exhibit certain structural similarities, operate at equivalent rates, and undergo cyclical conformational changes during transport of their substrates. They differ in that uniporters can only accelerate thermodynamically favorable transport down a concentration gradient, whereas cotransporters can harness the energy of a coupled favorable reaction to actively transport molecules against a concentration gradient.

When the transported molecule and cotransported ion move in the same direction, the process is called **symport**; when they move in opposite directions, the process is called **antiport** (see Figure 7-2). Some cotransporters transport only positive ions (cations), while others transport only negative ions (anions). An important example of a cation cotransporter is the  $\text{Na}^+/\text{H}^+$  *antiporter*, which exports  $\text{H}^+$  from cells coupled to the energetically favorable import of  $\text{Na}^+$ . An example of an anion cotransporter is the *AE1 anion antiporter protein*, which catalyzes the one-for-one exchange of  $\text{Cl}^-$  and  $\text{HCO}_3^-$  across the plasma membrane. Yet other cotransporters mediate movement of both cations and anions together. In this section, we describe the operation and physiological role of several widely distributed symporters and antiporters.

### $\text{Na}^+$ -Linked Symporters Import Amino Acids and Glucose into Animal Cells Against High Concentration Gradients

Most body cells import glucose from the blood down its concentration gradient, utilizing one or another GLUT protein to

facilitate this transport. However, certain cells, such as those lining the small intestine and the kidney tubules, need to import glucose from the intestinal lumen or forming urine against a very large concentration gradient. Such cells utilize a *two- $\text{Na}^+$ /one-glucose symporter*, a protein that couples import of one glucose molecule to the import of two  $\text{Na}^+$  ions:



Quantitatively, the free-energy change for the symport transport of two  $\text{Na}^+$  ions and one glucose molecule can be written

$$\Delta G = RT \ln \frac{[\text{glucose}_{\text{in}}]}{[\text{glucose}_{\text{out}}]} + 2RT \ln \frac{[\text{Na}^+_{\text{in}}]}{[\text{Na}^+_{\text{out}}]} + 2FE \quad (7-7)$$

Thus the  $\Delta G$  for the overall reaction is the sum of the free-energy changes generated by the glucose concentration gradient (1 molecule transported), the  $\text{Na}^+$  concentration gradient (2  $\text{Na}^+$  ions transported), and the membrane potential (2  $\text{Na}^+$  ions transported). At equilibrium  $\Delta G = 0$ . As illustrated in Figure 7-20, the free energy released by movement of  $\text{Na}^+$  into mammalian cells down its electrochemical gradient has a free-energy change  $\Delta G$  of about  $-3$  kcal per mole of  $\text{Na}^+$  transported. Thus the  $\Delta G$  for transport of two moles of  $\text{Na}^+$  inward is about  $-6$  kcal. By substituting this value into Equation 7-7 and setting  $\Delta G = 0$ , we see that

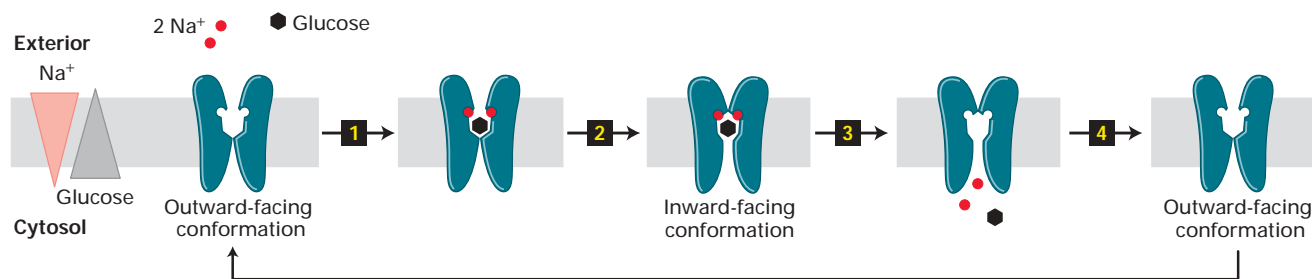
$$0 = RT \ln \frac{[\text{glucose}_{\text{in}}]}{[\text{glucose}_{\text{out}}]} - 6 \text{ kcal}$$

and we can calculate that at equilibrium the ratio  $\text{glucose}_{\text{in}}/\text{glucose}_{\text{out}} = \approx 30,000$ . Thus the inward flow of two moles of  $\text{Na}^+$  can generate an intracellular glucose concentration that is  $\approx 30,000$  times greater than the exterior concentration. If only one  $\text{Na}^+$  ion were imported ( $\Delta G$  of  $-3$  kcal/mol) per glucose molecule, then the available energy could generate a glucose concentration gradient (inside  $>$  outside) of only about 170-fold. Thus by coupling the transport of two  $\text{Na}^+$  ions to the transport of one glucose, the two- $\text{Na}^+$ /one-glucose symporter permits cells to accumulate a very high concentration of glucose relative to the external concentration.

The two- $\text{Na}^+$ /glucose symporter is thought to contain 14 transmembrane  $\alpha$  helices with both its N- and C-termini extending into the cytosol. A truncated recombinant protein consisting of only the five C-terminal transmembrane  $\alpha$  helices can transport glucose independently of  $\text{Na}^+$  across the plasma membrane, *down* its concentration gradient. This portion of the molecule thus functions as a glucose uniporter. The N-terminal portion of the protein, including helices 1–9, is required to couple  $\text{Na}^+$  binding and influx to the transport of glucose against a concentration gradient.

Figure 7-21 depicts the current model of transport by  $\text{Na}^+$ /glucose symporters. This model entails conformational changes in the protein analogous to those that occur in uniporter transporters, such as GLUT1, which do not require a cotransported ion (see Figure 7-4). Binding of all substrates to their sites on the extracellular domain is required before





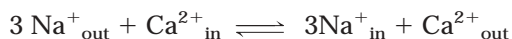
▲ **FIGURE 7-21 Operational model for the two- $\text{Na}^+$ /one-glucose symporter.** Simultaneous binding of  $\text{Na}^+$  and glucose to the conformation with outward-facing binding sites (step **1**) generates a second conformation with inward-facing sites (step **2**). Dissociation of the bound  $\text{Na}^+$  and glucose into the

cytosol (step **3**) allows the protein to revert to its original outward-facing conformation (step **4**), ready to transport additional substrate. [See M. Panayotova-Heiermann et al., 1997, *J. Biol. Chem.* **272**:20324, for details on the structure and function of this and related transporters.]

the protein undergoes the conformational change that changes the substrate-binding sites from outward- to inward-facing; this ensures that inward transport of glucose and  $\text{Na}^+$  ions are coupled.

### $\text{Na}^+$ -Linked Antiporter Exports $\text{Ca}^{2+}$ from Cardiac Muscle Cells

In cardiac muscle cells a *three- $\text{Na}^+$ /one- $\text{Ca}^{2+}$  antiporter*, rather than the plasma membrane  $\text{Ca}^{2+}$  ATPase discussed earlier, plays the principal role in maintaining a low concentration of  $\text{Ca}^{2+}$  in the cytosol. The transport reaction mediated by this *cation antiporter* can be written



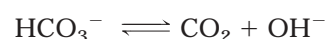
Note that the movement of three  $\text{Na}^+$  ions is required to power the export of one  $\text{Ca}^{2+}$  ion from the cytosol with a  $[\text{Ca}^{2+}]$  of  $\approx 2 \times 10^{-7}$  M to the extracellular medium with a  $[\text{Ca}^{2+}]$  of  $2 \times 10^{-3}$  M, a gradient of some 10,000-fold. As in other muscle cells, a rise in the cytosolic  $\text{Ca}^{2+}$  concentration in cardiac muscle triggers contraction. By lowering cytosolic  $\text{Ca}^{2+}$ , operation of the  $\text{Na}^+/\text{Ca}^{2+}$  antiporter reduces the strength of heart muscle contraction.



The  $\text{Na}^+/\text{K}^+$  ATPase in the plasma membrane of cardiac cells, as in other body cells, creates the  $\text{Na}^+$  concentration gradient necessary for export of  $\text{Ca}^{2+}$  by the  $\text{Na}^+$ -linked  $\text{Ca}^{2+}$  antiporter. As mentioned earlier, inhibition of the  $\text{Na}^+/\text{K}^+$  ATPase by the drugs ouabain and digoxin lowers the cytosolic  $\text{K}^+$  concentration and, more important, increases cytosolic  $\text{Na}^+$ . The resulting reduced  $\text{Na}^+$  electrochemical gradient across the membrane causes the  $\text{Na}^+$ -linked  $\text{Ca}^{2+}$  antiporter to function less efficiently. As a result, fewer  $\text{Ca}^{2+}$  ions are exported and the cytosolic  $\text{Ca}^{2+}$  concentration increases, causing the muscle to contract more strongly. Because of their ability to increase the force of heart muscle contractions, inhibitors of the  $\text{Na}^+/\text{K}^+$  ATPase are widely used in the treatment of congestive heart failure. ■

### Several Cotransporters Regulate Cytosolic pH

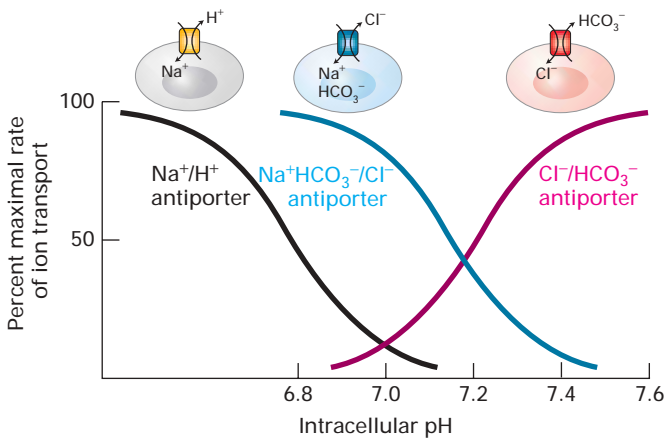
The anaerobic metabolism of glucose yields lactic acid, and aerobic metabolism yields  $\text{CO}_2$ , which adds water to form carbonic acid ( $\text{H}_2\text{CO}_3$ ). These weak acids dissociate, yielding  $\text{H}^+$  ions (protons); if these excess protons were not removed from cells, the cytosolic pH would drop precipitously, endangering cellular functions. Two types of cotransport proteins help remove some of the “excess” protons generated during metabolism in animal cells. One is a  *$\text{Na}^+/\text{HCO}_3^-/\text{Cl}^-$  antiporter*, which imports one  $\text{Na}^+$  ion down its concentration gradient, together with one  $\text{HCO}_3^-$ , in exchange for export of one  $\text{Cl}^-$  ion against its concentration gradient. The cytosolic enzyme *carbonic anhydrase* catalyzes dissociation of the imported  $\text{HCO}_3^-$  ions into  $\text{CO}_2$  and an  $\text{OH}^-$  (hydroxyl) ion:



The  $\text{CO}_2$  diffuses out of the cell, and the  $\text{OH}^-$  ions combine with intracellular protons, forming water. Thus the overall action of this transporter is to consume cytosolic  $\text{H}^+$  ions, thereby raising the cytosolic pH. Also important in raising cytosolic pH is a  *$\text{Na}^+/\text{H}^+$  antiporter*, which couples entry of one  $\text{Na}^+$  ion into the cell down its concentration gradient to the export of one  $\text{H}^+$  ion.

Under certain circumstances the cytosolic pH can rise beyond the normal range of 7.2–7.5. To cope with the excess  $\text{OH}^-$  ions associated with elevated pH, many animal cells utilize an *anion antiporter* that catalyzes the one-for-one exchange of  $\text{HCO}_3^-$  and  $\text{Cl}^-$  across the plasma membrane. At high pH, this  *$\text{Cl}^-/\text{HCO}_3^-$  antiporter* exports  $\text{HCO}_3^-$  (which can be viewed as a “complex” of  $\text{OH}^-$  and  $\text{CO}_2$ ) in exchange for  $\text{Cl}^-$ , thus lowering the cytosolic pH. The import of  $\text{Cl}^-$  down its concentration gradient ( $\text{Cl}^-_{\text{medium}} > \text{Cl}^-_{\text{cytosol}}$ ) powers the reaction.

The activity of all three of these antiport proteins depends on pH, providing cells with a fine-tuned mechanism



▲ **EXPERIMENTAL FIGURE 7-22** The activity of membrane transport proteins that regulate the cytosolic pH of mammalian cells changes with pH. Direction of ion transport is indicated above the curve for each protein. See the text for discussion. [See S. L. Alper et al., 2001, *J. Pancreas* 2:171, and S. L. Alper, 1991, *Ann. Rev. Physiol.* 53:549.]

for controlling the cytosolic pH (Figure 7-22). The two antiporters that operate to increase cytosolic pH are activated when the pH of the cytosol falls. Similarly, a rise in pH above 7.2 stimulates the  $\text{Cl}^-/\text{HCO}_3^-$  antiporter, leading to a more rapid export of  $\text{HCO}_3^-$  and decrease in the cytosolic pH. In this manner the cytosolic pH of growing cells is maintained very close to pH 7.4.

## Numerous Transport Proteins Enable Plant Vacuoles to Accumulate Metabolites and Ions



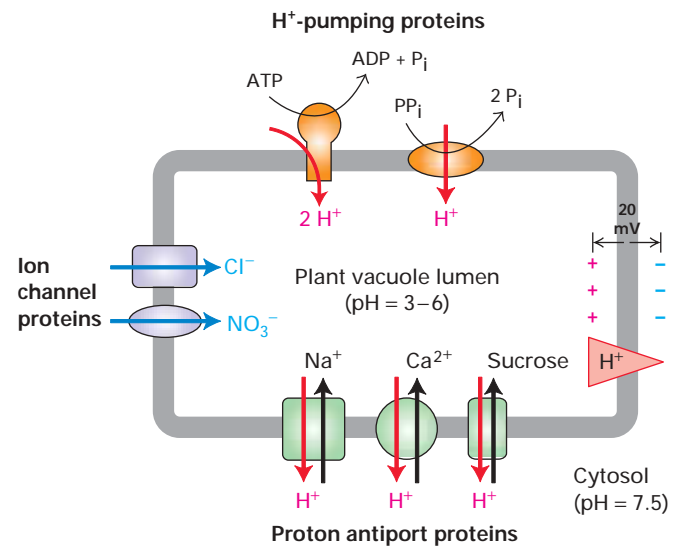
The lumen of plant vacuoles is much more acidic (pH 3 to 6) than is the cytosol (pH 7.5). The acidity of vacuoles is maintained by a V-class ATP-powered proton pump (see Figure 7-6) and by a  $\text{PP}_i$ -powered pump that is unique to plants. Both of these pumps, located in the vacuolar membrane, import  $\text{H}^+$  ions into the vacuolar lumen against a concentration gradient. The vacuolar membrane also contains  $\text{Cl}^-$  and  $\text{NO}_3^-$  channels that transport these anions from the cytosol into the vacuole. Entry of these anions against their concentration gradients is driven by the inside-positive potential generated by the  $\text{H}^+$  pumps. The combined operation of these proton pumps and anion channels produces an inside-positive electric potential of about 20 mV across the vacuolar membrane and also a substantial pH gradient (Figure 7-23).

The proton electrochemical gradient across the plant vacuole membrane is used in much the same way as the  $\text{Na}^+$  electrochemical gradient across the animal-cell plasma membrane: to power the selective uptake or extrusion of ions and small molecules by various antiporters. In the leaf, for example, excess sucrose generated during photosynthesis in the day is

stored in the vacuole; during the night the stored sucrose moves into the cytoplasm and is metabolized to  $\text{CO}_2$  and  $\text{H}_2\text{O}$  with concomitant generation of ATP from ADP and  $\text{P}_i$ . A *proton/sucrose antiporter* in the vacuolar membrane operates to accumulate sucrose in plant vacuoles. The inward movement of sucrose is powered by the outward movement of  $\text{H}^+$ , which is favored by its concentration gradient (lumen > cytosol) and by the cytosolic-negative potential across the vacuolar membrane (see Figure 7-23). Uptake of  $\text{Ca}^{2+}$  and  $\text{Na}^+$  into the vacuole from the cytosol against their concentration gradients is similarly mediated by proton antiporters. ■



Understanding of the transport proteins in plant vacuolar membranes has the potential for increasing agricultural production in high-salt ( $\text{NaCl}$ ) soils, which are found throughout the world. Because most agriculturally useful crops cannot grow in such saline soils, agricultural scientists have long sought to develop salt-tolerant plants by traditional breeding methods. With the availability of the cloned gene encoding the vacuolar  $\text{Na}^+/\text{H}^+$  antiporter, researchers can now produce transgenic plants that overexpress this transport protein, leading to in-



▲ **FIGURE 7-23** Concentration of ions and sucrose by the plant vacuole. The vacuolar membrane contains two types of proton pumps (orange): a V-class  $\text{H}^+$  ATPase (left) and a pyrophosphate-hydrolyzing proton pump (right) that differs from all other ion-transport proteins and probably is unique to plants. These pumps generate a low luminal pH as well as an inside-positive electric potential across the vacuolar membrane owing to the inward pumping of  $\text{H}^+$  ions. The inside-positive potential powers the movement of  $\text{Cl}^-$  and  $\text{NO}_3^-$  from the cytosol through separate channel proteins (purple). Proton antiporters (green), powered by the  $\text{H}^+$  gradient, accumulate  $\text{Na}^+$ ,  $\text{Ca}^{2+}$ , and sucrose inside the vacuole. [After P. Rea and D. Sanders, 1987, *Physiol. Plant* 71:131; J. M. Maathuis and D. Sanders, 1992, *Curr. Opin. Cell Biol.* 4:661; P. A. Rea et al., 1992, *Trends Biochem. Sci.* 17:348.]

creased sequestration of  $\text{Na}^+$  in the vacuole. For instance, transgenic tomato plants that overexpress the vacuolar  $\text{Na}^+/\text{H}^+$  antiporter have been shown to grow, flower, and produce fruit in the presence of soil  $\text{NaCl}$  concentrations that kill wild-type plants. Interestingly, although the leaves of these transgenic tomato plants accumulate large amounts of salt, the fruit has a very low salt content. ■

#### KEY CONCEPTS OF SECTION 7.4

##### Cotransport by Symporters and Antiporters

- Cotransporters use the energy released by movement of an ion (usually  $\text{H}^+$  or  $\text{Na}^+$ ) down its electrochemical gradient to power the import or export of a small molecule or different ion against its concentration gradient.
- The cells lining the small intestine and kidney tubules express symport proteins that couple the energetically favorable entry of  $\text{Na}^+$  to the import of glucose and amino acids against their concentration gradients (see Figure 7-21).
- In cardiac muscle cells, the export of  $\text{Ca}^{2+}$  is coupled to and powered by the import of  $\text{Na}^+$  by a cation antiporter, which transports 3  $\text{Na}^+$  ions inward for each  $\text{Ca}^{2+}$  ion exported.
- Two cotransporters that are activated at low pH help maintain the cytosolic pH in animal cells very close to 7.4 despite metabolic production of carbonic and lactic acids. One, a  $\text{Na}^+/\text{H}^+$  antiporter, exports excess protons. The other, a  $\text{Na}^+\text{HCO}_3^-/\text{Cl}^-$  cotransporter, imports  $\text{HCO}_3^-$ , which dissociates in the cytosol to yield pH-raising  $\text{OH}^-$  ions.
- A  $\text{Cl}^-/\text{HCO}_3^-$  antiporter that is activated at high pH functions to export  $\text{HCO}_3^-$  when the cytosolic pH rises above normal, and causes a decrease in pH.
- Uptake of sucrose,  $\text{Na}^+$ ,  $\text{Ca}^{2+}$ , and other substances into plant vacuoles is carried out by proton antiporters in the vacuolar membrane. Ion channels and proton pumps in the membrane are critical in generating a large enough proton concentration gradient to power accumulation of ions and metabolites in vacuoles by these proton antiporters (see Figure 7-23).

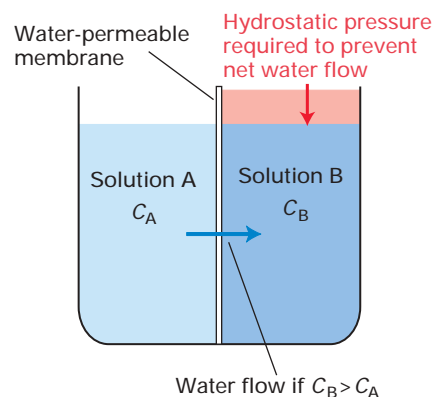
## 7.5 Movement of Water

In this section, we describe the factors that influence the movement of water in and out of cells, an important feature of the life of both plants and animals. The following section discusses other transport phenomena that are critical to essential physiological processes, focusing on the asymmetrical distribution of certain transport proteins in epithelial cells. We will see how this permits absorption of nutrients from the intestinal lumen and acidification of the stomach lumen.

### Osmotic Pressure Causes Water to Move Across Membranes

Water tends to move across a semipermeable membrane from a solution of low solute concentration to one of high concentration, a process termed **osmosis**, or osmotic flow. In other words, since solutions with a high concentration of dissolved solute have a lower concentration of water, water will spontaneously move from a solution of high water concentration to one of lower. In effect, osmosis is equivalent to “diffusion” of water. **Osmotic pressure** is defined as the hydrostatic pressure required to stop the net flow of water across a membrane separating solutions of different compositions (Figure 7-24). In this context, the “membrane” may be a layer of cells or a plasma membrane that is permeable to water but not to the solutes. The osmotic pressure is directly proportional to the difference in the concentration of the total number of solute molecules on each side of the membrane. For example, a 0.5 M  $\text{NaCl}$  solution is actually 0.5 M  $\text{Na}^+$  ions and 0.5 M  $\text{Cl}^-$  ions and has the same osmotic pressure as a 1 M solution of glucose or sucrose.

Pure phospholipid bilayers are essentially impermeable to water, but most cellular membranes contain water-channel proteins that facilitate the rapid movement of water in and out of cells. Such movement of water across the epithelial layer lining the kidney tubules of vertebrates is responsible for concentrating the urine. If this did not happen, one would excrete several liters of urine a day! In higher plants, water and minerals are absorbed from the soil by the roots and move up the plant through conducting tubes (the xylem); water loss from the plant, mainly by evaporation



▲ FIGURE 7-24 **Osmotic pressure.** Solutions A and B are separated by a membrane that is permeable to water but impermeable to all solutes. If  $C_B$  (the total concentration of solutes in solution B) is greater than  $C_A$ , water will tend to flow across the membrane from solution A to solution B. The osmotic pressure  $\pi$  between the solutions is the hydrostatic pressure that would have to be applied to solution B to prevent this water flow. From the van't Hoff equation, osmotic pressure is given by  $\pi = RT(C_B - C_A)$ , where  $R$  is the gas constant and  $T$  is the absolute temperature.

from the leaves, drives these movements of water. The movement of water across the plasma membrane also determines the volume of individual cells, which must be regulated to avoid damage to the cell. In all cases, osmotic pressure is the force powering the movement of water in biological systems.

### Different Cells Have Various Mechanisms for Controlling Cell Volume

When placed in a **hypotonic** solution (i.e., one in which the concentration of solutes is *lower* than in the cytosol), animal cells swell owing to the osmotic flow of water inward. Conversely, when placed in a **hypertonic** solution (i.e., one in which the concentration of solutes is *higher* than in the cytosol), animal cells shrink as cytosolic water leaves the cell by osmotic flow. Consequently, cultured animal cells must be maintained in an **isotonic** medium, which has a solute concentration identical with that of the cell cytosol (see Figure 5-18).

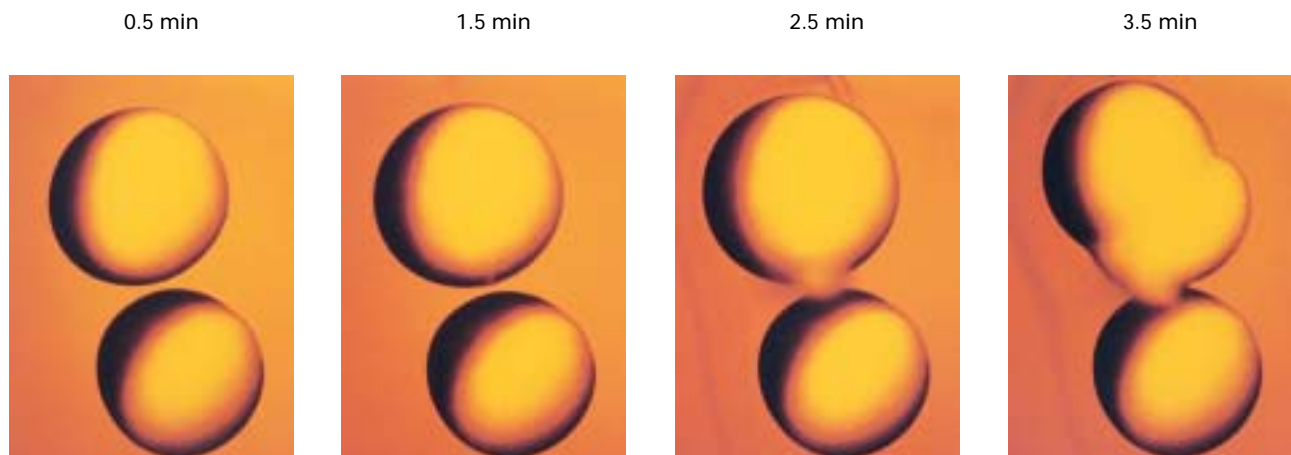
Even in an isotonic environment, however, animal cells face a problem in maintaining their cell volume within a limited range, thereby avoiding lysis. Not only do cells contain a large number of charged macromolecules and small metabolites, which attract oppositely charged ions from the exterior, but there also is a slow inward leakage of extracellular ions, particularly  $\text{Na}^+$  and  $\text{Cl}^-$ , down their concentration gradients. In the absence of some countervailing mechanism, the osmolarity of the cytosol would increase beyond that of the surrounding fluid, causing an osmotic influx of water and eventual cell lysis. To prevent this, animal cells actively export inorganic ions. The net export of cations by the ATP-powered  $\text{Na}^+/\text{K}^+$  pump (3  $\text{Na}^+$  out for 2  $\text{K}^+$  in) plays the major role

in this mechanism for preventing cell swelling. If cultured cells are treated with an inhibitor that prevents production of ATP, they swell and eventually burst, demonstrating the importance of active transport in maintaining cell volume.



Unlike animal cells, plant, algal, fungal, and bacterial cells are surrounded by a rigid cell wall. Because of the cell wall, the osmotic influx of water that occurs when such cells are placed in a hypotonic solution (even pure water) leads to an increase in intracellular pressure but not in cell volume. In plant cells, the concentration of solutes (e.g., sugars and salts) usually is higher in the vacuole than in the cytosol, which in turn has a higher solute concentration than the extracellular space. The osmotic pressure, called **turgor pressure**, generated from the entry of water into the cytosol and then into the vacuole pushes the cytosol and the plasma membrane against the resistant cell wall. Cell elongation during growth occurs by a hormone-induced localized loosening of a region of the cell wall, followed by influx of water into the vacuole, increasing its size. ■

Although most protozoans (like animal cells) do not have a rigid cell wall, many contain a contractile vacuole that permits them to avoid osmotic lysis. A contractile vacuole takes up water from the cytosol and, unlike a plant vacuole, periodically discharges its contents through fusion with the plasma membrane. Thus, even though water continuously enters the protozoan cell by osmotic flow, the contractile vacuole prevents too much water from accumulating in the cell and swelling it to the bursting point.



▲ **EXPERIMENTAL FIGURE 7-25** Expression of aquaporin by frog oocytes increases their permeability to water. Frog oocytes, which normally do not express aquaporin, were microinjected with mRNA encoding aquaporin. These photographs show control oocytes (bottom cell in each panel) and microinjected oocytes (top cell in each panel) at the indicated times after

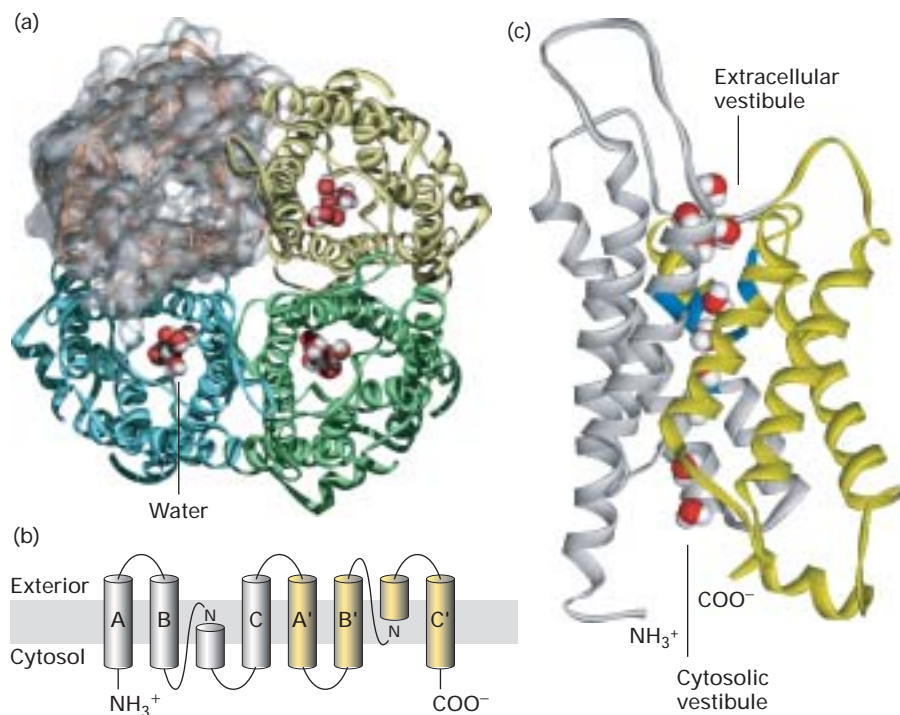
transfer from an isotonic salt solution (0.1 mM) to a hypotonic salt solution (0.035 M). The volume of the control oocytes remained unchanged because they are poorly permeable to water. In contrast, the microinjected oocytes expressing aquaporin swelled because of an osmotic influx of water, indicating that aquaporin is a water-channel protein. [Courtesy of Gregory M. Preston and Peter Agre, Johns Hopkins University School of Medicine.]



## Aquaporins Increase the Water Permeability of Cell Membranes

As just noted, small changes in extracellular osmotic strength cause most animal cells to swell or shrink rapidly. In contrast, frog oocytes and eggs do not swell when placed in pond water of very low osmotic strength even though their internal salt (mainly KCl) concentration is comparable to that of other cells ( $\approx 150$  mM KCl). These observations first led investigators to suspect that the plasma membranes of erythrocytes and other cell types, but not frog oocytes, contain water-channel proteins that accelerate the osmotic flow of water. The experimental results shown in Figure 7-25 demonstrate that the erythrocyte cell-surface protein known as *aquaporin* functions as a water channel.

In its functional form, aquaporin is a tetramer of identical 28-kDa subunits (Figure 7-26a). Each subunit contains six membrane-spanning  $\alpha$  helices that form a central pore through which water moves (Figure 7-26b, c). At its center the  $\approx 2$ -nm-long water-selective gate, or pore, is only 0.28 nm in diameter, which is only slightly larger than the diameter of a water molecule. The molecular sieving properties of the constriction are determined by several conserved hydrophilic amino acid residues whose side-chain and carbonyl groups extend into the middle of the channel. Several water molecules move simultaneously through the channel, each of which sequentially forms specific hydrogen bonds and displaces another water molecule downstream. The formation of hydrogen bonds between the oxygen atom of water and the amino groups of the side chains ensures that only water passes through the channel; even protons cannot pass through.



**▲ FIGURE 7-26 Structure of the water-channel protein aquaporin.** (a) Structural model of the tetrameric protein comprising four identical subunits. Each subunit forms a water channel, as seen in this end-on view from the exoplasmic surface. One of the monomers is shown with a molecular surface in which the pore entrance can be seen. (b) Schematic diagram of the topology of a single aquaporin subunit in relation to the membrane. Three pairs of homologous transmembrane  $\alpha$  helices (A and A', B and B', and C and C') are oriented in the opposite direction with respect to the membrane and are connected by two hydrophilic loops containing short non-membrane-spanning helices and conserved asparagine (N) residues. The loops bend into the cavity formed by the six transmembrane helices, meeting in the middle to form part of

the water-selective gate. (c) Side view of the pore in a single aquaporin subunit in which several water molecules (red oxygens and white hydrogens) are seen within the 2-nm-long water-selective gate that separates the water filled cytosolic and extracellular vestibules. The gate contains highly conserved arginine and histidine residues, as well as the two asparagine residues (blue) whose side chains form hydrogen bonds with transported waters. (Key gate residues are highlighted in blue.) Transported waters also form hydrogen bonds to the main-chain carbonyl group of a cysteine residue. The arrangement of these hydrogen bonds and the narrow pore diameter of 0.28 nm prevent passage of protons (i.e.,  $\text{H}_3\text{O}^+$ ) or other ions. [After H. Sui et al., 2001, *Nature* **414**:872. See also T. Zeuthen, 2001, *Trends Biochem. Sci.* **26**:77, and K. Murata et al., 2000, *Nature* **407**:599.]



As is the case for glucose transporters, mammals express a family of aquaporins. Aquaporin 1 is expressed in abundance in erythrocytes; the homologous aquaporin 2 is found in the kidney epithelial cells that resorb water from the urine. Inactivating mutations in both alleles of the aquaporin 2 gene cause diabetes insipidus, a disease marked by excretion of large volumes of dilute urine. This finding establishes the etiology of the disease and demonstrates that the level of aquaporin 2 is rate-limiting for water transport by the kidney. Other members of the aquaporin family transport hydroxyl-containing molecules such as glycerol rather than water. ■

## KEY CONCEPTS OF SECTION 7.5

### Movement of Water

- Most biological membranes are semipermeable, more permeable to water than to ions or most other solutes. Water moves by osmosis across membranes from a solution of lower solute concentration to one of higher solute concentration.
- Animal cells swell or shrink when placed in hypotonic or hypertonic solutions, respectively. By maintaining the normal osmotic balance inside and outside cells, the  $\text{Na}^+/\text{K}^+$  ATPase and other ion-transporting proteins in the plasma membrane control cell volume.
- The rigid cell wall surrounding plant cells prevents their swelling and leads to generation of turgor pressure in response to the osmotic influx of water.
- In response to the entry of water, protozoans maintain their normal cell volume by extruding water from contractile vacuoles.
- Aquaporins are water-channel proteins that specifically increase the permeability of biomembranes for water (see Figure 7-26). Aquaporin 2 in the plasma membrane of certain kidney cells is essential for resorption of water from the forming urine; its absence leads to a form of diabetes.

## 7.6 Transepithelial Transport

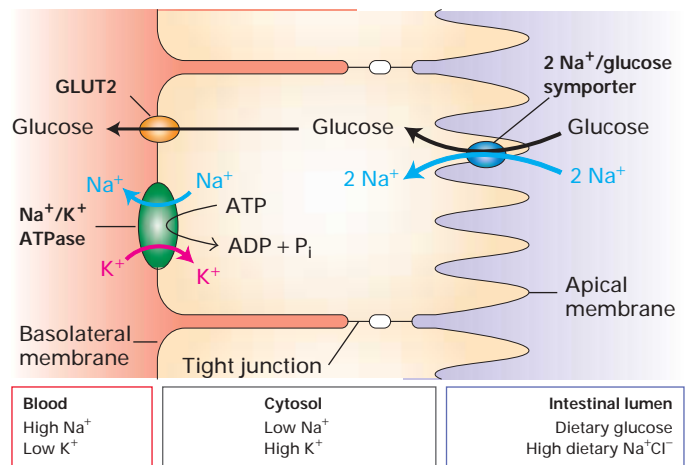
We saw in Chapter 6 that several types of specialized regions of the plasma membrane, called *cell junctions*, connect epithelial cells forming the sheetlike lining of the intestines and other body surfaces (see Figure 6-5). Of concern to us here are **tight junctions**, which prevent water-soluble materials on one side of an epithelium from moving across to the other side through the extracellular space between cells. For this reason, absorption of nutrients from the intestinal lumen occurs by the import of molecules on the luminal side of intestinal epithelial cells and their export on the blood-

facing (serosal) side, a two-stage process called *transcellular transport*.

An intestinal epithelial cell, like all epithelial cells, is said to be **polarized** because the apical and basolateral domains of the plasma membrane contain different sets of proteins. These two plasma-membrane domains are separated by the tight junctions between cells. The apical portion of the plasma membrane, which faces the intestinal lumen, is specialized for absorption of sugars, amino acids, and other molecules that are produced from food by various digestive enzymes. Numerous fingerlike projections (100 nm in diameter) called **microvilli** greatly increase the area of the apical surface and thus the number of transport proteins it can contain, enhancing the cell's absorptive capacity.

### Multiple Transport Proteins Are Needed to Move Glucose and Amino Acids Across Epithelia

Figure 7-27 depicts the proteins that mediate absorption of glucose from the intestinal lumen into the blood. In the first stage of this process, a two- $\text{Na}^+$ /one-glucose symporter located in microvillar membranes imports glucose, against its concentration gradient, from the intestinal lumen across the apical surface of the epithelial cells. As noted above, this symporter couples the energetically unfavorable inward



▲ **FIGURE 7-27 Transcellular transport of glucose from the intestinal lumen into the blood.** The  $\text{Na}^+/\text{K}^+$  ATPase in the basolateral surface membrane generates  $\text{Na}^+$  and  $\text{K}^+$  concentration gradients. The outward movement of  $\text{K}^+$  ions through nongated  $\text{K}^+$  channels (not shown) generates an inside-negative membrane potential. Both the  $\text{Na}^+$  concentration gradient and the membrane potential are used to drive the uptake of glucose from the intestinal lumen by the two- $\text{Na}^+$ /one-glucose symporter located in the apical surface membrane. Glucose leaves the cell via facilitated diffusion catalyzed by GLUT2, a glucose uniporter located in the basolateral membrane.

movement of one glucose molecule to the energetically favorable inward transport of two  $\text{Na}^+$  ions (see Figure 7-21). In the steady state, all the  $\text{Na}^+$  ions transported from the intestinal lumen into the cell during  $\text{Na}^+$ /glucose symport, or the similar process of  $\text{Na}^+$ /amino acid symport, are pumped out across the basolateral membrane, which faces the underlying tissue. Thus the low intracellular  $\text{Na}^+$  concentration is maintained. The  $\text{Na}^+/\text{K}^+$  ATPase that accomplishes this is found exclusively in the basolateral membrane of intestinal epithelial cells. The coordinated operation of these two transport proteins allows uphill movement of glucose and amino acids from the intestine into the cell. This first stage in transcellular transport ultimately is powered by ATP hydrolysis by the  $\text{Na}^+/\text{K}^+$  ATPase.

In the second stage, glucose and amino acids concentrated inside intestinal cells by symporters are exported down their concentration gradients into the blood via uniport proteins in the basolateral membrane. In the case of glucose, this movement is mediated by GLUT2 (see Figure 7-27). As noted earlier, this GLUT isoform has a relatively low affinity for glucose but increases its rate of transport substantially when the glucose gradient across the membrane rises (see Figure 7-3).

The net result of this two-stage process is movement of  $\text{Na}^+$  ions, glucose, and amino acids from the intestinal lumen across the intestinal epithelium into the extracellular medium that surrounds the basolateral surface of intestinal epithelial cells. Tight junctions between the epithelial cells prevent these molecules from diffusing back into the intestinal lumen, and eventually they move into the blood. The increased osmotic pressure created by transcellular transport of salt, glucose, and amino acids across the intestinal epithelium draws water from the intestinal lumen into the extracellular medium that surrounds the basolateral surface. In a sense, salts, glucose, and amino acids “carry” the water along with them.

### Simple Rehydration Therapy Depends on the Osmotic Gradient Created by Absorption of Glucose and $\text{Na}^+$



An understanding of osmosis and the intestinal absorption of salt and glucose forms the basis for a simple therapy that saves millions of lives each year, particularly in less-developed countries. In these countries, cholera and other intestinal pathogens are major causes of death of young children. A toxin released by the bacteria activates chloride secretion by the intestinal epithelial cells into the lumen; water follows osmotically, and the resultant massive loss of water causes diarrhea, dehydration, and ultimately death. A cure demands not only killing the bacteria with antibiotics, but also *rehydration*—replacement of the water that is lost from the blood and other tissues.

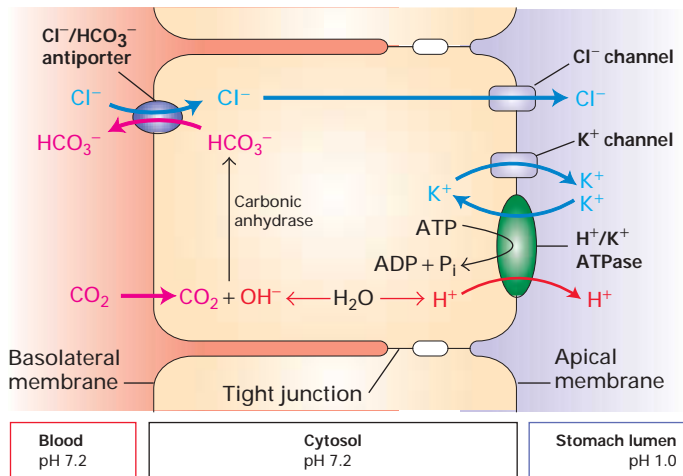
Simply drinking water does not help, because it is excreted from the gastrointestinal tract almost as soon as it enters. However, as we have just learned, the coordinated transport of glucose and  $\text{Na}^+$  across the intestinal epithelium creates a transepithelial osmotic gradient, forcing movement of water from the intestinal lumen across the cell layer. Thus, giving affected children a solution of sugar and salt to drink (but not sugar or salt alone) causes the osmotic flow of water into the blood from the intestinal lumen and leads to rehydration. Similar sugar/salt solutions are the basis of popular drinks used by athletes to get sugar as well as water into the body quickly and efficiently. ■

### Parietal Cells Acidify the Stomach Contents While Maintaining a Neutral Cytosolic pH

The mammalian stomach contains a 0.1 M solution of hydrochloric acid (HCl). This strongly acidic medium kills many ingested pathogens and denatures many ingested proteins before they are degraded by proteolytic enzymes (e.g., pepsin) that function at acidic pH. Hydrochloric acid is secreted into the stomach by specialized epithelial cells called *parietal cells* (also known as *oxyntic cells*) in the gastric lining. These cells contain a  $\text{H}^+/\text{K}^+$  ATPase in their apical membrane, which faces the stomach lumen and generates a millionfold  $\text{H}^+$  concentration gradient:  $\text{pH} = 1.0$  in the stomach lumen versus  $\text{pH} = 7.0$  in the cell cytosol. This transport protein is a P-class ATP-powered ion pump similar in structure and function to the plasma-membrane  $\text{Na}^+/\text{K}^+$  ATPase discussed earlier. The numerous mitochondria in parietal cells produce abundant ATP for use by the  $\text{H}^+/\text{K}^+$  ATPase.

If parietal cells simply exported  $\text{H}^+$  ions in exchange for  $\text{K}^+$  ions, the loss of protons would lead to a rise in the concentration of  $\text{OH}^-$  ions in the cytosol and thus a marked increase in cytosolic pH. (Recall that  $[\text{H}^+] \times [\text{OH}^-]$  always is a constant,  $10^{-14} \text{ M}^2$ .) Parietal cells avoid this rise in cytosolic pH in conjunction with acidification of the stomach lumen by using  $\text{Cl}^-/\text{HCO}_3^-$  antiporters in the basolateral membrane to export the “excess”  $\text{OH}^-$  ions in the cytosol into the blood. As noted earlier, this anion antiporter is activated at high cytosolic pH (see Figure 7-22).

The overall process by which parietal cells acidify the stomach lumen is illustrated in Figure 7-28. In a reaction catalyzed by carbonic anhydrase the “excess” cytosolic  $\text{OH}^-$  combines with  $\text{CO}_2$  that diffuses in from the blood, forming  $\text{HCO}_3^-$ . Catalyzed by the basolateral anion antiporter, this bicarbonate ion is exported across the basolateral membrane (and ultimately into the blood) in exchange for a  $\text{Cl}^-$  ion. The  $\text{Cl}^-$  ions then exit through  $\text{Cl}^-$  channels in the apical membrane, entering the stomach lumen. To preserve electroneutrality, each  $\text{Cl}^-$  ion that moves into the stomach lumen across the apical membrane is accompanied by a  $\text{K}^+$  ion that moves outward through a separate  $\text{K}^+$  channel. In this way, the excess  $\text{K}^+$  ions pumped inward by the  $\text{H}^+/\text{K}^+$



▲ **FIGURE 7-28 Acidification of the stomach lumen by parietal cells in the gastric lining.** The apical membrane of parietal cells contains an  $H^+/K^+$  ATPase (a P-class pump) as well as  $Cl^-$  and  $K^+$  channel proteins. Note the cyclic  $K^+$  transport across the apical membrane:  $K^+$  ions are pumped inward by the  $H^+/K^+$  ATPase and exit via a  $K^+$  channel. The basolateral membrane contains an anion antiporter that exchanges  $HCO_3^-$  and  $Cl^-$  ions. The combined operation of these four different transport proteins and carbonic anhydrase acidifies the stomach lumen while maintaining the neutral pH and electroneutrality of the cytosol. See the text for more details.

ATPase are returned to the stomach lumen, thus maintaining the normal intracellular  $K^+$  concentration. The net result is secretion of equal amounts of  $H^+$  and  $Cl^-$  ions (i.e., HCl) into the stomach lumen, while the pH of the cytosol remains neutral and the excess  $OH^-$  ions, as  $HCO_3^-$ , are transported into the blood.

## KEY CONCEPTS OF SECTION 7.6

### Transepithelial Transport

- The apical and basolateral plasma membrane domains of epithelial cells contain different transport proteins and carry out quite different transport processes.
- In the intestinal epithelial cell, the coordinated operation of  $Na^+$ -linked symporters in the apical membrane with  $Na^+/K^+$  ATPases and uniporters in the basolateral membrane mediates transcellular transport of amino acids and glucose from the intestinal lumen to the blood (see Figure 7-27).
- The combined action of carbonic anhydrase and four different transport proteins permits parietal cells in the stomach lining to secrete HCl into the lumen while maintaining their cytosolic pH near neutrality (see Figure 7-28).

## 7.7 Voltage-Gated Ion Channels and the Propagation of Action Potentials in Nerve Cells

In the previous section, we examined how different transport proteins work together to absorb nutrients across the intestinal epithelium and to acidify the stomach. The nervous system, however, provides the most striking example of the interplay of various ion channels, transporters, and ion pumps in carrying out physiological functions. **Neurons** (nerve cells) and certain muscle cells are specialized to generate and conduct a particular type of electric impulse, the **action potential**. This alteration of the electric potential across the cell membrane is caused by the opening and closing of certain voltage-gated ion channels.

In this section, we first introduce some of the key properties of neurons and action potentials, which move down the axon very rapidly. We then describe how the voltage-gated channels responsible for propagating action potentials in neurons operate. In the following section, we examine how arrival of an action potential at the axon terminus causes secretion of chemicals called **neurotransmitters**. These chemicals, in turn, bind to receptors on adjacent cells and cause changes in the membrane potential of these cells. Thus electric signals carry information within a nerve cell, while chemical signals transmit information from one neuron to another or from a neuron to a muscle or other target cell.

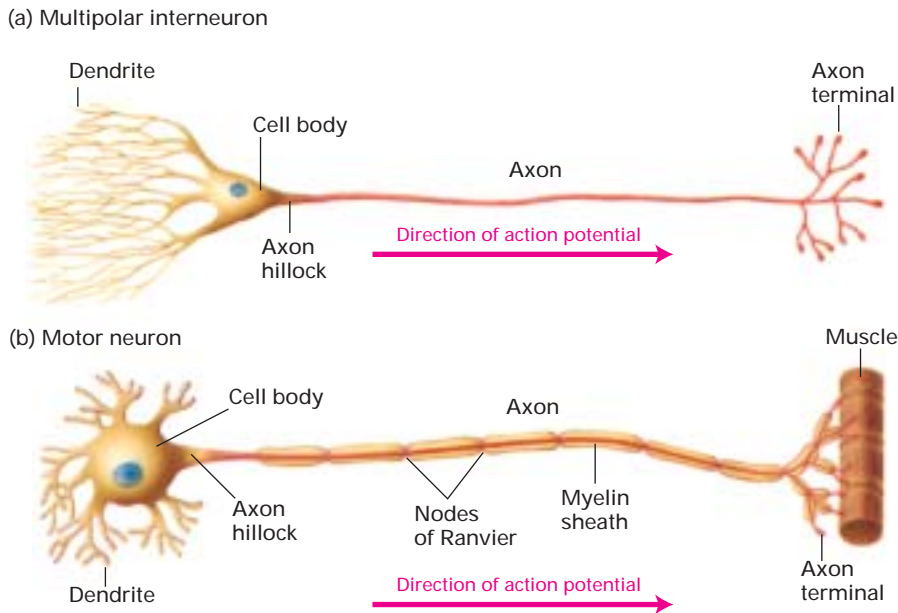
### Specialized Regions of Neurons Carry Out Different Functions

Although the morphology of various types of neurons differs in some respects, they all contain four distinct regions with differing functions: the cell body, the axon, the axon terminals, and the dendrites (Figure 7-29).

The *cell body* contains the nucleus and is the site of synthesis of virtually all neuronal proteins and membranes. Some proteins are synthesized in dendrites, but none are made in axons or axon terminals. Special transport processes involving microtubules move proteins and membranes from their sites of synthesis in the cell body down the length of the axon to the terminals (Chapter 20).

**Axons**, whose diameter varies from a micrometer in certain nerves of the human brain to a millimeter in the giant fiber of the squid, are specialized for conduction of action potentials. An action potential is a series of sudden changes in the voltage, or equivalently the electric potential, across the plasma membrane. When a neuron is in the resting (nonstimulated) state, the electric potential across the axonal membrane is approximately  $-60$  mV (the inside negative relative to the outside); this *resting potential* is similar to that of the membrane potential in most non-neuronal cells. At the peak of an action potential, the membrane potential can be as much as  $+50$  mV (inside positive), a net change of  $\approx 110$  mV.



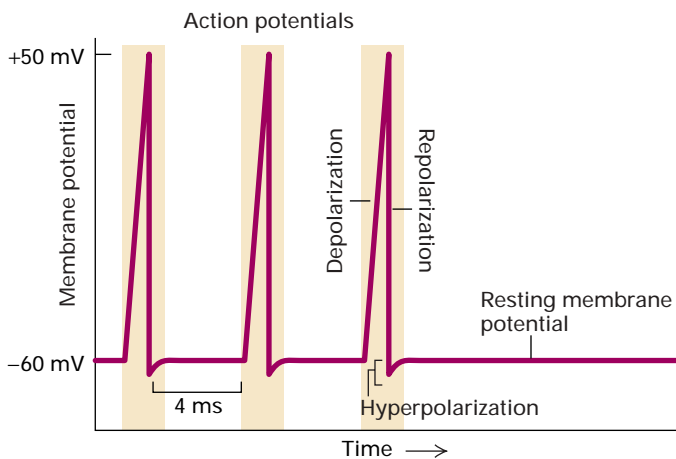


◀ **FIGURE 7-29 Typical morphology of two types of mammalian neurons.**

Action potentials arise in the axon hillock and are conducted toward the axon terminus. (a) A multipolar interneuron has profusely branched dendrites, which receive signals at synapses with several hundred other neurons. A single long axon that branches laterally at its terminus transmits signals to other neurons. (b) A motor neuron innervating a muscle cell typically has a single long axon extending from the cell body to the effector cell. In mammalian motor neurons, an insulating sheath of myelin usually covers all parts of the axon except at the nodes of Ranvier and the axon terminals.

This **depolarization** of the membrane is followed by a rapid repolarization, returning the membrane potential to the resting value (Figure 7-30).

An action potential originates at the *axon hillock*, the junction of the axon and cell body, and is actively conducted down the axon to the *axon terminals*, small branches of the axon that form the **synapses**, or connections, with other cells.

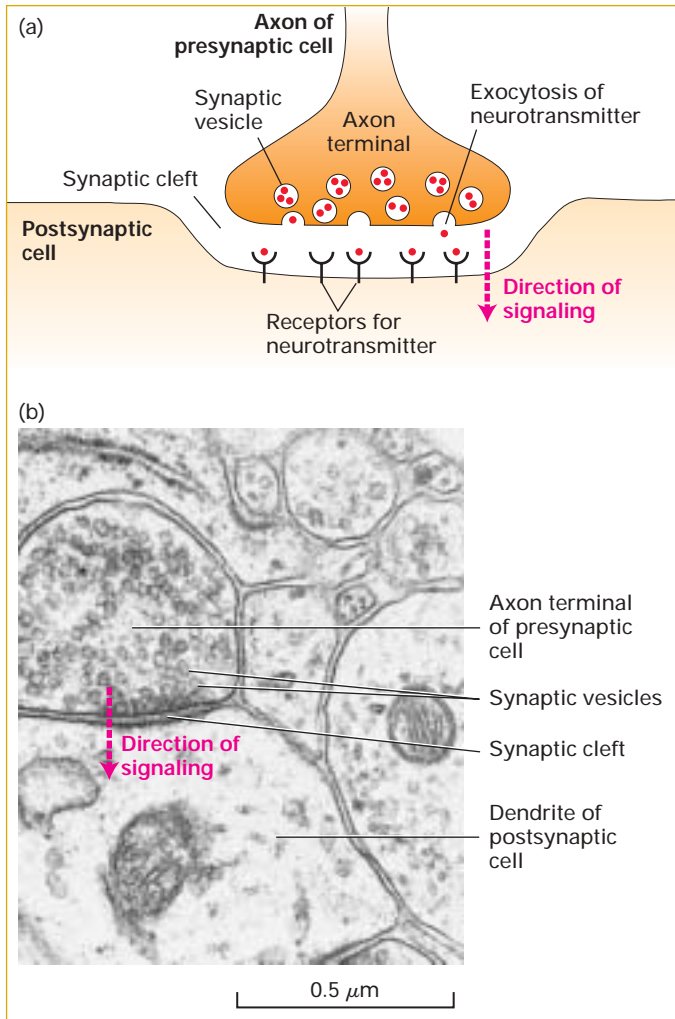


▲ **EXPERIMENTAL FIGURE 7-30 Recording of an axonal membrane potential over time reveals the amplitude and frequency of action potentials.** An action potential is a sudden, transient depolarization of the membrane, followed by repolarization to the resting potential of about  $-60$  mV. The axonal membrane potential can be measured with a small electrode placed into it (see Figure 7-14). This recording of the axonal membrane potential in this neuron shows that it is generating one action potential about every 4 milliseconds.

Action potentials move at speeds up to 100 meters per second. In humans, for instance, axons may be more than a meter long, yet it takes only a few milliseconds for an action potential to move along their length. Arrival of an action potential at an axon terminal leads to opening of voltage-sensitive  $\text{Ca}^{2+}$  channels and an influx of  $\text{Ca}^{2+}$ , causing a localized rise in the cytosolic  $\text{Ca}^{2+}$  concentration in the axon terminus. The rise in  $\text{Ca}^{2+}$  in turn triggers fusion of small vesicles containing neurotransmitters with the plasma membrane, releasing neurotransmitters from this *presynaptic cell* into the synaptic cleft, the narrow space separating it from *postsynaptic cells* (Figure 7-31).

It takes about 0.5 millisecond (ms) for neurotransmitters to diffuse across the synaptic cleft and bind to a receptor on the postsynaptic cells. Binding of neurotransmitter triggers opening or closing of specific ion channels in the plasma membrane of postsynaptic cells, leading to changes in the membrane potential at this point. A single axon in the central nervous system can synapse with many neurons and induce responses in all of them simultaneously.

Most neurons have multiple **dendrites**, which extend outward from the cell body and are specialized to receive chemical signals from the axon termini of other neurons. Dendrites convert these signals into small electric impulses and conduct them toward the cell body. Neuronal cell bodies can also form synapses and thus receive signals. Particularly in the central nervous system, neurons have extremely long dendrites with complex branches. This allows them to form synapses with and receive signals from a large number of other neurons, perhaps up to a thousand (see Figure 7-29a). Membrane depolarizations or hyperpolarizations generated in the dendrites or cell body spread to the axon hillock. If the membrane depolarization at that



**▲ FIGURE 7-31 A chemical synapse.** (a) A narrow region—the synaptic cleft—separates the plasma membranes of the presynaptic and postsynaptic cells. Arrival of action potentials at a synapse causes release of neurotransmitters (red circles) by the presynaptic cell, their diffusion across the synaptic cleft, and their binding by specific receptors on the plasma membrane of the postsynaptic cell. Generally these signals depolarize the postsynaptic membrane (making the potential inside less negative), tending to induce an action potential in it. (b) Electron micrograph shows a dendrite synapsing with an axon terminal filled with synaptic vesicles. In the synaptic region, the plasma membrane of the presynaptic cell is specialized for vesicle exocytosis; synaptic vesicles containing a neurotransmitter are clustered in these regions. The opposing membrane of the postsynaptic cell (in this case, a neuron) contains receptors for the neurotransmitter. [Part (b) from C. Raine et al., eds., 1981, *Basic Neurochemistry*, 3d ed., Little, Brown, p. 32.]

point is great enough, an action potential will originate and will be actively conducted down the axon.

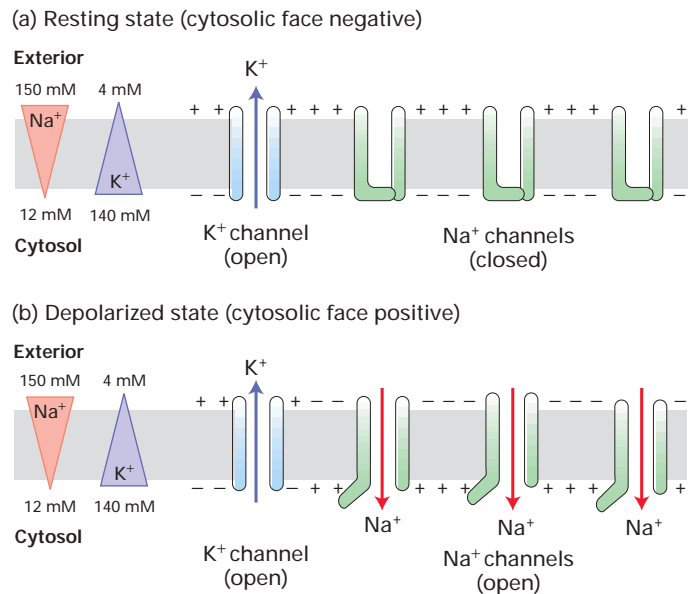
Thus neurons use changes in the membrane potential, the action potentials, to conduct signals along their length, and small molecules, the neurotransmitters, to send signals from cell to cell.

### Magnitude of the Action Potential Is Close to $E_{Na}$

Earlier in this chapter we saw how operation of the  $Na^+/K^+$  pump generates a high concentration of  $K^+$  and a low concentration of  $Na^+$  in the cytosol, relative to those in the extracellular medium. The subsequent outward movement of  $K^+$  ions through nongated  $K^+$  channels is driven by the  $K^+$  concentration gradient (cytosol > medium), generating the resting membrane potential. The entry of  $Na^+$  ions into the cytosol from the medium also is thermodynamically favored, driven by the  $Na^+$  concentration gradient (medium > cytosol) and the inside-negative membrane potential (see Figure 7-20). However, most  $Na^+$  channels in the plasma membrane are closed in resting cells, so little inward movement of  $Na^+$  ions can occur (Figure 7-32a).

If enough  $Na^+$  channels open, the resulting influx of  $Na^+$  ions will overwhelm the efflux of  $K^+$  ions through open resting  $K^+$  channels. The result would be a *net* inward movement of cations, generating an excess of positive charges on the cytosolic face and a corresponding excess of negative charges (due to the  $Cl^-$  ions “left behind” in the extracellular medium after influx of  $Na^+$  ions) on the extracellular face (Figure 7-32b). In other words, the plasma membrane is depolarized to such an extent that the inside face becomes positive.

The magnitude of the membrane potential at the peak of depolarization in an action potential is very close to the  $Na^+$



**▲ FIGURE 7-32 Depolarization of the plasma membrane due to opening of gated  $Na^+$  channels.** (a) In resting neurons, nongated  $K^+$  channels are open, but the more numerous gated  $Na^+$  channels are closed. The movement of  $K^+$  ions outward establishes the inside-negative membrane potential characteristic of most cells. (b) Opening of gated  $Na^+$  channels permits an influx of sufficient  $Na^+$  ions to cause a reversal of the membrane potential. See text for details.

equilibrium potential  $E_{\text{Na}}$  given by the Nernst equation (Equation 7-2), as would be expected if opening of voltage-gated  $\text{Na}^+$  channels is responsible for generating action potentials. For example, the measured peak value of the action potential for the squid giant axon is 35 mV, which is close to the calculated value of  $E_{\text{Na}}$  (55 mV) based on  $\text{Na}^+$  concentrations of 440 mM outside and 50 mM inside. The relationship between the magnitude of the action potential and the concentration of  $\text{Na}^+$  ions inside and outside the cell has been confirmed experimentally. For instance, if the concentration of  $\text{Na}^+$  ions in the solution bathing the squid axon is reduced to one-third of normal, the magnitude of the depolarization is reduced by 40 mV, nearly as predicted.

### Sequential Opening and Closing of Voltage-Gated $\text{Na}^+$ and $\text{K}^+$ Channels Generate Action Potentials

The cycle of membrane depolarization, hyperpolarization, and return to the resting value that constitutes an action potential lasts 1–2 milliseconds and can occur hundreds of times a second in a typical neuron (see Figure 7-30). These cyclical changes in the membrane potential result from the sequential opening and closing first of *voltage-gated  $\text{Na}^+$  channels* and then of *voltage-gated  $\text{K}^+$  channels*. The role of these channels in the generation of action potentials was elucidated in classic studies done on the giant axon of the squid, in which multiple microelectrodes can be inserted without causing damage to the integrity of the plasma membrane. However, the same basic mechanism is used by all neurons.

**Voltage-Gated  $\text{Na}^+$  Channels** As just discussed, voltage-gated  $\text{Na}^+$  channels are closed in resting neurons. A small depolarization of the membrane causes a conformational change in these channel proteins that opens a gate on the cytosolic surface of the pore, permitting  $\text{Na}^+$  ions to pass through the pore into the cell. The greater the initial membrane depolarization, the more voltage-gated  $\text{Na}^+$  channels that open and the more  $\text{Na}^+$  ions enter.

As  $\text{Na}^+$  ions flow inward through opened channels, the excess positive charges on the cytosolic face and negative charges on the exoplasmic face diffuse a short distance away from the initial site of depolarization. This *passive spread* of positive and negative charges depolarizes (makes the inside less negative) adjacent segments of the plasma membrane, causing opening of additional voltage-gated  $\text{Na}^+$  channels in these segments and an increase in  $\text{Na}^+$  influx. As more  $\text{Na}^+$  ions enter the cell, the inside of the cell membrane becomes more depolarized, causing the opening of yet more voltage-gated  $\text{Na}^+$  channels and even more membrane depolarization, setting into motion an explosive entry of  $\text{Na}^+$  ions. For a fraction of a millisecond, the permeability of this region of the membrane to  $\text{Na}^+$  becomes vastly greater than that for  $\text{K}^+$ , and the membrane potential approaches  $E_{\text{Na}}$ , the equilibrium potential for a membrane permeable only to  $\text{Na}^+$  ions. As the membrane potential approaches  $E_{\text{Na}}$ , however, further net inward movement of  $\text{Na}^+$  ions ceases, since the

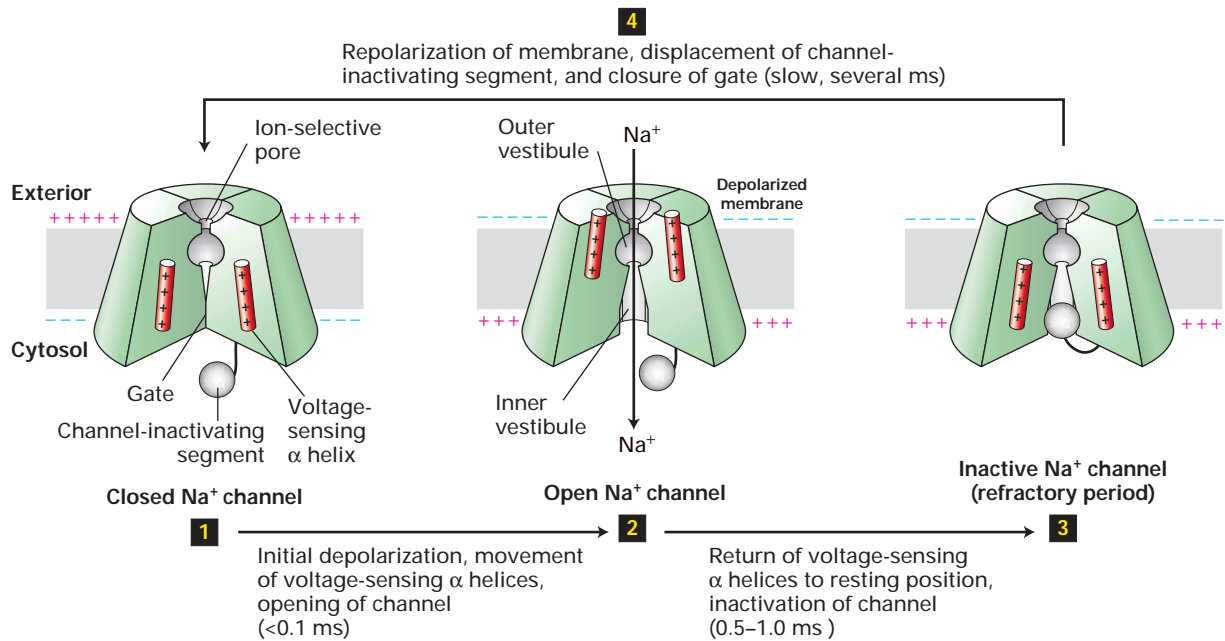
concentration gradient of  $\text{Na}^+$  ions (outside > inside) is now offset by the inside-positive membrane potential  $E_{\text{Na}}$ . The action potential is at its peak, close to the value of  $E_{\text{Na}}$ .

Figure 7-33 schematically depicts the critical structural features of voltage-gated  $\text{Na}^+$  channels and the conformational changes that cause their opening and closing. In the resting state, a segment of the protein on the cytosolic face—the “gate”—obstructs the central pore, preventing passage of ions. A small depolarization of the membrane triggers movement of positively charged *voltage-sensing*  $\alpha$  helices toward the exoplasmic surface, causing a conformational change in the gate that opens the channel and allows ion flow. After about 1 millisecond, further  $\text{Na}^+$  influx is prevented by movement of the cytosol-facing *channel-inactivating segment* into the open channel. As long as the membrane remains depolarized, the channel-inactivating segment remains in the channel opening; during this *refractory period*, the channel is inactivated and cannot be reopened. A few milliseconds after the inside-negative resting potential is reestablished, the channel-inactivating segment swings away from the pore and the channel returns to the closed resting state, once again able to be opened by depolarization.

**Voltage-Gated  $\text{K}^+$  Channels** The repolarization of the membrane that occurs during the refractory period is due largely to opening of voltage-gated  $\text{K}^+$  channels. The subsequent increased efflux of  $\text{K}^+$  from the cytosol removes the excess positive charges from the cytosolic face of the plasma membrane (i.e., makes it more negative), thereby restoring the inside-negative resting potential. Actually, for a brief instant the membrane becomes hyperpolarized, with the potential approaching  $E_{\text{K}}$ , which is more negative than the resting potential (see Figure 7-30).

Opening of the voltage-gated  $\text{K}^+$  channels is induced by the large depolarization of the action potential. Unlike voltage-gated  $\text{Na}^+$  channels, most types of voltage-gated  $\text{K}^+$  channels remain open as long as the membrane is depolarized, and close only when the membrane potential has returned to an inside-negative value. Because the voltage-gated  $\text{K}^+$  channels open slightly after the initial depolarization, at the height of the action potential, they sometimes are called *delayed  $\text{K}^+$  channels*. Eventually all the voltage-gated  $\text{K}^+$  and  $\text{Na}^+$  channels return to their closed resting state. The only open channels in this baseline condition are the nongated  $\text{K}^+$  channels that generate the resting membrane potential, which soon returns to its usual value (see Figure 7-32a).

The patch-clamp tracings in Figure 7-34 reveal the essential properties of voltage-gated  $\text{K}^+$  channels. In this experiment, small segments of a neuronal plasma membrane were held “clamped” at different potentials, and the flux of electric charges through the patch due to flow of  $\text{K}^+$  ions through open  $\text{K}^+$  channels was measured. At the depolarizing voltage of  $-10$  mV, the channels in the membrane patch open infrequently and remain open for only a few milliseconds, as judged, respectively, by the number and width of the “upward blips” on the tracings. Further, the ion flux through

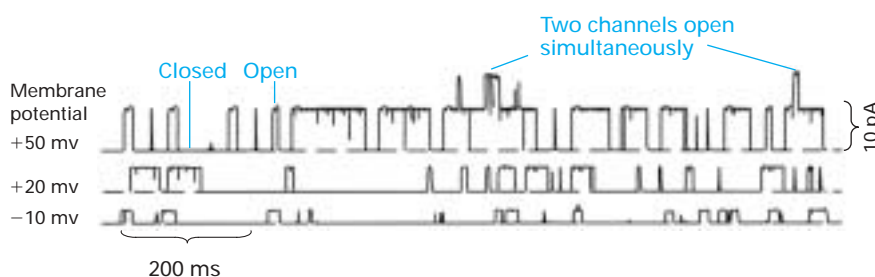


**▲ FIGURE 7-33 Operational model of the voltage-gated  $\text{Na}^+$  channel.** Four transmembrane domains in the protein contribute to the central pore through which ions move. The critical components that control movement of  $\text{Na}^+$  ions are shown here in the cutaway views depicting three of the four transmembrane domains. **1** In the closed, resting state, the voltage-sensing  $\alpha$  helices, which have positively charged side chains every third residue, are attracted to the negative charges on the cytosolic side of the resting membrane. This keeps the gate segment in a position that blocks the channel, preventing entry of  $\text{Na}^+$  ions. **2** In response to a small depolarization, the

voltage-sensing helices rotate in a screwlike manner toward the outer membrane surface, causing an immediate conformational change in the gate segment that opens the channel. **3** The voltage-sensing helices rapidly return to the resting position and the channel-inactivating segment moves into the open channel, preventing passage of further ions. **4** Once the membrane is repolarized, the channel-inactivating segment is displaced from the channel opening and the gate closes; the protein reverts to the closed, resting state and can be opened again by depolarization. [See W. A. Catterall, 2001, *Nature* **409**:988; M. Zhou et al., 2001, *Nature* **411**:657; and B. A. Yi and L. Y. Jan, 2000, *Neuron* **27**:423.]

them is rather small, as measured by the electric current passing through each open channel (the height of the blips). Depolarizing the membrane further to +20 mV causes these channels to open about twice as frequently. Also, more  $\text{K}^+$  ions move through each open channel (the height of the blips is greater) because the force driving cytosolic  $\text{K}^+$  ions out-

ward is greater at a membrane potential of +20 mV than at -10 mV. Depolarizing the membrane further to +50 mV, the value at the peak of an action potential, causes opening of more  $\text{K}^+$  channels and also increases the flux of  $\text{K}^+$  through them. Thus, by opening during the peak of the action potential, these  $\text{K}^+$  channels permit the outward movement of  $\text{K}^+$



**▲ EXPERIMENTAL FIGURE 7-34 Probability of channel opening and current flux through individual voltage-gated  $\text{K}^+$  channels increases with the extent of membrane depolarization.** These patch-clamp tracings were obtained from patches of neuronal plasma membrane clamped at three different potentials, +50, +20, and -10 mV. The upward deviations in the current indicate the opening of  $\text{K}^+$  channels and movement of  $\text{K}^+$

ions outward (cytosolic to exoplasmic face) across the membrane. Increasing the membrane depolarization (i.e., the clamping voltage) from -10 mV to +50 mV increases the probability a channel will open, the time it stays open, and the amount of electric current (numbers of ions) that pass through it. [From B. Pallota et al., 1981, *Nature* **293**:471, as modified by B. Hille, 1992, *Ion Channels of Excitable Membranes*, 2d ed., Sinauer Associates, p. 122.]

ions and repolarization of the membrane potential while the voltage-gated  $\text{Na}^+$  channels are closed and inactivated.

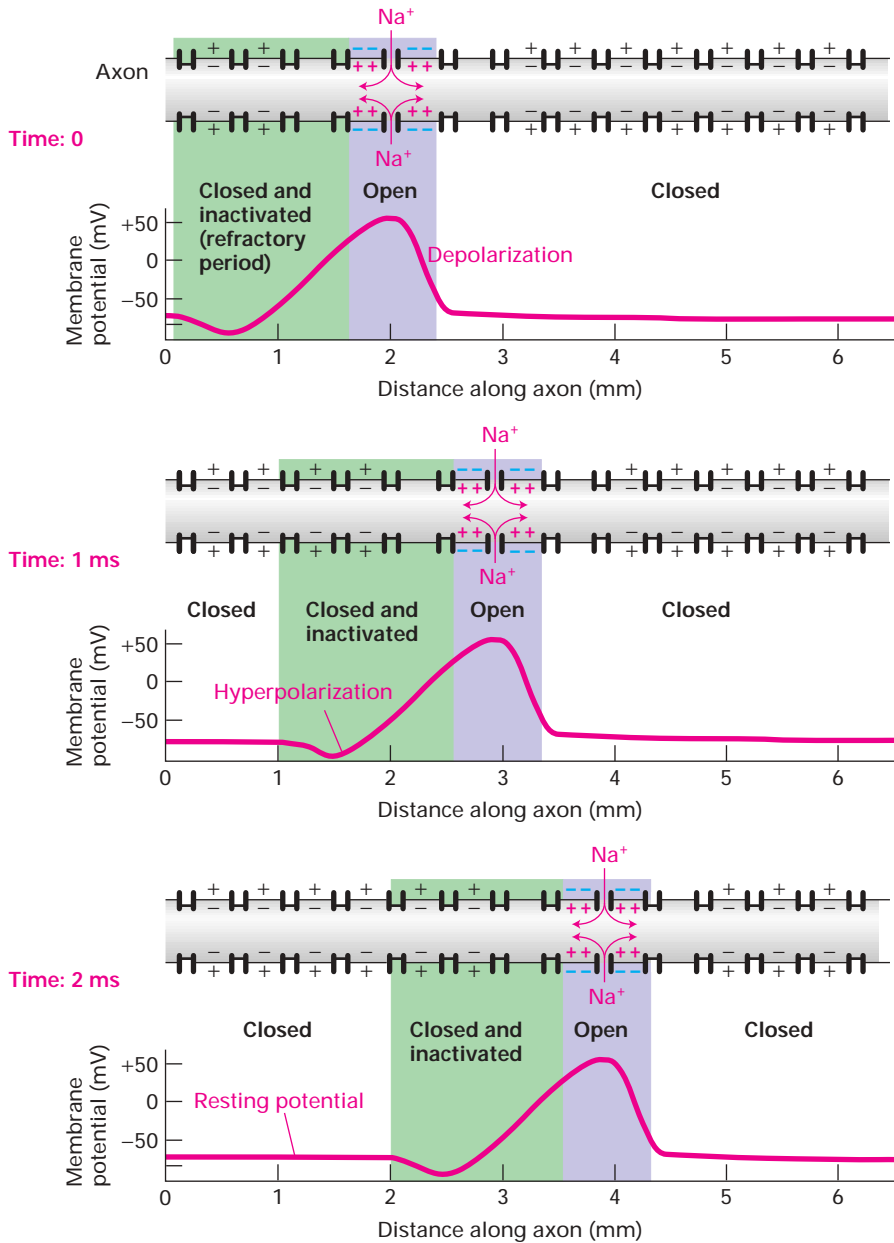
More than 100 voltage-gated  $\text{K}^+$  channel proteins have been isolated from humans and other vertebrates. As we discuss later, all these channel proteins have a similar overall structure, but they exhibit different voltage dependencies, conductivities, channel kinetics, and other functional properties. However, many open only at strongly depolarizing voltages, a property required for generation of the maximal depolarization characteristic of the action potential before repolarization of the membrane begins.

### Action Potentials Are Propagated Unidirectionally Without Diminution

The generation of an action potential just described relates to the changes that occur in a small patch of the neuronal

plasma membrane. At the peak of the action potential, passive spread of the membrane depolarization is sufficient to depolarize a neighboring segment of membrane. This causes a few voltage-gated  $\text{Na}^+$  channels in this region to open, thereby increasing the extent of depolarization in this region and causing an explosive opening of more  $\text{Na}^+$  channels and generation of an action potential. This depolarization soon triggers opening of voltage-gated  $\text{K}^+$  channels and restoration of the resting potential. The action potential thus spreads as a traveling wave away from its initial site without diminution.

As noted earlier, during the refractory period voltage-gated  $\text{Na}^+$  channels are inactivated for several milliseconds. Such previously opened channels cannot open during this period even if the membrane is depolarized due to passive spread. As illustrated in Figure 7-35, the inability of  $\text{Na}^+$  channels to reopen during the refractory period ensures that



◀ **FIGURE 7-35 Unidirectional conduction of an action potential due to transient inactivation of voltage-gated  $\text{Na}^+$  channels.** At time 0, an action potential (red) is at the 2-mm position on the axon; the  $\text{Na}^+$  channels at this position are open and  $\text{Na}^+$  ions are flowing inward. The excess  $\text{Na}^+$  ions diffuse in both directions along the inside of the membrane, passively spreading the depolarization. Because the  $\text{Na}^+$  channels at the 1-mm position are still inactivated (green), they cannot yet be reopened by the small depolarization caused by passive spread; the  $\text{Na}^+$  channels at the 3-mm position, in contrast, begin to open. Each region of the membrane is refractory (inactive) for a few milliseconds after an action potential has passed. Thus, the depolarization at the 2-mm site at time 0 triggers action potentials downstream only; at 1 ms an action potential is passing the 3-mm position, and at 2 ms, an action potential is passing the 4-mm position.

action potentials are propagated only in one direction, from the axon hillock where they originate to the axon terminus. This property of the  $\text{Na}^+$  channels also limits the number of action potentials per second that a neuron can conduct. Re-opening of  $\text{Na}^+$  channels “upstream” of an action potential (i.e., closer to the cell body) also is delayed by the membrane hyperpolarization that results from opening of voltage-gated  $\text{K}^+$  channels.

### Nerve Cells Can Conduct Many Action Potentials in the Absence of ATP

It is important to note that the depolarization of the membrane characteristic of an action potential results from movement of just a small number of  $\text{Na}^+$  ions into a neuron and does not significantly affect the intracellular  $\text{Na}^+$  concentration gradient. A typical nerve cell has about 10 voltage-gated  $\text{Na}^+$  channels per square micrometer ( $\mu\text{m}^2$ ) of plasma membrane. Since each channel passes  $\approx 5000$ – $10,000$  ions during the millisecond it is open (see Figure 7-18), a maximum of  $10^5$  ions per  $\mu\text{m}^2$  of plasma membrane will move inward during each action potential.

To assess the effect of this ion flux on the cytosolic  $\text{Na}^+$  concentration of 10 mM (0.01 mol/L), typical of a resting axon, we focus on a segment of axon 1 micrometer ( $\mu\text{m}$ ) long and 10  $\mu\text{m}$  in diameter. The volume of this segment is  $78 \mu\text{m}^3$  or  $7.8 \times 10^{-14}$  liters, and it contains  $4.7 \times 10^8$   $\text{Na}^+$  ions:  $(10^{-2} \text{ mol/L}) (7.8 \times 10^{-14} \text{ L}) (6 \times 10^{23} \text{ Na}^+/\text{mol})$ . The surface area of this segment of the axon is  $31 \mu\text{m}^2$ , and during passage of one action potential,  $10^5$   $\text{Na}^+$  ions will enter per  $\mu\text{m}^2$  of membrane. Thus this  $\text{Na}^+$  influx increases the number of  $\text{Na}^+$  ions in this segment by only one part in about 150:  $(4.7 \times 10^8) \div (3.1 \times 10^6)$ . Likewise, the repolarization of the membrane due to the efflux of  $\text{K}^+$  ions through voltage-gated  $\text{K}^+$  channels does not significantly change the intracellular  $\text{K}^+$  concentration.

Because so few  $\text{Na}^+$  and  $\text{K}^+$  ions move across the plasma membrane during each action potential, the  $\text{Na}^+/\text{K}^+$  pump that maintains the usual ion gradients plays no direct role in impulse conduction. When this pump is experimentally inhibited by dinitrophenol or another inhibitor of ATP production, the concentrations of  $\text{Na}^+$  and  $\text{K}^+$  gradually become the same inside and outside the cell, and the membrane potential falls to zero. This elimination of the usual  $\text{Na}^+$  and  $\text{K}^+$  electrochemical gradients occurs extremely slowly in large squid neurons but takes about 5 minutes in smaller mammalian neurons. In either case, the electrochemical gradients are essentially independent of the supply of ATP over the short time spans required for nerve cells to generate and conduct action potentials. Since the ion movements during each action potential involve only a minute fraction of the cell's  $\text{K}^+$  and  $\text{Na}^+$  ions, a nerve cell can fire hundreds or even thousands of times in the absence of ATP.

### All Voltage-Gated Ion Channels Have Similar Structures

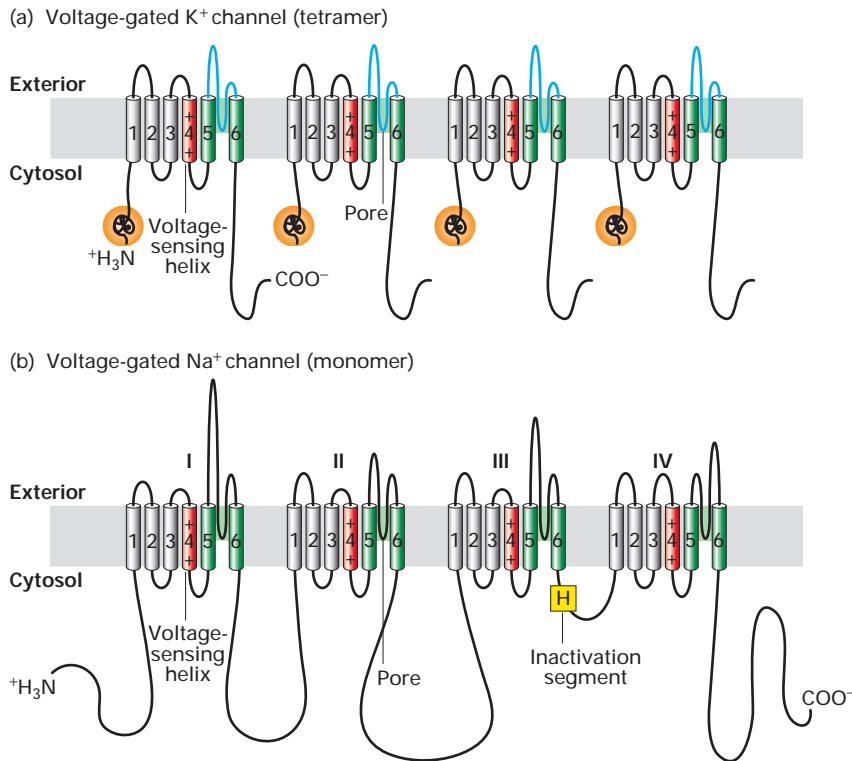
Having explained how the action potential is dependent on regulated opening and closing of voltage-gated channels, we turn to a molecular dissection of these remarkable proteins. After describing the basic structure of these channels, we focus on three questions:

- How do these proteins sense changes in membrane potential?
- How is this change transduced into opening of the channel?
- What causes these channels to become inactivated shortly after opening?

The initial breakthrough in understanding voltage-gated ion channels came from analysis of fruit flies (*Drosophila melanogaster*) carrying the *shaker* mutation. These flies shake vigorously under ether anesthesia, reflecting a loss of motor control and a defect in certain motor neurons that have an abnormally prolonged action potential. This phenotype suggested that the *shaker* mutation causes a defect in voltage-gated  $\text{K}^+$  channels that prevents them from opening normally immediately upon depolarization. To show that the wild-type *shaker* gene encoded a  $\text{K}^+$  channel, cloned wild-type *shaker* cDNA was used as a template to produce *shaker* mRNA in a cell-free system. Expression of this mRNA in frog oocytes and patch-clamp measurements on the newly synthesized channel protein showed that its functional properties were identical to those of the voltage-gated  $\text{K}^+$  channel in the neuronal membrane, demonstrating conclusively that the *shaker* gene encodes this  $\text{K}^+$ -channel protein.

The Shaker  $\text{K}^+$  channel and most other voltage-gated  $\text{K}^+$  channels that have been identified are tetrameric proteins composed of four identical subunits arranged in the membrane around a central pore. Each subunit is constructed of six membrane-spanning  $\alpha$  helices, designated S1–S6, and a P segment (Figure 7-36a). The S5 and S6 helices and the P segment are structurally and functionally homologous to those in the nongated resting  $\text{K}^+$  channel discussed earlier (see Figure 7-15). The S4 helix, which contains numerous positively charged lysine and arginine residues, acts as a voltage sensor; the N-terminal “ball” extending into the cytosol from S1 is the channel-inactivating segment.

Voltage-gated  $\text{Na}^+$  channels and  $\text{Ca}^{2+}$  channels are monomeric proteins organized into four homologous domains, I–IV (Figure 7-36b). Each of these domains is similar to a subunit of a voltage-gated  $\text{K}^+$  channel. However, in contrast to voltage-gated  $\text{K}^+$  channels, which have four channel-inactivating segments, the monomeric voltage-gated channels have a single channel-inactivating segment. Except for this minor structural difference and their varying ion permeabilities, all voltage-gated ion channels are thought to function in a similar manner and to have evolved from a monomeric ancestral channel protein that contained six transmembrane  $\alpha$  helices.



◀ **FIGURE 7-36 Schematic depictions of the secondary structures of voltage-gated  $K^+$  and  $Na^+$  channels.** (a) Voltage-gated  $K^+$  channels are composed of four identical subunits, each containing 600–700 amino acids, and six membrane-spanning  $\alpha$  helices, S1–S6. The N-terminus of each subunit, located in the cytosol, forms a globular domain (orange ball) essential for inactivation of the open channel. The S5 and S6 helices (green) and the P segment (blue) are homologous to those in nongated resting  $K^+$  channels, but each subunit contains four additional transmembrane  $\alpha$  helices. One of these, S4 (red), is the voltage-sensing  $\alpha$  helix. (b) Voltage-gated  $Na^+$  channels are monomers containing 1800–2000 amino acids organized into four transmembrane domains (I–IV) that are similar to the subunits in voltage-gated  $K^+$  channels. The single channel-inactivating segment, located in the cytosol between domains III and IV, contains a conserved hydrophobic motif (H). Voltage-gated  $Ca^{2+}$  channels have a similar overall structure. Most voltage-gated ion channels also contain regulatory ( $\beta$ ) subunits that are not depicted here. [Part (a) adapted from C. Miller, 1992, *Curr. Biol.* **2**:573, and H. Larsson et al., 1996, *Neuron* **16**:387. Part (b) adapted from W. A. Catterall, 2001, *Nature* **409**:988.]

### Voltage-Sensing S4 $\alpha$ Helices Move in Response to Membrane Depolarization

Sensitive electric measurements suggest that the opening of a voltage-gated  $Na^+$  or  $K^+$  channel is accompanied by the movement of 10 to 12 protein-bound positive charges from the cytosolic to the exoplasmic surface of the membrane; alternatively, a larger number of charges may move a shorter distance across the membrane. The movement of these gating charges (or voltage sensors) under the force of the electric field triggers a conformational change in the protein that opens the channel. The four voltage-sensing S4 transmembrane  $\alpha$  helices, often called *gating helices*, are present in all voltage-gated channels and generally have a positively charged lysine or arginine every third or fourth residue. In the closed resting state, the C-terminal half of each S4 helix is exposed to the cytosol; when the membrane is depolarized, these amino acids move outward, probably rotate 180°, and become exposed to the exoplasmic surface of the channel (see Figure 7-33).

Studies with mutant Shaker  $K^+$  channels support this model for operation of the S4 helix in voltage sensing. When one or more arginine or lysine residues in the S4 helix of the Shaker  $K^+$  channel were replaced with neutral or acidic residues, fewer positive charges than normal moved across the membrane in response to a membrane depolarization, indicating that arginine and lysine residues in the S4 helix do indeed move across the membrane. In other studies, mutant

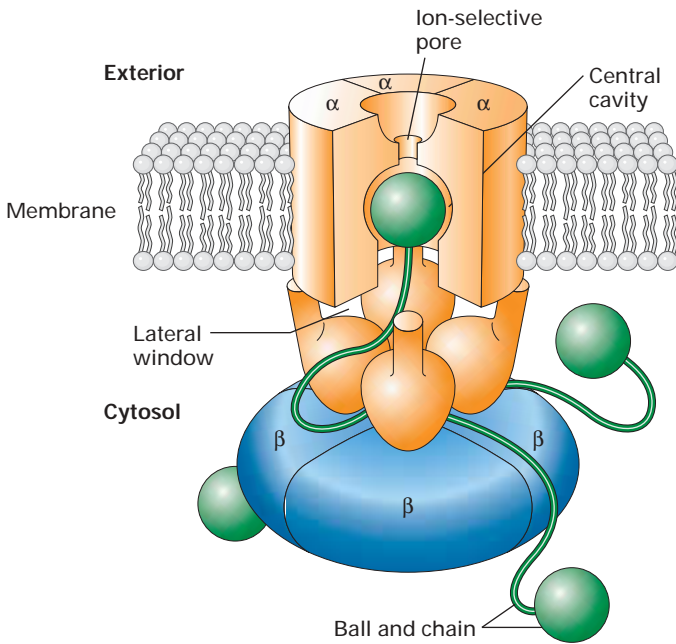
Shaker proteins in which various S4 residues were converted to cysteine were tested for their reactivity with a water-soluble cysteine-modifying chemical agent that cannot cross the membrane. On the basis of whether the cysteines reacted with the agent added to one side or other of the membrane, the results indicated that in the resting state amino acids near the C-terminus of the S4 helix face the cytosol; after the membrane is depolarized, some of these same amino acids become exposed to the exoplasmic surface of the channel. These experiments directly demonstrate movement of the S4 helix across the membrane, as schematically depicted in Figure 7-33 for voltage-gated  $Na^+$  channels.

The gate itself is thought to comprise the cytosolic facing N-termini of the four S5 helices and the C-termini of the four S6 helices (see Figure 7-36). By analogy to the bacterial  $K^+$  channel, the ends of these helices most likely come together just below the actual ion-selectivity filter, thereby blocking the pore in the closed state (see Figure 7-15). X-ray crystallographic studies of bacterial channels indicate that in the open state, the ends of these helices have moved outward, leaving a hole in the middle sufficient for ions to move through. Thus the gates probably are composed of the cytosol-facing ends of the S5 and S6 helices. However, since the molecular structure of no voltage-gated channel has been determined to date, we do not yet know how this putative conformational change is induced by movements of the voltage-sensing S4 helices.

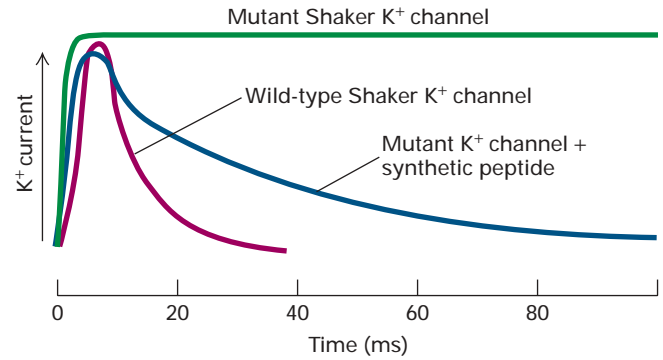
### Movement of the Channel-Inactivating Segment into the Open Pore Blocks Ion Flow

An important characteristic of most voltage-gated channels is inactivation; that is, soon after opening they close spontaneously, forming an inactive channel that will not reopen until the membrane is repolarized. In the resting state, the positively charged globular balls at the N-termini of the four subunits in a voltage-gated  $K^+$  channel are free in the cytosol. Several milliseconds after the channel is opened by depolarization, one ball moves through an opening (“lateral window”) between two of the subunits and binds in a hydrophobic pocket in the pore’s central cavity, blocking the flow of  $K^+$  ions (Figure 7-37). After a few milliseconds, the ball is displaced from the pore, and the protein reverts to the closed, resting state. The ball-and-chain domains in  $K^+$  channels are functionally equivalent to the channel-inactivating segment in  $Na^+$  channels.

The experimental results shown in Figure 7-38 demonstrate that inactivation of  $K^+$  channels depends on the ball domains, occurs after channel opening, and does not require the ball domains to be covalently linked to the channel protein. In other experiments, mutant  $K^+$  channels lacking portions of the  $\approx 40$ -residue chain connecting the ball to the S1 helix were expressed in frog oocytes. Patch-clamp measurements of channel activity showed that the shorter the chain,



▲ FIGURE 7-37 **Ball-and-chain model for inactivation of voltage-gated  $K^+$  channels.** Three-dimensional cutaway view of the channel in the inactive state. The globular domain (green ball) at the terminus of one subunit has moved through a lateral window to block the central pore. In addition to the four  $\alpha$  subunits (orange) that form the channel, these channel proteins also have four regulatory  $\beta$  subunits (blue). See text for discussion. [Adapted from R. Aldrich, 2001, *Nature* 411:643, and M. Zhou et al., 2001, *Nature* 411:657.]



▲ EXPERIMENTAL FIGURE 7-38 **Experiments with a mutant  $K^+$  channel lacking the N-terminal globular domains support the ball-and-chain inactivation model.** The wild-type Shaker  $K^+$  channel and a mutant form lacking the amino acids composing the N-terminal ball were expressed in *Xenopus* oocytes. The activity of the channels then was monitored by the patch-clamp technique. When patches were depolarized from  $-0$  to  $+30$  mV, the wild-type channel opened for  $\approx 5$  ms and then closed (red curve), whereas the mutant channel opened normally, but could not close (green curve). When a chemically synthesized ball peptide was added to the cytosolic face of the patch, the mutant channel opened normally and then closed (blue curve). This demonstrated that the added peptide inactivated the channel after it opened and that the ball does not have to be tethered to the protein in order to function. [From W. N. Zagotta et al., 1990, *Science* 250:568.]

the more rapid the inactivation, as if a ball attached to a shorter chain can move into the open channel more readily. Conversely, addition of random amino acids to lengthen the normal chain slows channel inactivation.

The single channel-inactivating segment in voltage-gated  $Na^+$  channels contains a conserved hydrophobic motif composed of isoleucine, phenylalanine, methionine, and threonine (see Figure 7-36b). Like the longer ball-and-chain domain in  $K^+$  channels, this segment folds into and blocks the  $Na^+$ -conducting pore until the membrane is repolarized (see Figure 7-33).

### Myelination Increases the Velocity of Impulse Conduction

As we have seen, action potentials can move down an axon without diminution at speeds up to 1 meter per second. But even such fast speeds are insufficient to permit the complex movements typical of animals. In humans, for instance, the cell bodies of motor neurons innervating leg muscles are located in the spinal cord, and the axons are about a meter in length. The coordinated muscle contractions required for walking, running, and similar movements would be impossible if it took one second for an action potential to move from the spinal cord down the axon of a motor neuron to a leg muscle. The presence of a **myelin sheath** around an axon increases the velocity of impulse conduction to 10–100 meters

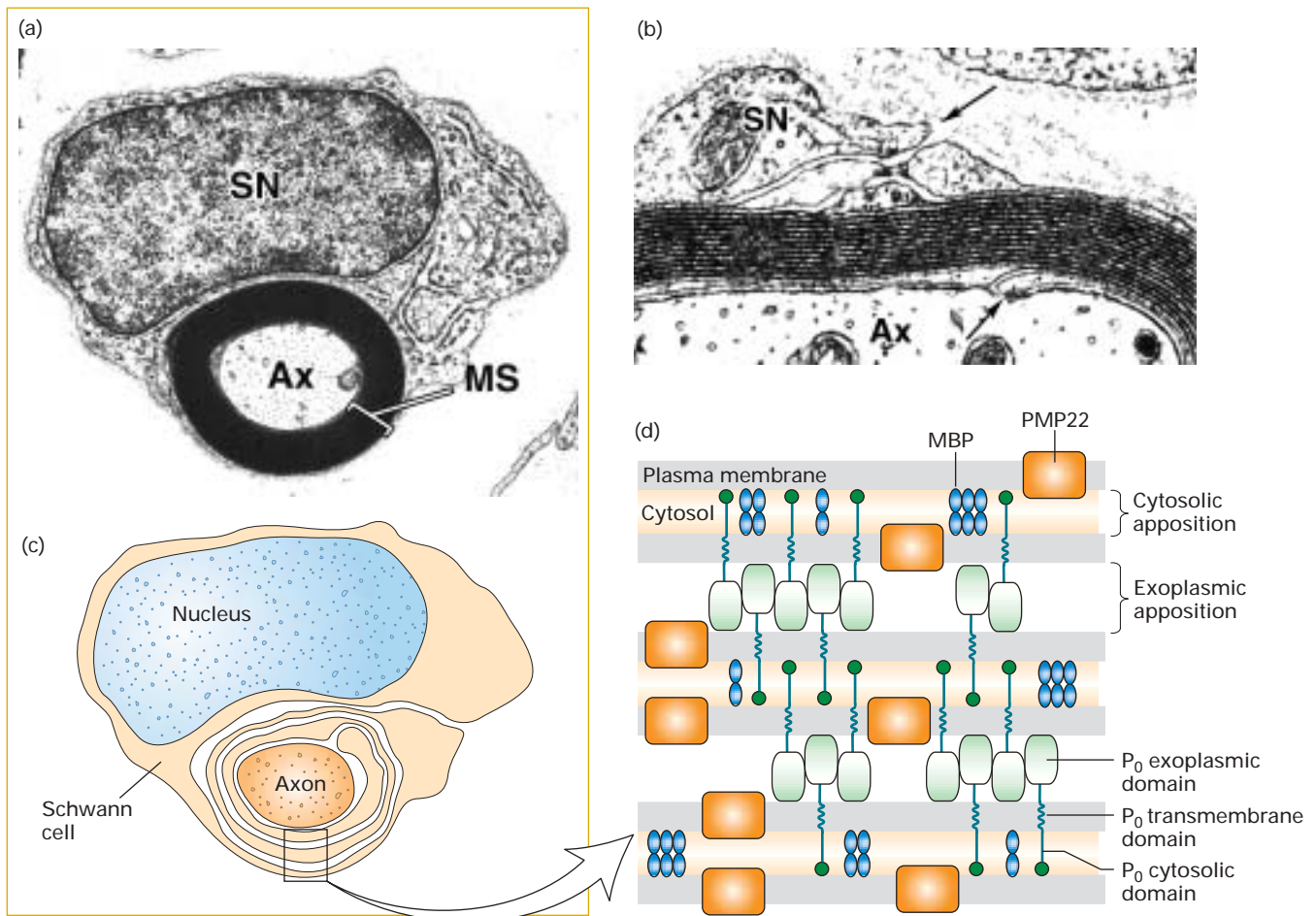


per second. As a result, in a typical human motor neuron, an action potential can travel the length of a 1-meter-long axon and stimulate a muscle to contract within 0.01 seconds.

In nonmyelinated neurons, the conduction velocity of an action potential is roughly proportional to the diameter of the axon, because a thicker axon will have a greater number of ions that can diffuse. The human brain is packed with relatively small, myelinated neurons. If the neurons in the

human brain were not myelinated, their axonal diameters would have to increase about 10,000-fold to achieve the same conduction velocities as myelinated neurons. Thus vertebrate brains, with their densely packed neurons, never could have evolved without myelin.

The myelin sheath is a stack of specialized plasma membrane sheets produced by a glial cell that wraps itself around the axon (Figure 7-39). In the peripheral nervous system,



▲ **FIGURE 7-39 Formation and structure of a myelin sheath in the peripheral nervous system.**

Myelinated axons are surrounded by an insulating layer of compressed membranes. (a) Electron micrograph of a cross section through an axon (Ax) surrounded by a myelin sheath (MS) and Schwann cell (SN). (b) At higher magnification this specialized spiral membrane appears as a series of layers, or lamellae, of phospholipid bilayers. In this image, the termini of both the outer and innermost wraps are evident (arrows). (c) As a Schwann cell repeatedly wraps around an axon, all the spaces between its plasma membranes, both cytosolic and exoplasmic, are reduced. Eventually all the cytosol is forced out and a structure of compact stacked plasma membranes, the myelin sheath, is formed. (d) The two most abundant membrane proteins, P<sub>0</sub> and PMP22, in peripheral myelin are expressed only by Schwann cells. The exoplasmic

domain of a P<sub>0</sub> protein, which has an immunoglobulin fold, associates with similar domains emanating from P<sub>0</sub> proteins in the opposite membrane surface, thereby “zippering” together the exoplasmic membrane surfaces in close apposition. These interactions are stabilized by binding of a tryptophan residue on the tip of the exoplasmic domain to lipids in the opposite membrane. Close apposition of the cytosolic faces of the membrane may result from binding of the cytosolic tail of each P<sub>0</sub> protein to phospholipids in the opposite membrane. PMP22 may also contribute to membrane compaction. Myelin basic protein (MBP), a cytosolic protein, remains between the closely apposed membranes as the cytosol is squeezed out. [Parts (a) and (b) courtesy Grahame Kidd, Lerner Research Institute. Part (d) adapted from L. Shapiro et al., 1996, *Neuron* 17:435, and E. J. Arroyo and S. S. Scherer, 2000, *Histochem. Cell Biol.* 113:1.]

these glial cells are called *Schwann cells*. In the central nervous system, they are called *oligodendrocytes*. In both vertebrates and some invertebrates, glial cells accompany axons along their length, but specialization of these glial cells to form myelin occurs predominantly in vertebrates. Vertebrate glial cells that will later form myelin have on their surface a myelin-associated glycoprotein and other proteins that bind to adjacent axons and trigger the formation of myelin.

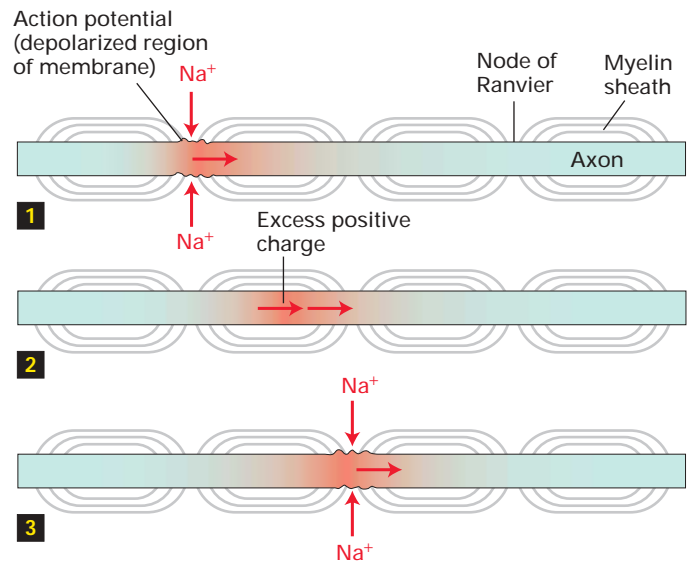
Figure 7-39d illustrates the formation and basic structure of a myelin sheath, which contains both membrane and cytosolic components. A myelin membrane, like all biomembranes, has a basic phospholipid bilayer structure, but it contains far fewer types of proteins than found in most other membranes. Two proteins predominate in the myelin membrane around peripheral axons:  $P_0$ , which causes adjacent plasma membranes to stack tightly together, and *PMP22*. Gene knockout studies in mice have recently identified *PMP22* as essential for myelination. In the central nervous system, a different membrane protein and a proteolipid together function similarly to  $P_0$ . The major cytosolic protein in all myelin sheaths is *myelin basic protein* (MBP). Mice that contain the *shiverer* mutation in the MBP gene exhibit severe neurological problems, evidence for the importance of myelination in the normal functioning of the nervous system.

### Action Potentials “Jump” from Node to Node in Myelinated Axons

The myelin sheath surrounding an axon is formed from many glial cells. Each region of myelin formed by an individual glial cell is separated from the next region by an unmyelinated area of axonal membrane about  $1\ \mu\text{m}$  in length called the *node of Ranvier* (or simply, node). The axonal membrane is in direct contact with the extracellular fluid only at the nodes. Moreover, all the voltage-gated  $\text{Na}^+$  channels and all the  $\text{Na}^+/\text{K}^+$  pumps, which maintain the ionic gradients in the axon, are located in the nodes.

As a consequence of this localization, the inward movement of  $\text{Na}^+$  ions that generates the action potential can occur only at the myelin-free nodes (Figure 7-40). The excess cytosolic positive ions generated at a node during the membrane depolarization associated with an action potential spread passively through the axonal cytosol to the next node with very little loss or attenuation, since they cannot cross the myelinated axonal membrane. This causes a depolarization at one node to spread rapidly to the next node, permitting, in effect, the action potential to “jump” from node to node. This phenomenon explains why the conduction velocity of myelinated neurons is about the same as that of much larger diameter unmyelinated neurons. For instance, a  $12\text{-}\mu\text{m}$ -diameter myelinated vertebrate axon and a  $600\text{-}\mu\text{m}$ -diameter unmyelinated squid axon both conduct impulses at  $12\ \text{m/s}$ .

Several factors contribute to the clustering of voltage-gated  $\text{Na}^+$  channels and  $\text{Na}^+/\text{K}^+$  pumps at the nodes of



▲ **FIGURE 7-40 Conduction of action potentials in myelinated axons.** Because voltage-gated  $\text{Na}^+$  channels are localized to the axonal membrane at the nodes of Ranvier, the influx of  $\text{Na}^+$  ions associated with an action potential can occur only at nodes. When an action potential is generated at one node (step **1**), the excess positive ions in the cytosol, which cannot move outward across the sheath, diffuse rapidly down the axon, causing sufficient depolarization at the next node (step **2**) to induce an action potential at that node (step **3**). By this mechanism the action potential jumps from node to node along the axon.

Ranvier. Both of these transport proteins interact with two cytoskeletal proteins, ankyrin and spectrin, similar to those in the erythrocyte membrane (see Figure 5-31). The extracellular domain of the  $\beta 1$  subunit of the  $\text{Na}^+$  channel also binds to the extracellular domain of Nr-CAM, a type of adhesive protein that is localized to the node. As a result of these multiple protein-protein interactions, the concentration of  $\text{Na}^+$  channels is roughly a hundredfold higher in the nodal membrane of myelinated axons than in the axonal membrane of nonmyelinated neurons. In addition, glial cells secrete protein hormones that somehow trigger the clustering of these nerve membrane proteins at the nodes. Finally, tight junctions between the axon and the glial cell plasma membrane in the paranodal junctions immediately adjacent to the nodes may prevent diffusion of  $\text{Na}^+$  channels and  $\text{Na}^+/\text{K}^+$  pumps away from the nodes.



One prevalent neurological disease among human adults is multiple sclerosis (MS), usually characterized by spasms and weakness in one or more limbs, bladder dysfunction, local sensory losses, and visual disturbances. This disorder—the prototype *demyelinating disease*—is caused by patchy loss of myelin in areas of the brain and spinal cord. In MS patients, conduction of action potentials by the demyelinated neurons is slowed, and the

Na<sup>+</sup> channels spread outward from the nodes, lowering their nodal concentration. The cause of the disease is not known but appears to involve either the body's production of autoantibodies (antibodies that bind to normal body proteins) that react with myelin basic protein or the secretion of proteases that destroy myelin proteins. ■

## KEY CONCEPTS OF SECTION 7.7

### Voltage-Gated Ion Channels and the Propagation of Action Potentials in Nerve Cells

- Action potentials are sudden membrane depolarizations followed by a rapid repolarization. They originate at the axon hillock and move down the axon toward the axon terminals, where the electric impulse is transmitted to other cells via a synapse (see Figures 7-29 and 7-31).
- An action potential results from the sequential opening and closing of voltage-gated Na<sup>+</sup> and K<sup>+</sup> channels in the plasma membrane of neurons and muscle cells.
- Opening of voltage-gated Na<sup>+</sup> channels permits influx of Na<sup>+</sup> ions for about 1 ms, causing a sudden large depolarization of a segment of the membrane. The channels then close and become unable to open (refractory) for several milliseconds, preventing further Na<sup>+</sup> flow (see Figure 7-33).
- As the action potential reaches its peak, opening of voltage-gated K<sup>+</sup> channels permits efflux of K<sup>+</sup> ions, which repolarizes and then hyperpolarizes the membrane. As these channels close, the membrane returns to its resting potential (see Figure 7-30).
- The excess cytosolic cations associated with an action potential generated at one point on an axon spread passively to the adjacent segment, triggering opening of voltage-gated Na<sup>+</sup> channels and movement of the action potential along the axon.
- Because of the absolute refractory period of the voltage-gated Na<sup>+</sup> channels and the brief hyperpolarization resulting from K<sup>+</sup> efflux, the action potential is propagated in one direction only, toward the axon terminus.
- Voltage-gated Na<sup>+</sup> and Ca<sup>2+</sup> channels are monomeric proteins containing four domains that are structurally and functionally similar to each of the subunits in the tetrameric voltage-gated K<sup>+</sup> channels.
- Each domain or subunit in voltage-gated cation channels contains six transmembrane  $\alpha$  helices and a nonhelical P segment that forms the ion-selectivity pore (see Figure 7-36).
- Opening of voltage-gated channels results from outward movement of the positively charged S4  $\alpha$  helices in response to a depolarization of sufficient magnitude.
- Closing and inactivation of voltage-gated cation chan-

nels result from movement of a cytosolic segment into the open pore (see Figure 7-37).

- Myelination, which increases the rate of impulse conduction up to a hundredfold, permits the close packing of neurons characteristic of vertebrate brains.
- In myelinated neurons, voltage-gated Na<sup>+</sup> channels are concentrated at the nodes of Ranvier. Depolarization at one node spreads rapidly with little attenuation to the next node, so that the action potential “jumps” from node to node (see Figure 7-40).

## 7.8 Neurotransmitters and Receptor and Transport Proteins in Signal Transmission at Synapses

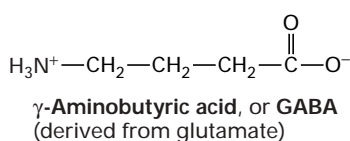
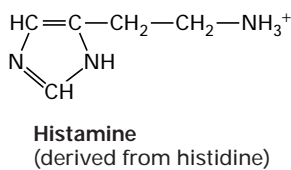
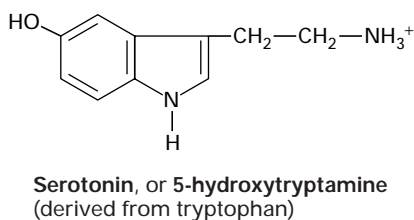
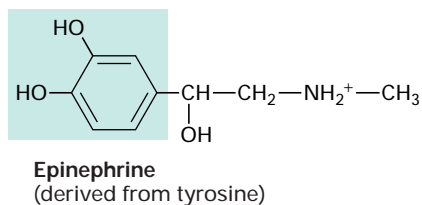
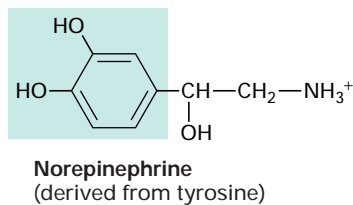
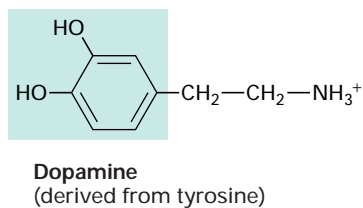
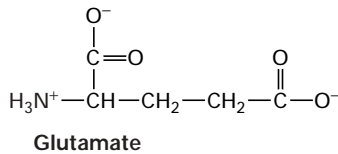
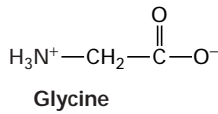
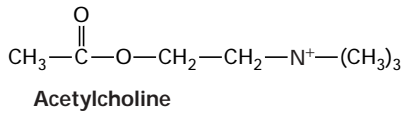
As noted earlier, synapses are the junctions where neurons release a chemical neurotransmitter that acts on a postsynaptic target cell, which can be another neuron or a muscle or gland cell (see Figure 7-31). In this section, we focus on several key issues related to impulse transmission:

- How neurotransmitters are packaged in membrane-bounded *synaptic vesicles* in the axon terminus
- How arrival of an action potential at axon termini in presynaptic cells triggers secretion of neurotransmitters
- How binding of neurotransmitters by receptors on postsynaptic cells leads to changes in their membrane potential
- How neurotransmitters are removed from the synaptic cleft after stimulating postsynaptic cells

Neurotransmitter receptors fall into two broad classes: ligand-gated ion channels, which open immediately upon neurotransmitter binding, and G protein-coupled receptors. Neurotransmitter binding to a G protein-coupled receptor induces the opening or closing of a *separate* ion channel protein over a period of seconds to minutes. These “slow” neurotransmitter receptors are discussed in Chapter 13 along with G protein-coupled receptors that bind different types of ligands and modulate the activity of cytosolic proteins other than ion channels. Here we examine the structure and operation of the *nicotinic acetylcholine receptor* found at many nerve-muscle synapses. The first ligand-gated ion channel to be purified, cloned, and characterized at the molecular level, this receptor provides a paradigm for other neurotransmitter-gated ion channels.

### Neurotransmitters Are Transported into Synaptic Vesicles by H<sup>+</sup>-Linked Antiport Proteins

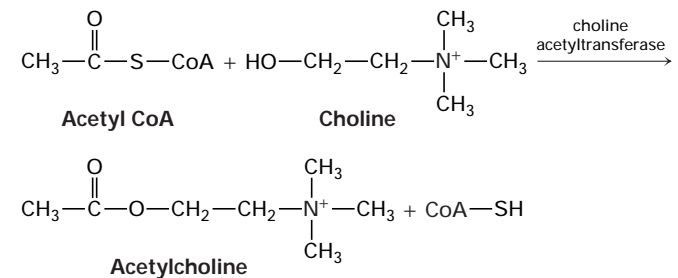
Numerous small molecules function as neurotransmitters at various synapses. With the exception of **acetylcholine**, the



neurotransmitters shown in Figure 7-41 are amino acids or derivatives of amino acids. Nucleotides such as ATP and the corresponding nucleosides, which lack phosphate groups, also function as neurotransmitters. Each neuron generally produces just one type of neurotransmitter.

All the “classic” neurotransmitters are synthesized in the cytosol and imported into membrane-bound synaptic vesicles within axon terminals, where they are stored. These vesicles are 40–50 nm in diameter, and their lumen has a low pH, generated by operation of a V-class proton pump in the vesicle membrane. Similar to the accumulation of metabolites in plant vacuoles (see Figure 7-23), this proton concentration gradient (vesicle lumen > cytosol) powers neurotransmitter import by ligand-specific  $\text{H}^+$ -linked antiporters in the vesicle membrane.

For example, acetylcholine is synthesized from acetyl coenzyme A (acetyl CoA), an intermediate in the degradation of glucose and fatty acids, and choline in a reaction catalyzed by choline acetyltransferase:



Synaptic vesicles take up and concentrate acetylcholine from the cytosol against a steep concentration gradient, using an  $\text{H}^+$ /acetylcholine antiporter in the vesicle membrane. Curiously, the gene encoding this antiporter is contained entirely within the first intron of the gene encoding choline acetyltransferase, a mechanism conserved throughout evolution for ensuring coordinate expression of these two proteins. Different  $\text{H}^+$ /neurotransmitter antiport proteins are used for import of other neurotransmitters into synaptic vesicles.

### Influx of $\text{Ca}^{2+}$ Through Voltage-Gated $\text{Ca}^{2+}$ Channels Triggers Release of Neurotransmitters

Neurotransmitters are released by **exocytosis**, a process in which neurotransmitter-filled synaptic vesicles fuse with the axonal membrane, releasing their contents into the synaptic cleft. The exocytosis of neurotransmitters from synaptic vesicles involves vesicle-targeting and fusion events similar to those that occur during the intracellular transport of secreted and plasma-membrane proteins (Chapter 17). Two features

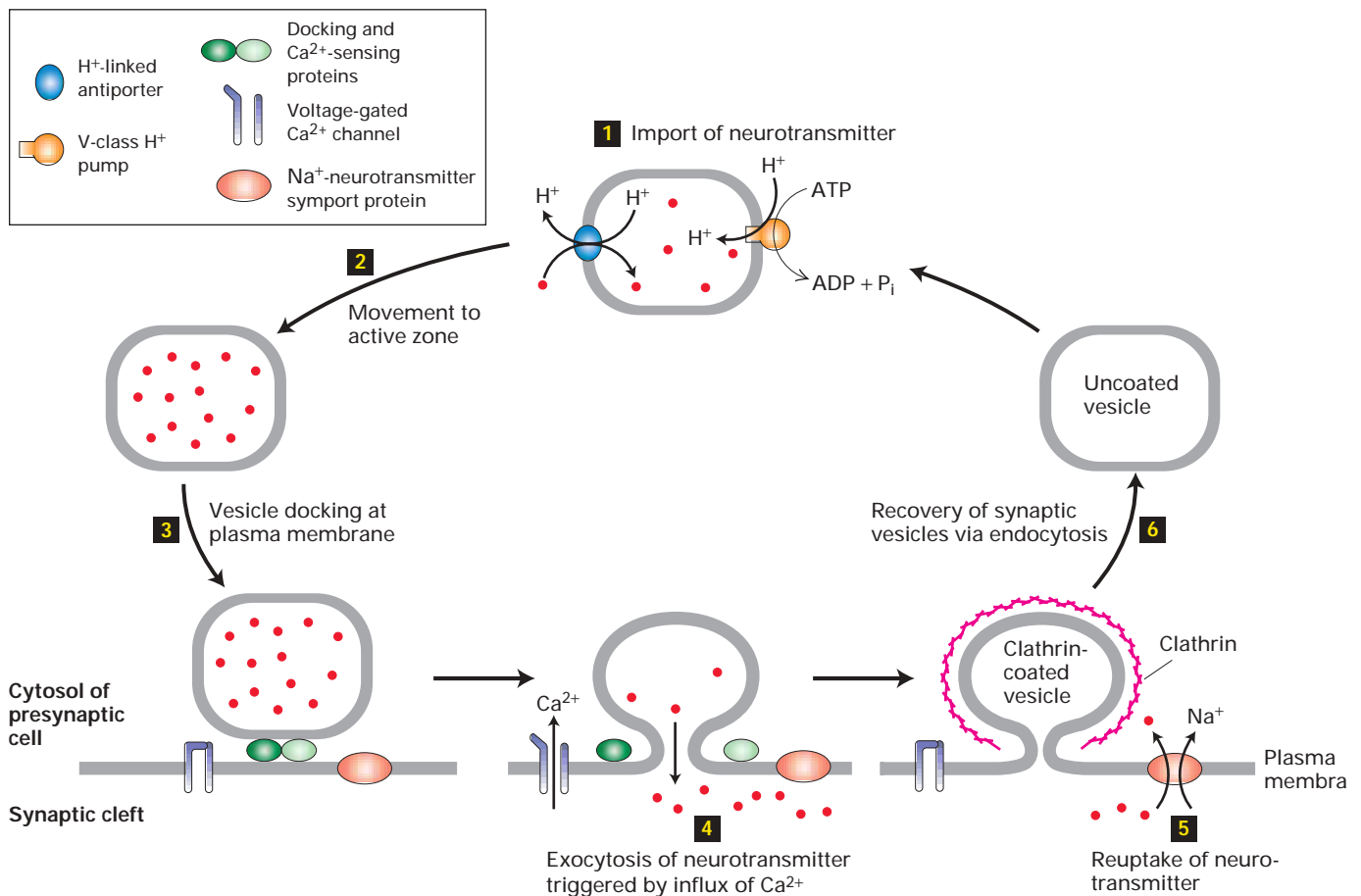
◀ **FIGURE 7-41 Structures of several small molecules that function as neurotransmitters.** Except for acetylcholine, all these are amino acids (glycine and glutamate) or derived from the indicated amino acids. The three transmitters synthesized from tyrosine, which contain the catechol moiety (blue highlight), are referred to as catecholamines.

critical to synapse function differ from other secretory pathways: (a) secretion is tightly coupled to arrival of an action potential at the axon terminus, and (b) synaptic vesicles are recycled locally to the axon terminus after fusion with the plasma membrane. Figure 7-42 shows the entire cycle whereby synaptic vesicles are filled with neurotransmitter, release their contents, and are recycled.

Depolarization of the plasma membrane cannot, by itself, cause synaptic vesicles to fuse with the plasma membrane. In order to trigger vesicle fusion, an action potential must be converted into a chemical signal—namely, a localized rise in the cytosolic  $\text{Ca}^{2+}$  concentration. The transducers of the electric signals are *voltage-gated  $\text{Ca}^{2+}$  channels* localized to the region of the plasma membrane adjacent to the synaptic vesicles. The membrane depolarization due to arrival of an action potential opens these channels, permitting an influx

of  $\text{Ca}^{2+}$  ions from the extracellular medium into the axon terminal. This ion flux raises the local cytosolic  $\text{Ca}^{2+}$  concentration near the synaptic vesicles from  $<0.1 \mu\text{M}$ , characteristic of the resting state, to  $1\text{--}100 \mu\text{M}$ . Binding of  $\text{Ca}^{2+}$  ions to proteins that connect the synaptic vesicle with the plasma membrane induces membrane fusion and thus exocytosis of the neurotransmitter. The subsequent export of extra  $\text{Ca}^{2+}$  ions by ATP-powered  $\text{Ca}^{2+}$  pumps in the plasma membrane rapidly lowers the cytosolic  $\text{Ca}^{2+}$  level to that of the resting state, enabling the axon terminus to respond to the arrival of another action potential.

A simple experiment demonstrates the importance of voltage-gated  $\text{Ca}^{2+}$  channels in release of neurotransmitters. A preparation of neurons in a  $\text{Ca}^{2+}$ -containing medium is treated with tetrodotoxin, a drug that blocks voltage-gated  $\text{Na}^+$  channels and thus prevents conduction of action



▲ **FIGURE 7-42 Cycling of neurotransmitters and of synaptic vesicles in axon terminals.** The entire cycle depicted here typically takes about 60 seconds. Note that several transport proteins participate in the filling of synaptic vesicles with neurotransmitter (red circles), its release by exocytosis, and subsequent reuptake from the synaptic cleft. Once synaptic-vesicle membrane proteins (e.g., pumps, antiporters, and fusion

proteins needed for exocytosis) are specifically recovered by endocytosis in clathrin-coated vesicles, the clathrin coat is depolymerized, yielding vesicles that can be filled with neurotransmitter. Unlike most neurotransmitters, acetylcholine is not recycled. [See T. Südhof and R. Jahn, 1991, *Neuron* 6:665; K. Takei et al., 1996, *J. Cell. Biol.* 133:1237; and V. Murthy and C. Stevens, 1998, *Nature* 392:497.]

potentials. As expected, no neurotransmitters are secreted into the culture medium. If the axonal membrane then is artificially depolarized by making the medium  $\approx 100$  mM KCl, neurotransmitters are released from the cells because of the influx of  $\text{Ca}^{2+}$  through open voltage-gated  $\text{Ca}^{2+}$  channels. Indeed, patch-clamping experiments show that voltage-gated  $\text{Ca}^{2+}$  channels, like voltage-gated  $\text{Na}^+$  channels, open transiently upon depolarization of the membrane.

Two pools of neurotransmitter-filled synaptic vesicles are present in axon terminals: those “docked” at the plasma membrane, which can be readily exocytosed, and those in reserve in the *active zone* near the plasma membrane. Each rise in  $\text{Ca}^{2+}$  triggers exocytosis of about 10 percent of the docked vesicles. Membrane proteins unique to synaptic vesicles then are specifically internalized by **endocytosis**, usually via the same types of clathrin-coated vesicles used to recover other plasma-membrane proteins by other types of cells. After the endocytosed vesicles lose their clathrin coat, they are rapidly refilled with neurotransmitter. The ability of many neurons to fire 50 times a second is clear evidence that the recycling of vesicle membrane proteins occurs quite rapidly.

### Signaling at Synapses Usually Is Terminated by Degradation or Reuptake of Neurotransmitters

Following their release from a presynaptic cell, neurotransmitters must be removed or destroyed to prevent continued stimulation of the postsynaptic cell. Signaling can be terminated by diffusion of a transmitter away from the synaptic cleft, but this is a slow process. Instead, one of two more rapid mechanisms terminates the action of neurotransmitters at most synapses.

Signaling by acetylcholine is terminated when it is hydrolyzed to acetate and choline by *acetylcholinesterase*, an enzyme localized to the synaptic cleft. Choline released in this reaction is transported back into the presynaptic axon terminal by a  $\text{Na}^+$ /choline symporter and used in synthesis of more acetylcholine. The operation of this transporter is similar to that of the  $\text{Na}^+$ -linked symporters used to transport glucose into cells against a concentration gradient (see Figure 7-21).

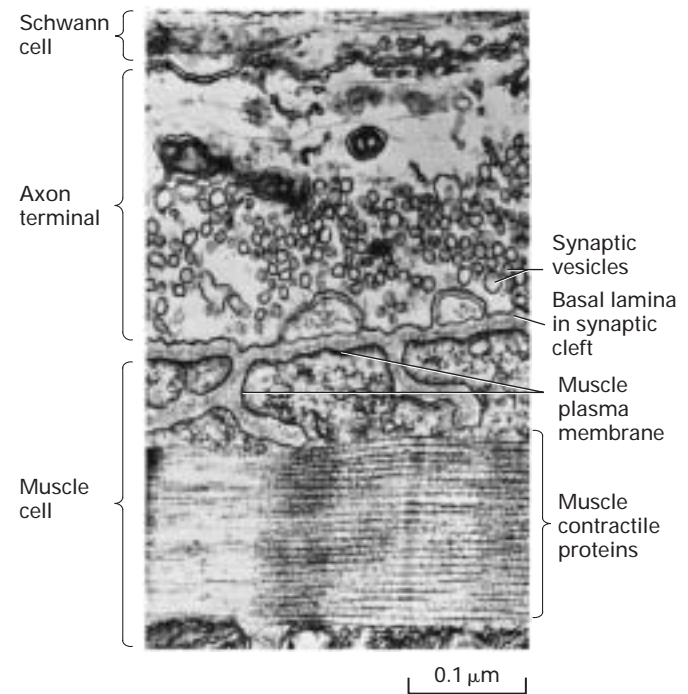
With the exception of acetylcholine, all the neurotransmitters shown in Figure 7-41 are removed from the synaptic cleft by transport into the axon terminals that released them. Thus these transmitters are recycled intact, as depicted in Figure 7-42 (step 5). Transporters for GABA, norepinephrine, dopamine, and serotonin were the first to be cloned and studied. These four transport proteins are all  $\text{Na}^+$ -linked symporters. They are 60–70 percent identical in their amino acid sequences, and each is thought to contain 12 transmembrane  $\alpha$  helices. As with other  $\text{Na}^+$  symporters, the movement of  $\text{Na}^+$  into the cell down its electrochemical gradient provides the energy for uptake of the neurotransmitter. To maintain electroneutrality,  $\text{Cl}^-$  often is transported via an ion channel along with the  $\text{Na}^+$  and neurotransmitter.



Cocaine inhibits the transporters for norepinephrine, serotonin, and dopamine. Binding of cocaine to the dopamine transporter inhibits reuptake of dopamine, thus prolonging signaling at key brain synapses; indeed, the dopamine transporter is the principal brain “cocaine receptor.” Therapeutic agents such as the antidepressant drugs fluoxetine (Prozac) and imipramine block serotonin uptake, and the tricyclic antidepressant desipramine blocks norepinephrine uptake. ■

### Opening of Acetylcholine-Gated Cation Channels Leads to Muscle Contraction

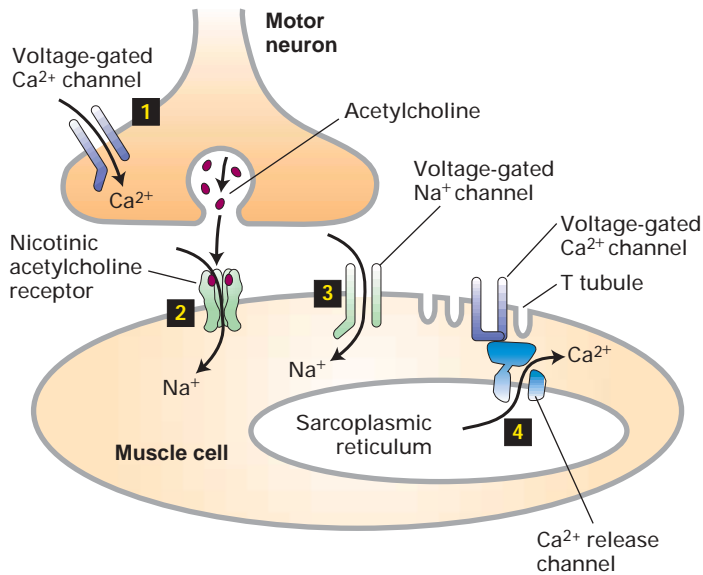
Acetylcholine is the neurotransmitter at synapses between motor neurons and muscle cells, often called *neuromuscular junctions*. A single axon terminus of a frog motor neuron may contain a million or more synaptic vesicles, each containing 1000–10,000 molecules of acetylcholine; these vesicles often accumulate in rows in the active zone (Figure 7-43). Such a neuron can form synapses with a single skeletal muscle cell at several hundred points.



#### ▲ FIGURE 7-43 Synaptic vesicles in the axon terminal near the region where neurotransmitter is released.

In this longitudinal section through a neuromuscular junction, the basal lamina lies in the synaptic cleft separating the neuron from the muscle membrane, which is extensively folded. Acetylcholine receptors are concentrated in the postsynaptic muscle membrane at the top and part way down the sides of the folds in the membrane. A Schwann cell surrounds the axon terminal.

[From J. E. Heuser and T. Reese, 1977, in E. R. Kandel, ed., *The Nervous System*, vol. 1, *Handbook of Physiology*, Williams & Wilkins, p. 266.]



**▲ FIGURE 7-44 Sequential activation of gated ion channels at a neuromuscular junction.** Arrival of an action potential at the terminus of a presynaptic motor neuron induces opening of voltage-gated  $\text{Ca}^{2+}$  channels (step **1**) and subsequent release of acetylcholine, which triggers opening of the ligand-gated acetylcholine receptors in the muscle plasma membrane (step **2**). The resulting influx of  $\text{Na}^+$  produces a localized depolarization of the membrane, leading to opening of voltage-gated  $\text{Na}^+$  channels and generation of an action potential (step **3**). When the spreading depolarization reaches T tubules, it is sensed by voltage-gated  $\text{Ca}^{2+}$  channels in the plasma membrane. This leads to opening of  $\text{Ca}^{2+}$ -release channels in the sarcoplasmic reticulum membrane, releasing stored  $\text{Ca}^{2+}$  into the cytosol (step **4**). The resulting rise in cytosolic  $\text{Ca}^{2+}$  causes muscle contraction by mechanisms discussed in Chapter 19.

The nicotinic acetylcholine receptor, which is expressed in muscle cells, is a ligand-gated channel that admits both  $\text{K}^+$  and  $\text{Na}^+$ . The effect of acetylcholine on this receptor can be determined by patch-clamping studies on isolated outside-out patches of muscle plasma membranes (see Figure 7-17c). Such measurements have shown that acetylcholine causes opening of a cation channel in the receptor capable of transmitting 15,000–30,000  $\text{Na}^+$  or  $\text{K}^+$  ions per millisecond. However, since the resting potential of the muscle plasma membrane is near  $E_{\text{K}}$ , the potassium equilibrium potential, opening of acetylcholine receptor channels causes little increase in the efflux of  $\text{K}^+$  ions;  $\text{Na}^+$  ions, on the other hand, flow into the muscle cell driven by the  $\text{Na}^+$  electrochemical gradient.

The simultaneous increase in permeability to  $\text{Na}^+$  and  $\text{K}^+$  ions following binding of acetylcholine produces a net depolarization to about  $-15$  mV from the muscle resting potential of  $-85$  to  $-90$  mV. As shown in Figure 7-44, this localized depolarization of the muscle plasma membrane triggers opening of voltage-gated  $\text{Na}^+$  channels, leading to generation and conduction of an action potential in the muscle cell surface membrane by the same mechanisms described

previously for neurons. When the membrane depolarization reaches T tubules, specialized invaginations of the plasma membrane, it affects  $\text{Ca}^{2+}$  channels in the plasma membrane apparently without causing them to open. Somehow this causes opening of adjacent  $\text{Ca}^{2+}$ -release channels in the sarcoplasmic reticulum membrane. The subsequent flow of stored  $\text{Ca}^{2+}$  ions from the sarcoplasmic reticulum into the cytosol raises the cytosolic  $\text{Ca}^{2+}$  concentration sufficiently to induce muscle contraction.

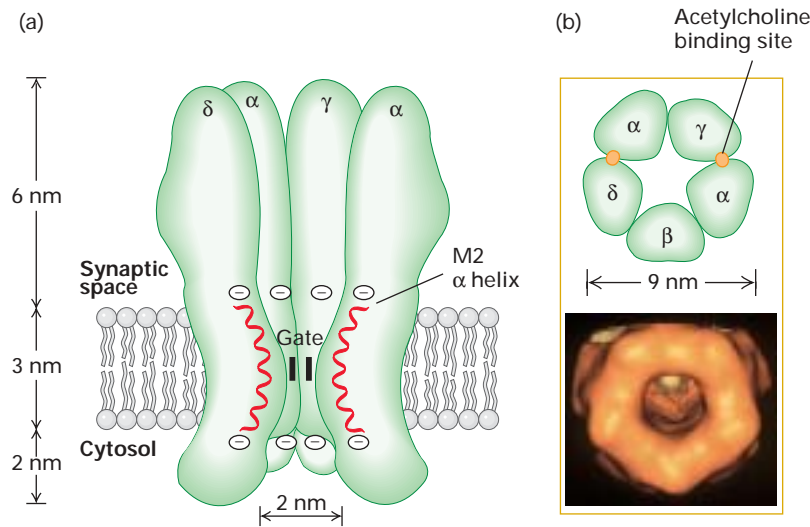
Careful monitoring of the membrane potential of the muscle membrane at a synapse with a cholinergic motor neuron has demonstrated spontaneous, intermittent, and random  $\approx 2$ -ms depolarizations of about 0.5–1.0 mV in the absence of stimulation of the motor neuron. Each of these depolarizations is caused by the spontaneous release of acetylcholine from a single synaptic vesicle. Indeed, demonstration of such spontaneous small depolarizations led to the notion of the quantal release of acetylcholine (later applied to other neurotransmitters) and thereby led to the hypothesis of vesicle exocytosis at synapses. The release of one acetylcholine-containing synaptic vesicle results in the opening of about 3000 ion channels in the postsynaptic membrane, far short of the number needed to reach the threshold depolarization that induces an action potential. Clearly, stimulation of muscle contraction by a motor neuron requires the nearly simultaneous release of acetylcholine from numerous synaptic vesicles.

### All Five Subunits in the Nicotinic Acetylcholine Receptor Contribute to the Ion Channel

The acetylcholine receptor from skeletal muscle is a pentameric protein with a subunit composition of  $\alpha_2\beta\gamma\delta$ . The  $\alpha$ ,  $\beta$ ,  $\gamma$ , and  $\delta$  subunits have considerable sequence homology; on average, about 35–40 percent of the residues in any two subunits are similar. The complete receptor has fivefold symmetry, and the actual cation channel is a tapered central pore lined by homologous segments from each of the five subunits (Figure 7-45).

The channel opens when the receptor cooperatively binds two acetylcholine molecules to sites located at the interfaces of the  $\alpha\delta$  and  $\alpha\gamma$  subunits. Once acetylcholine is bound to a receptor, the channel is opened within a few microseconds. Studies measuring the permeability of different small cations suggest that the open ion channel is, at its narrowest, about 0.65–0.80 nm in diameter, in agreement with estimates from electron micrographs. This would be sufficient to allow passage of both  $\text{Na}^+$  and  $\text{K}^+$  ions with their shell of bound water molecules. Thus the acetylcholine receptor probably transports hydrated ions, unlike  $\text{Na}^+$  and  $\text{K}^+$  channels, both of which allow passage only of nonhydrated ions (see Figure 7-16).

Although the structure of the central ion channel is not known in molecular detail, much evidence indicates that it is lined by five homologous transmembrane M2  $\alpha$  helices, one from each of the five subunits. The M2 helices are



▲ **FIGURE 7-45 Three-dimensional structure of the nicotinic acetylcholine receptor.** (a) Schematic cutaway model of the pentameric receptor in the membrane; for clarity, the  $\beta$  subunit is not shown. Each subunit contains an M2  $\alpha$  helix (red) that faces the central pore. Aspartate and glutamate side chains at both ends of the M2 helices form two rings of negative charges that help exclude anions from and attract cations to the channel. The gate, which is opened by binding of acetylcholine, lies within the pore. (b) *Top*: Cross section of the exoplasmic face of the

receptor showing the arrangement of subunits around the central pore. The two acetylcholine binding sites are located about 3 nm from the membrane surface. *Bottom*: Top-down view looking into the synaptic entrance of the channel. The tunnel-like entrance narrows abruptly after a distance of about 6 nm. These models are based on amino acid sequence data, computer-generated averaging of high-resolution electron micrographs, and information from site-specific mutations. [Part (b) from N. Unwin, 1993, *Cell* **72**, and *Neuron*, **10** (suppl.), p. 31.]

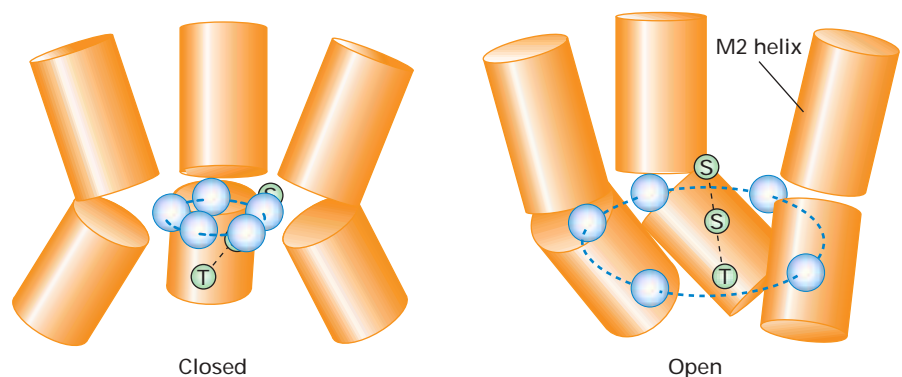
composed largely of hydrophobic or uncharged polar amino acids, but negatively charged aspartate or glutamate residues are located at each end, near the membrane faces, and several serine or threonine residues are near the middle. Mutant acetylcholine receptors in which a single negatively charged glutamate or aspartate in one M2 helix is replaced by a positively charged lysine have been expressed in frog oocytes. Patch-clamping measurements indicate that such altered proteins can function as channels, but the number of ions that pass through during the open state is reduced. The greater the number of glutamate or aspartate residues mutated (in one or multiple M2 helices), the greater the reduction in ion conductivity. These findings suggest that aspartate and glutamate residues form a ring of negative charges on

the external surface of the pore that help to screen out anions and attract  $\text{Na}^+$  or  $\text{K}^+$  ions as they enter the channel. A similar ring of negative charges lining the cytosolic pore surface also helps select cations for passage (see Figure 7-45).

The two acetylcholine binding sites in the extracellular domain of the receptor lie  $\approx 4$  to 5 nm from the center of the pore. Binding of acetylcholine thus must trigger conformational changes in the receptor subunits that can cause channel opening at some distance from the binding sites. Receptors in isolated postsynaptic membranes can be trapped in the open or closed state by rapid freezing in liquid nitrogen. Images of such preparations suggest that the five M2 helices rotate relative to the vertical axis of the channel during opening and closing (Figure 7-46).

► **FIGURE 7-46 Schematic models of the pore-lining M2 helices in the closed and opened states.** In the closed state, the kink in the center of each M2 helix points inward, constricting the passageway, whose perimeter is indicated by the blue spheres. In the open state, the kinks rotate to one side, so that the helices are farther apart. The green spheres denote the hydroxyl groups of serine (S) and threonine (T) residues in the center of the M2 helices; in the open state these are parallel to the channel axis and allow ions to flow.

[Adapted from N. Unwin, 1995, *Nature* **373**:37.]

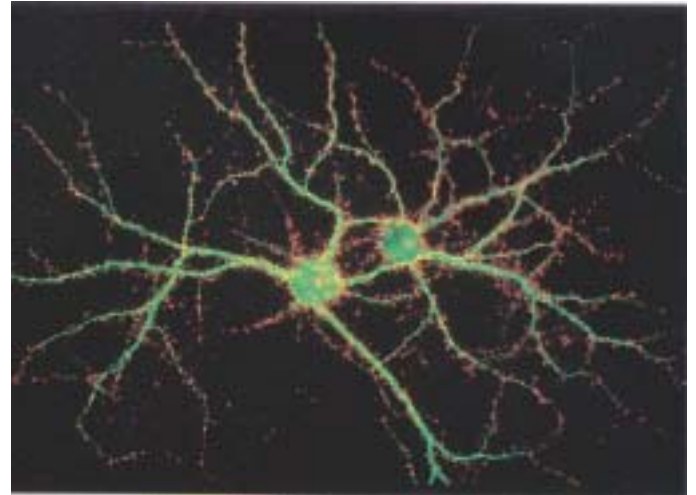




## Nerve Cells Make an All-or-None Decision to Generate an Action Potential

At the neuromuscular junction, virtually every action potential in the presynaptic motor neuron triggers an action potential in the postsynaptic muscle cell. The situation at synapses between neurons, especially those in the brain, is much more complex because the postsynaptic neuron commonly receives signals from many presynaptic neurons (Figure 7-47). The neurotransmitters released from presynaptic neurons may bind to an *excitatory receptor* on the postsynaptic neuron, thereby opening a channel that admits  $\text{Na}^+$  ions or both  $\text{Na}^+$  and  $\text{K}^+$  ions. The acetylcholine receptor just discussed is one of many excitatory receptors, and opening of such ion channels leads to depolarization of the postsynaptic plasma membrane, promoting generation of an action potential. In contrast, binding of a neurotransmitter to an *inhibitory receptor* on the postsynaptic cell causes opening of  $\text{K}^+$  or  $\text{Cl}^-$  channels, leading to an efflux of additional  $\text{K}^+$  ions from the cytosol or an influx of  $\text{Cl}^-$  ions. In either case, the ion flow tends to hyperpolarize the plasma membrane, which inhibits generation of an action potential in the postsynaptic cell.

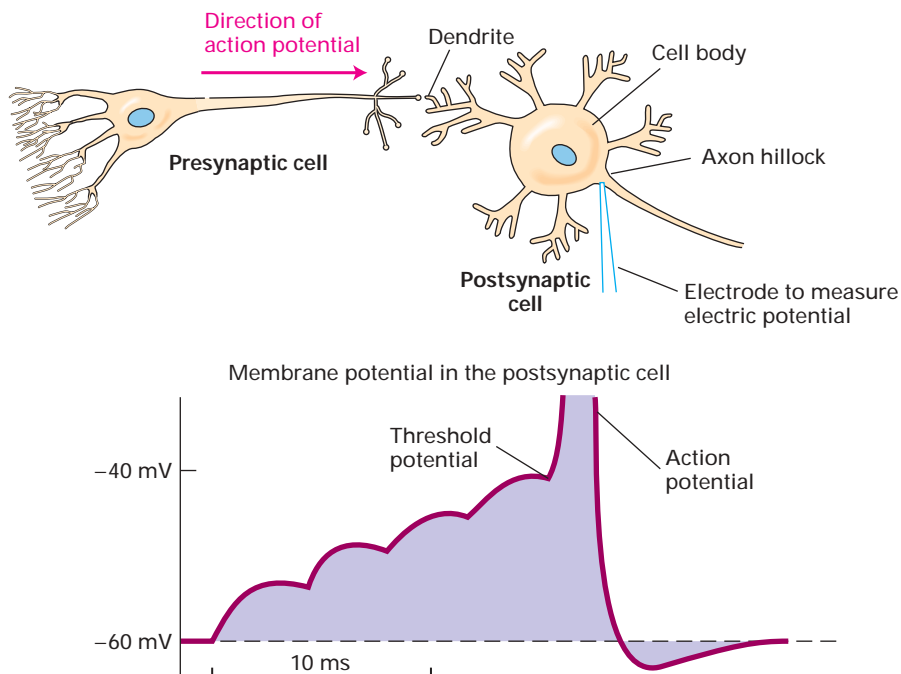
A single neuron can be affected simultaneously by signals received at multiple excitatory and inhibitory synapses. The neuron continuously integrates these signals and determines whether or not to generate an action potential. In this process, the various small depolarizations and hyperpolarizations generated at synapses move along the plasma membrane from the dendrites to the cell body and then to the axon hillock, where they are summed together. An action potential is generated whenever the membrane at the axon hillock becomes depolarized to a certain voltage called the *threshold potential* (Figure 7-48). Thus an action potential



### ▲ EXPERIMENTAL FIGURE 7-47 A fluorescent micrograph of two interneurons reveals that many other neurons synapse with them.

These cells, from the hippocampal region of the brain, were stained with two fluorescent antibodies: one specific for the microtubule-associated protein MAP2 (green), which is found only in dendrites and cell bodies, and the other specific for synaptotagmin (orange-red), a protein found in presynaptic axon terminals. The numerous orange-red dots, which represent presynaptic axon terminals from neurons that are not visible in this field, indicate that these interneurons receive signals from many other cells. [Courtesy of O. Mundigl and P. deCamilli.]

is generated in an all-or-nothing fashion: Depolarization to the threshold always leads to an action potential, whereas any depolarization that does not reach the threshold potential never induces it.



### ◀ EXPERIMENTAL FIGURE 7-48 Incoming signals must reach the threshold potential to trigger an action potential in a postsynaptic cell.

In this example, the presynaptic neuron is generating about one action potential every 4 milliseconds. Arrival of each action potential at the synapse causes a small change in the membrane potential at the axon hillock of the postsynaptic cell, in this example a depolarization of  $\approx 5$  mV. When multiple stimuli cause the membrane of this postsynaptic cell to become depolarized to the threshold potential, here approximately  $-40$  mV, an action potential is induced in it.

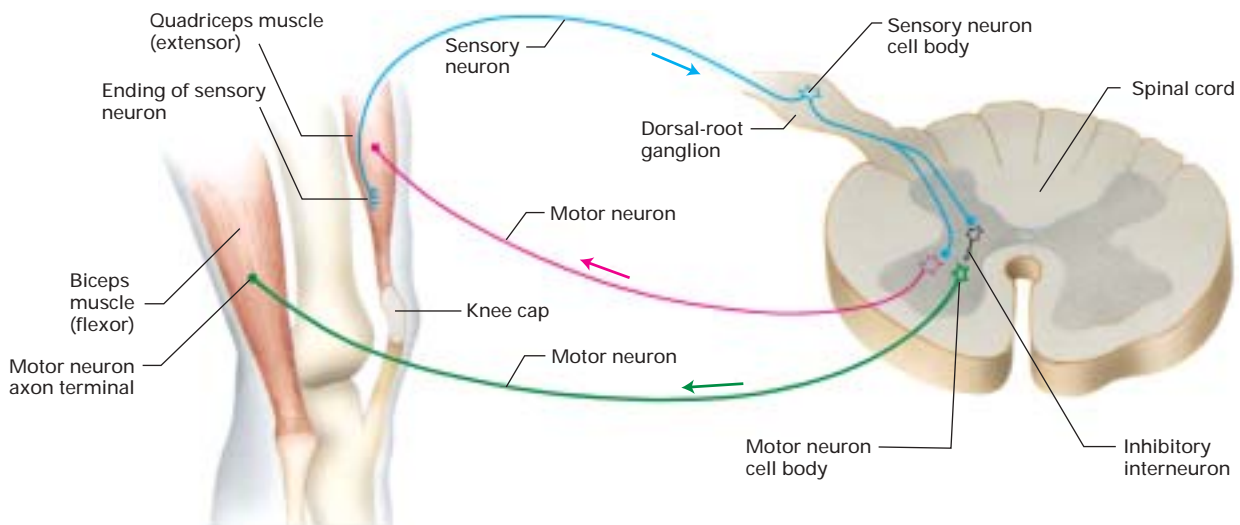
Whether a neuron generates an action potential in the axon hillock depends on the balance of the timing, amplitude, and localization of all the various inputs it receives; this signal computation differs for each type of neuron. In a sense, each neuron is a tiny computer that averages all the receptor activations and electric disturbances on its membrane and makes a decision whether to trigger an action potential and conduct it down the axon. An action potential will always have the same *magnitude* in any particular neuron. The *frequency* with which action potentials are generated in a particular neuron is the important parameter in its ability to signal other cells.

### The Nervous System Uses Signaling Circuits Composed of Multiple Neurons

In complex multicellular animals, such as insects and mammals, various types of neurons form signaling circuits. In the simple type of circuit, called a *reflex arc*, interneurons connect multiple sensory and motor neurons, allowing one sensory neuron to affect multiple motor neurons and one motor neuron to be affected by multiple sensory neurons; in this

way interneurons integrate and enhance reflexes. For example, the knee-jerk reflex in humans involves a complex reflex arc in which one muscle is stimulated to contract while another is inhibited from contracting (Figure 7-49). Such circuits allow an organism to respond to a sensory input by the coordinated action of sets of muscles that together achieve a single purpose.

These simple signaling circuits, however, do not directly explain higher-order brain functions such as reasoning, computation, and memory development. Typical neurons in the brain receive signals from up to a thousand other neurons and, in turn, can direct chemical signals to many other neurons. The output of the nervous system depends on its circuit properties, that is, the wiring, or interconnections, between neurons and the strength of these interconnections. Complex aspects of the nervous system, such as vision and consciousness, cannot be understood at the single-cell level, but only at the level of networks of nerve cells that can be studied by techniques of systems analysis. The nervous system is constantly changing; alterations in the number and nature of the interconnections between individual neurons occur, for example, in the development of new memories.



▲ FIGURE 7-49 The knee-jerk reflex arc in the human.

Positioning and movement of the knee joint are accomplished by two muscles that have opposite actions: Contraction of the quadriceps muscle straightens the leg, whereas contraction of the biceps muscle bends the leg. The knee-jerk response, a sudden extension of the leg, is stimulated by a blow just below the kneecap. The blow directly stimulates sensory neurons (blue) located in the tendon of the quadriceps muscle. The axon of each sensory neuron extends from the tendon to its cell body in a dorsal root ganglion. The sensory axon then continues to the

spinal cord, where it branches and synapses with two neurons: (1) a motor neuron (red) that innervates the quadriceps muscle and (2) an inhibitory interneuron (black) that synapses with a motor neuron (green) innervating the biceps muscle. Stimulation of the sensory neuron causes a contraction of the quadriceps and, via the inhibitory neuron, a simultaneous inhibition of contraction of the biceps muscle. The net result is an extension of the leg at the knee joint. Each cell illustrated here actually represents a nerve, that is, a population of neurons.

## KEY CONCEPTS OF SECTION 7.8

### Neurotransmitters and Receptor and Transport Proteins in Signal Transmission at Synapses

- Neurotransmitter receptors fall into two classes: ligand-gated ion channels, which permit ion passage when open, and G protein-coupled receptors, which are linked to a separate ion channel.
- At synapses impulses are transmitted by neurotransmitters released from the axon terminal of the presynaptic cell and subsequently bound to specific receptors on the postsynaptic cell (see Figure 7-31).
- Low-molecular-weight neurotransmitters (e.g., acetylcholine, dopamine, epinephrine) are imported from the cytosol into synaptic vesicles by H<sup>+</sup>-linked antiporters. V-class proton pumps maintain the low intravesicular pH that drives neurotransmitter import against a concentration gradient.
- Arrival of an action potential at a presynaptic axon terminal opens voltage-gated Ca<sup>2+</sup> channels, leading to a localized rise in the cytosolic Ca<sup>2+</sup> level that triggers exocytosis of synaptic vesicles. Following neurotransmitter release, vesicles are formed by endocytosis and recycled (see Figure 7-42).
- Coordinated operation of four gated ion channels at the synapse of a motor neuron and striated muscle cell leads to release of acetylcholine from the axon terminal, depolarization of the muscle membrane, generation of an action potential, and then contraction (see Figure 7-44).
- The nicotinic acetylcholine receptor, a ligand-gated cation channel, contains five subunits, each of which has a transmembrane  $\alpha$  helix (M2) that lines the channel (see Figure 7-45).
- A postsynaptic neuron generates an action potential only when the plasma membrane at the axon hillock is depolarized to the threshold potential by the summation of small depolarizations and hyperpolarizations caused by activation of multiple neuronal receptors (see Figure 7-48).

## PERSPECTIVES FOR THE FUTURE

In this chapter, we have explained certain aspects of human physiology in terms of the action of specific membrane transport proteins. Such a molecular physiology approach has many medical applications. Even today, specific inhibitors or activators of channels, pumps, and transporters constitute the largest single class of drugs. For instance, an inhibitor of the gastric H<sup>+</sup>/K<sup>+</sup> ATPase that acidifies the stomach is the most widely used drug for treating stomach ulcers. Inhibitors of channel proteins in the kidney are widely used to control

hypertension (high blood pressure). By blocking resorption of water from the forming urine into the blood, these drugs reduce blood volume and thus blood pressure. Calcium-channel blockers are widely employed to control the intensity of contraction of the heart. And the Na<sup>+</sup>-linked symport proteins that are used by nerve cells for reuptake of neurotransmitters are specifically inhibited by many drugs of abuse (e.g., cocaine) and antidepressant medications (e.g., Prozac).

With the completion of the human genome project, we are positioned to learn the sequences of all human membrane transport proteins. Already we know that mutations in many of them cause disease. For example, mutation in a voltage-gated Na<sup>+</sup> channel that is expressed in the heart causes ventricular fibrillation and heart attacks. Mutations in other Na<sup>+</sup> channels, expressed mainly in the brain, cause epilepsy and febrile seizures. In some cases the molecular mechanisms are known. One type of missense mutation in a Na<sup>+</sup> channel that causes epilepsy affects the voltage dependence of channel opening and closing; another slows inactivation of the channel at depolarizing potentials, prolonging the influx of Na<sup>+</sup> ions. Studies in mice expressing mutant forms of these and many other membrane transport proteins are continuing to provide clues to their role in human physiology and disease.

This exploding basic knowledge will enable researchers to identify new types of compounds that inhibit or activate just one of these membrane transport proteins and not its homologs. An important challenge, however is to understand the role of an individual transport protein in each of the several tissues in which it is expressed. As an example, a drug that inhibits a particular ion channel in sensory neurons might be useful in treatment of chronic pain, but if this channel also is expressed in certain areas of the brain, its inhibition may have serious undesired actions (“side effects”).

A real understanding of the function of nerve cells requires knowledge of the three-dimensional structures of many different channels, neurotransmitter receptors, and other membrane proteins. Determination of the structure of the first voltage-gated K<sup>+</sup> channel should illuminate the mechanisms of channel gating, opening, and inactivation that may also apply to other voltage-gated channels. Similarly, the nicotinic acetylcholine, glutamate, GABA, and glycine receptors are all ligand-gated ion channels, but it is disputed whether they all have the same overall structures in the membrane. Resolving this issue will also require knowledge of their three-dimensional structures, which, in addition, should tell us in detail how neurotransmitter binding leads to channel opening.

How does a neuron achieve its very long, branching structure? Why does one part of a neuron become a dendrite and another an axon? Why are certain key membrane proteins clustered at particular points—neurotransmitter receptors in postsynaptic densities in dendrites, Ca<sup>2+</sup> channels in axon termini, and Na<sup>+</sup> channels in myelinated neurons at the nodes of Ranvier? Such questions of cell shape and

protein targeting also apply to other types of cells, but the morphological diversity of different types of neurons makes these particularly intriguing questions in the nervous system. Development of pure cultures of specific types of neurons that maintain their normal properties would enable many of these problems to be studied by techniques of molecular cell biology. Perhaps the most difficult questions concern the formation of specific synapses within the nervous system; that is, how does a neuron “know” to synapse with one type of cell and not another? Ongoing research on the development of the nervous system, which we briefly discuss in Chapter 15, is beginning to provide more complete answers about the complex wiring among neurons and how this relates to brain function.

## KEY TERMS

ABC superfamily 239	membrane potential 232
action potential 231	myelin sheath 270
active transport 233	Na <sup>+</sup> /K <sup>+</sup> ATPase 242
antiport 254	neurotransmitter 262
cotransport 254	passive diffusion 232
depolarization 263	patch clamping 251
electrochemical gradient 232	resting K <sup>+</sup> channels 248
facilitated diffusion 233	symport 254
gated channel 233	synapses 263
hypertonic 258	tight junctions 260
hypotonic 258	transcellular transport 260
isotonic 258	uniport 234

## REVIEW THE CONCEPTS

- The basic structural unit of biomembranes is the phospholipid bilayer. Acetic acid and ethanol are composed each of two carbons, hydrogen and oxygen, and both enter cells by passive diffusion. At pH 7, one is much more membrane permeant than the other. Which is the more permeable, and why? Predict how the permeability of each is altered when pH is reduced to 1.0, a value typical of the stomach.
- Uniporters and ion channels support facilitated diffusion across biomembranes. Although both are examples of facilitated diffusion, the rates of ion movement via a channel are roughly 10<sup>4</sup>- to 10<sup>5</sup>-fold faster than that of molecules via a uniporter. What key mechanistic difference results in this large difference in transport rate?
- Name the three classes of transporters. Explain which of these classes is able to move glucose or bicarbonate (HCO<sub>3</sub><sup>-</sup>), for example, against an electrochemical gradient. In the case of bicarbonate, but not glucose, the  $\Delta G$  of the transport process has two terms. What are these two terms, and why does the second not apply to glucose? Why are cotransporters often referred to as examples of secondary active transport?
- GLUT1, found in the plasma membrane of erythrocytes, is a classic example of a uniporter. Design a set of experiments to prove that GLUT1 is indeed a glucose-specific uniporter rather than a galactose- or mannose-specific uniporter. Glucose is a 6-carbon sugar while ribose is a 5-carbon sugar. Despite this smaller size, ribose is not efficiently transported by GLUT1. How can this be explained?
- Name the four classes of ATP-powered pumps that produce active transport of ions and molecules. Indicate which of these classes transport ions only and which transport primarily small molecules. In the case of one class of these ATP-powered pumps, the initial discovery of the class came from studying not the transport of a natural substrate but rather artificial substrates used as cancer chemotherapy drugs. What do investigators now think are common examples of the natural substrates of this particular class of ATP-powered pumps?
- Genome sequencing projects continue, and for an increasing number of organisms the complete genome sequence of that organism is known. How does this information allow us to state the total number of transporters or pumps of a given type in either mice or humans? Many of the sequence-identified transporters or pumps are “orphan” proteins, in the sense that their natural substrate or physiological role is not known. How can this be, and how might one establish the physiological role of an orphan protein?
- As cited in the section Perspectives for the Future, specific inhibitors or activators of channels, pumps, and transporters constitute the largest single class of drugs produced by the pharmaceutical industry. Skeletal muscle contraction is caused by elevation of Ca<sup>2+</sup> concentration in the cytosol. What is the expected effect on muscle contraction of selective drug inhibition of sarcoplasmic reticulum (SR) P-class Ca<sup>2+</sup> ATPase?
- The membrane potential in animal cells, but not in plants, depends largely on resting K<sup>+</sup> channels. How do these channels contribute to the resting potential? Why are these channels considered to be nongated channels? How do these channels achieve selectivity for K<sup>+</sup> versus Na<sup>+</sup>?
- Patch clamping can be used to measure the conductance properties of individual ion channels. Describe how patch clamping can be used to determine whether or not the gene coding for a putative K<sup>+</sup> channel actually codes for a K<sup>+</sup> or Na<sup>+</sup> channel.
- Plants use the proton electrochemical gradient across the vacuole membrane to power the accumulation of salts and sugars in the organelle. This creates a hypertonic situation. Why does this not result in the plant cell bursting? How does

the plasma membrane  $\text{Na}^+/\text{K}^+$  ATPase allow animal cells to avoid osmotic lysis even under isotonic conditions?

**11.** Movement of glucose from one side to the other side of the intestinal epithelium is a major example of transcellular transport. How does the  $\text{Na}^+/\text{K}^+$  ATPase power the process? Why are tight junctions essential for the process? Rehydration supplements such as sport drinks include a sugar and a salt. Why are both important to rehydration?

**12.** Name the three phases of an action potential. Describe for each the underlying molecular basis and the ion involved. Why is the term *voltage-gated channel* applied to  $\text{Na}^+$  channels involved in the generation of an action potential?

**13.** Myelination increases the velocity of action potential propagation along an axon. What is myelination? Myelination causes clustering of voltage-gated  $\text{Na}^+$  channels and  $\text{Na}^+/\text{K}^+$  pumps at nodes of Ranvier along the axon. Predict the consequences to action potential propagation of increasing the spacing between nodes of Ranvier by a factor of 10.

**14.** Compare the role of  $\text{H}^+$ -linked antiporters in the accumulation of neurotransmitters in synaptic vesicles and sucrose in the plant vacuole. Acetylcholine is a common neurotransmitter released at the synapse. Predict the consequences for muscle activation of decreased acetylcholine esterase activity at nerve-muscle synapses.

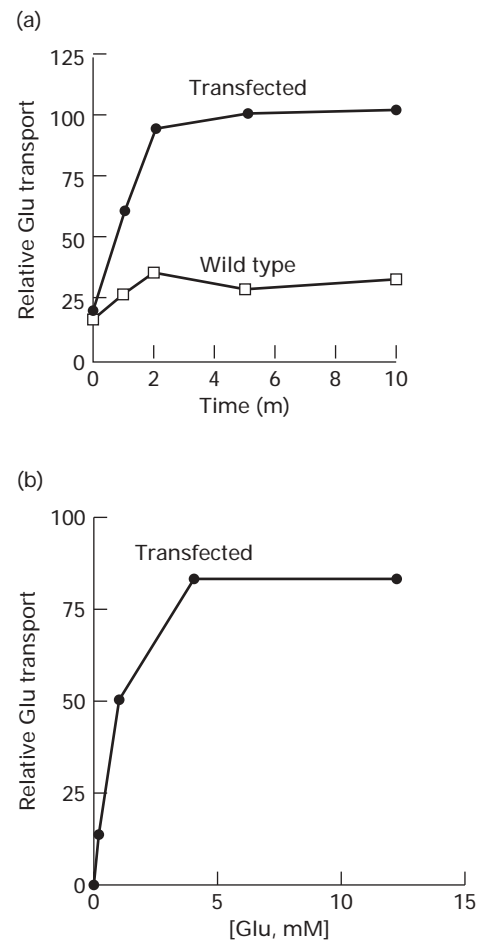
**15.** Neurons, particularly those in the brain, receive multiple excitatory and inhibitory signals. What is the name of the extension of the neuron at which such signals are received? How does the neuron integrate these signals to determine whether or not to generate an action potential?

## ANALYZE THE DATA

Imagine that you are evaluating candidates for the glutamate transporter resident in the membrane of synaptic vesicles of the brain. Glutamate is a major neurotransmitter. You conduct a thorough search of protein databases and literature and find that the *Caenorhabditis elegans* protein EAT-4 has many of the properties expected of a brain glutamate transporter. The protein is presynaptic in *C. elegans* and mutations in it are associated with glutamatergic defects. By sequence comparison, the mammalian homolog is BNP1. Related type I transporters are known to transport organic anions.

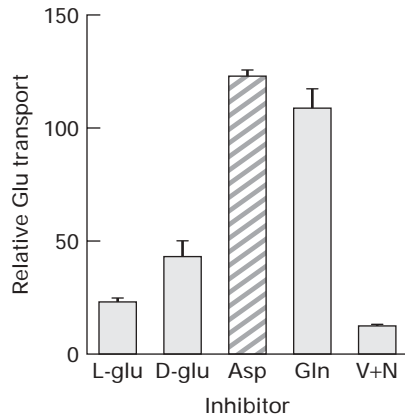
**a.** To determine whether BNP1 mediates the transport of glutamate into synaptic vesicles, you transfect BNP1 cDNA into PC12 cells, which lack detectable endogenous BNP1 protein. You then prepare a synaptic vesicle-like microvesicle population from transfected and untransfected cells. The glutamate transport properties of the isolated vesicles are shown in the figure at the right. How do these results indi-

cate transporter-dependent uptake of glutamate in transfected versus nontransfected, wild-type PC12 cell vesicles? What is the apparent  $K_m$  of the glutamate transporter? The literature reports  $K_m$  values of  $\sim 10\text{--}100\ \mu\text{M}$  for plasma membrane excitatory amino acid transporters. Is the  $K_m$  observed consistent with BNP1 being a plasma membrane amino acid transporter?



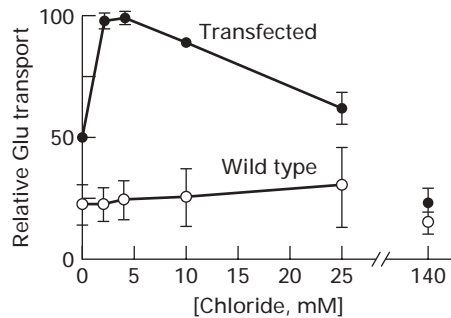
Effect of BNP1 transfection on glutamate uptake by PC12 cell vesicles.

**b.** You next decide to test the specificity of BNP1 for individual amino acids and whether or not glutamate uptake is dependent on the electrical gradient as predicted. For these experiments, you set up a series of incubation mixes with various amino acids as competitors and separately a mix with valinomycin (V) and nigericin (N) to dissipate selectively the electrical gradient. Based on the data shown in the following figure, does BNP1-dependent transport display the expected properties? Why are the chosen amino acids the logical choices for potential competitors?



Effect of amino acid competitors and valinomycin plus nigericin (V + N) on BNP1 transport.

c. As a final test, you determine the dependence of BNP1 transport on chloride concentration. Vesicular glutamate transport is known to exhibit a biphasic dependence on chloride concentration. The results of your experiment are shown in the figure below. Do these data indicate a biphasic chloride dependence? How may such a chloride dependence be explained?



Chloride dependence of transport by BNP1.

d. You conclude on the basis of the data that BNP1 is the synaptic vesicle glutamate transporter. How could you test in PC12 cells whether mutations modeled on the *C. elegans* EAT-4 protein were important in the mammalian protein?

## REFERENCES

### Overview of Membrane Transport

Hruz, P. W., and M. M. Mueckler. 2001. Structural analysis of the GLUT1 facilitative glucose transporter (review). *Mol. Memb. Biol.* **18**:183–193.

Malandro, M., and M. Kilberg. 1996. Molecular biology of mammalian amino acid transporters. *Ann. Rev. Biochem.* **66**:305–336.

Mueckler, M. 1994. Facilitative glucose transporters. *Eur. J. Biochem.* **219**:713–725.

### ATP-Powered Pumps and the Intracellular Ionic Environment

Borst, P., N. Zelcer, and A. van Helvoort. 2000. ABC transporters in lipid transport. *Biochim. Biophys. Acta* **1486**:128–144.

Carafoli, E., and M. Brini. 2000. Calcium pumps: structural basis for and mechanism of calcium transmembrane transport. *Curr. Opin. Chem. Biol.* **4**:152–161.

Davies, J., F. Chen, and Y. Ioannou. 2000. Transmembrane molecular pump activity of Niemann-Pick C1 protein. *Science* **290**:2295–2298.

Doige, C. A., and G. F. Ames. 1993. ATP-dependent transport systems in bacteria and humans: relevance to cystic fibrosis and multidrug resistance. *Ann. Rev. Microbiol.* **47**:291–319.

Gottesman, M. M. 2002. Mechanisms of cancer drug resistance. *Ann. Rev. Med.* **53**:615–627.

Gottesman, M. M., and S. V. Ambudkar. 2001. Overview: ABC transporters and human disease. *J. Bioenerg. Biomemb.* **33**:453–458.

Higgins, C. F., and K. J. Linton. 2001. Structural biology. The xyz of ABC transporters. *Science* **293**:1782–1784.

Holmgren, M., et al. 2000. Three distinct and sequential steps in the release of sodium ions by the Na<sup>+</sup>/K<sup>+</sup>-ATPase. *Nature* **403**:898–901.

Jencks, W. P. 1995. The mechanism of coupling chemical and physical reactions by the calcium ATPase of sarcoplasmic reticulum and other coupled vectorial systems. *Biosci. Rept.* **15**:283–287.

Nishi, T., and M. Forgac. 2002. The vacuolar (H<sup>+</sup>)-ATPases—nature's most versatile proton pumps. *Nature. Rev. Mol. Cell Biol.* **3**:94–103.

Ostedgaard, L. S., O. Baldursson, and M. J. Welsh. 2001. Regulation of the cystic fibrosis transmembrane conductance regulator Cl<sup>−</sup> channel by its R domain. *J. Biol. Chem.* **276**:7689–7692.

Raggers, R. J., et al. 2000. Lipid traffic: the ABC of transbilayer movement. *Traffic* **1**:226–234.

Rea, P. A., et al. 1992. Vacuolar H<sup>+</sup>-translocating pyrophosphatases: a new category of ion translocase. *Trends Biochem. Sci.* **17**:348–353.

Sweadner, K. J., and C. Donnet. 2001. Structural similarities of Na,K-ATPase and SERCA, the Ca(2<sup>+</sup>)-ATPase of the sarcoplasmic reticulum. *Biochem. J.* **356**:685–704.

Toyoshima, C., M. Nakasako, H. Nomura, and H. Ogawa. 2000. Crystal structure of the calcium pump of sarcoplasmic reticulum at 2.6 Å resolution. *Nature* **405**:647–655.

Xu, C., W. J. Rice, W. He, and D. L. Stokes. 2002. A structural model for the catalytic cycle of Ca(2<sup>+</sup>)-ATPase. *J. Mol. Biol.* **316**:201–211.

### Nongated Ion Channels and the Resting Membrane Potential

Clapham, D. 1999. Unlocking family secrets: K<sup>+</sup> channel transmembrane domains. *Cell* **97**:547–550.

Cooper, E. C., and L. Y. Jan. 1999. Ion channel genes and human neurological disease: recent progress, prospects, and challenges. *Proc. Nat'l. Acad. Sci. USA* **96**:4759–4766.

Dutzler, R., et al. 2002. X-ray structure of a ClC chloride channel at 3.0 Å reveals the molecular basis of anion selectivity. *Nature* **415**:287–294.

Gulbis, J. M., M. Zhou, S. Mann, and R. MacKinnon. 2000. Structure of the cytoplasmic beta subunit-T1 assembly of voltage-dependent K<sup>+</sup> channels. *Science* **289**:123–127.

Hanaoka, K., et al. 2000. Co-assembly of polycystin-1 and -2 produces unique cation-permeable currents. *Nature* **408**:990–994.

Hille, B. 2001. *Ion Channels of Excitable Membranes*, 3d ed. Sinauer Associates.

- Montell, C., L. Birnbaumer, and V. Flockerzi. 2002. The TRP channels, a remarkably functional family. *Cell* **108**:595–598.
- Neher, E. 1992. Ion channels for communication between and within cells. Nobel Lecture reprinted in *Neuron* **8**:605–612 and *Science* **256**:498–502.
- Neher, E., and B. Sakmann. 1992. The patch clamp technique. *Sci. Am.* **266**(3):28–35.
- Nichols, C., and A. Lopatin. 1997. Inward rectifier potassium channels. *Ann. Rev. Physiol.* **59**:171–192.
- Yi, B. A., et al. 2001. Controlling potassium channel activities: interplay between the membrane and intracellular factors. *Proc. Nat'l. Acad. Sci. USA* **98**:11016–11023.
- Zhou, M., J. H. Morais-Cabral, S. Mann, and R. MacKinnon. 2001. Potassium channel receptor site for the inactivation gate and quaternary amine inhibitors. *Nature* **411**:657–661.
- Zhou, Y., J. Morais-Cabral, A. Kaufman, and R. MacKinnon. 2001. Chemistry of ion coordination and hydration revealed by a K<sup>+</sup> channel–Fab complex at 2 Å resolution. *Nature* **414**:43–48.
- ### Cotransport by Symporters and Antiporters
- Alper, S. L., M. N. Chernova, and A. K. Stewart. 2001. Regulation of Na<sup>+</sup>-independent Cl<sup>-</sup>/HCO<sub>3</sub><sup>-</sup> exchangers by pH. *J. Pancreas* **2**:171–175.
- Barkla, B., and O. Pantoja. 1996. Physiology of ion transport across the tonoplast of higher plants. *Ann. Rev. Plant Physiol. Plant Mol. Biol.* **47**:159–184.
- Orlowski, J., and S. Grinstein. 1997. Na<sup>+</sup>/H<sup>+</sup> exchangers of mammalian cells. *J. Biol. Chem.* **272**:22373–22376.
- Shrode, L. D., H. Tapper, and S. Grinstein. 1997. Role of intracellular pH in proliferation, transformation, and apoptosis. *J. Bioenerg. Biomemb.* **29**:393–399.
- Wakabayashi, S., M. Shigekawa, and J. Pouyssegur. 1997. Molecular physiology of vertebrate Na<sup>+</sup>/H<sup>+</sup> exchangers. *Physiol. Rev.* **77**:51–74.
- Wright, E. M. 2001. Renal Na(+)-glucose cotransporters. *Am. J. Physiol. Renal Physiol.* **280**:F10–F18.
- Wright, E. M., and D. D. Loo. 2000. Coupling between Na<sup>+</sup>, sugar, and water transport across the intestine. *Ann. NY Acad. Sci.* **915**:54–66.
- Zhang, H.-X., and E. Blumwald. 2001. Transgenic salt-tolerant tomato plants accumulate salt in foliage but not in fruit. *Nature Biotech.* **19**:765–769.
- ### Movement of Water
- Agre, P., M. Bonhivers, and M. Borgina. 1998. The aquaporins, blueprints for cellular plumbing systems. *J. Biol. Chem.* **273**:14659.
- Engel, A., Y. Fujiyoshi, and P. Agre. 2000. The importance of aquaporin water channel protein structures. *EMBO J.* **19**:800–806.
- Maurel, C. 1997. Aquaporins and water permeability of plant membranes. *Ann. Rev. Plant Physiol. Plant Mol. Biol.* **48**:399–430.
- Nielsen, S., et al. 2002. Aquaporins in the kidney: from molecules to medicine. *Physiol. Rev.* **82**:205–244.
- Schultz, S. G. 2001. Epithelial water absorption: osmosis or co-transport? *Proc. Nat'l. Acad. Sci. USA* **98**:3628–3630.
- Sui, H., et al. 2001. Structural basis of water-specific transport through the AQP1 water channel. *Nature* **414**:872–878.
- Verkman, A. S. 2000. Physiological importance of aquaporins: lessons from knockout mice. *Curr. Opin. Nephrol. Hypertens.* **9**:517–522.
- ### Transepithelial Transport
- Cereijido, M., J. Valdés, L. Shoshani, and R. Conteras. 1998. Role of tight junctions in establishing and maintaining cell polarity. *Ann. Rev. Physiol.* **60**:161–177.
- Goodenough, D. A. 1999. Plugging the leaks. *Proc. Nat'l. Acad. Sci. USA* **96**:319.
- Mitic, L., and J. Anderson. 1998. Molecular architecture of tight junctions. *Ann. Rev. Physiol.* **60**:121–142.
- Schultz, S., et al., eds. 1997. *Molecular Biology of Membrane Transport Disorders*. Plenum Press.
- ### Propagation of Electric Impulses by Gated Ion Channels
- Aldrich, R. W. 2001. Fifty years of inactivation. *Nature* **411**:643–644.
- Armstrong, C., and B. Hille. 1998. Voltage-gated ion channels and electrical excitability. *Neuron* **20**:371–380.
- Catterall, W. A. 2000. From ionic currents to molecular mechanisms: the structure and function of voltage-gated sodium channels. *Neuron* **26**:13–25.
- Catterall, W. A. 2000. Structure and regulation of voltage-gated Ca<sup>2+</sup> channels. *Ann. Rev. Cell Dev. Biol.* **16**:521–555.
- Catterall, W. A. 2001. A 3D view of sodium channels. *Nature* **409**:988–989.
- del Camino, D., and G. Yellen. 2001. Tight steric closure at the intracellular activation gate of a voltage-gated K(+) channel. *Neuron* **32**:649–656.
- Doyle, D. A., et al. 1998. The structure of the potassium channel: molecular basis of K<sup>+</sup> conduction and selectivity. *Science* **280**:69–77.
- Hille, B. 2001. *Ion Channels of Excitable Membranes*, 3d ed. Sinauer Associates.
- Jan, Y. N., and L. Y. Jan. 2001. Dendrites. *Genes Dev.* **15**:2627–2641.
- Miller, C. 2000. Ion channel surprises: prokaryotes do it again! *Neuron* **25**:7–9.
- Sato, C., et al. 2001. The voltage-sensitive sodium channel is a bell-shaped molecule with several cavities. *Nature* **409**:1047–1051.
- Yi, B. A., and L. Y. Jan. 2000. Taking apart the gating of voltage-gated K<sup>+</sup> channels. *Neuron* **27**:423–425.
- ### Myelin
- Arroyo, E. J., and S. S. Scherer. 2000. On the molecular architecture of myelinated fibers. *Histochem. Cell Biol.* **113**:1–18.
- Pedraza, L., J. K. Huang, and D. R. Colman. 2001. Organizing principles of the axoglial apparatus. *Neuron* **30**:335–344.
- Salzer, J. L. 1997. Clustering sodium channels at the node of Ranvier: close encounters of the axon-glia kind. *Neuron* **18**:843–846.
- Trapp, B. D., and G. J. Kidd. 2000. Axo-glia septate junctions. The maestro of nodal formation and myelination? *J. Cell Biol.* **150**:F97–F100.
- ### Neurotransmitters and Transport Proteins in the Transmission of Electric Impulses
- Amara, S. G., and M. J. Kuhar. 1993. Neurotransmitter transporters: recent progress. *Ann. Rev. Neurosci.* **16**:73–93.
- Bajjalieh, S. M., and R. H. Scheller. 1995. The biochemistry of neurotransmitter secretion. *J. Biol. Chem.* **270**:1971–1974.
- Betz, W., and J. Angleson. 1998. The synaptic vesicle cycle. *Ann. Rev. Physiol.* **60**:347–364.
- Brejč, K., et al. 2001. Crystal structure of an ACh-binding protein reveals the ligand-binding domain of nicotinic receptors. *Nature* **411**:269–276.
- Fernandez, J. M. 1997. Cellular and molecular mechanics by atomic force microscopy: capturing the exocytotic fusion pore in vivo? *Proc. Nat'l. Acad. Sci. USA* **94**:9–10.
- Ikedo, S. R. 2001. Signal transduction. Calcium channels—link locally, act globally. *Science* **294**:318–319.

Jan, L. Y., and C. F. Stevens. 2000. Signaling mechanisms: a decade of signaling. *Curr. Opin. Neurobiol.* **10**:625–630.

Karlin, A. 2002. Emerging structure of the nicotinic acetylcholine receptors. *Nature Rev. Neurosci.* **3**:102–114.

Kavanaugh, M. P. 1998. Neurotransmitter transport: models in flux. *Proc. Nat'l. Acad. Sci. USA* **95**:12737–12738.

Lin, R. C., and R. H. Scheller. 2000. Mechanisms of synaptic vesicle exocytosis. *Ann. Rev. Cell Dev. Biol.* **16**:19–49.

Neher, E. 1998. Vesicle pools and  $\text{Ca}^{2+}$  microdomains: new tools for understanding their roles in neurotransmitter release. *Neuron* **20**:389–399.

Reith, M., ed. 1997. *Neurotransmitter Transporters: Structure, Function, and Regulation*. Humana Press.

Sakmann, B. 1992. Elementary steps in synaptic transmission revealed by currents through single ion channels. Nobel Lecture reprinted in *EMBO J.* **11**:2002–2016 and *Science* **256**:503–512.

Sudhof, T. C. 1995. The synaptic vesicle cycle: a cascade of protein-protein interactions. *Nature* **375**:645–653.

Usdin, T. B., L. E. Eiden, T. I. Bonner, and J. D. Erickson. 1995. Molecular biology of the vesicular ACh transporter. *Trends Neurosci.* **18**:218–224.